UNIVERSITY OF OKLAHOMA

GRADUATE COLLEGE

MEASURING RATE CONSTANTS FOR THE REACTION OF HYPOCHLOROUS ACID AND BIOLOGICALLY RELEVANT MOLECULES

A DISSERTATION

SUBMITTED TO THE GRADUATE FACULTY

in partial fulfillment of the requirements for the

Degree of

DOCTOR OF PHILOSOPHY

By

JENNIFER BEAL
Norman, Oklahoma
2012

Downloaded from SHAREOK. Persistent Handle URL: https://hdl.handle.net/11244/318542

MEASURING RATE CONSTANTS FOR THE REACTION OF
HYPOCHLOROUS ACID AND BIOLOGICALLY RELEVANT MOLECULES

A DISSERTATION APPROVED FOR THE
DEPARTMENT OF CHEMISTRY AND BIOCHEMISTRY

BY

Dr. Michael Ashby, Chair

Dr. Richard Taylor

Dr. Robert White

Dr. Roger Frech

Dr. John Moore-Furneaux

© Copyright by JENNIFER BEAL 2012
All Rights Reserved.

Acknowledgements

First, I would like to express my sincere gratitude to my research advisor Dr. Ashby for his guidance, knowledge, encouragement, and overall help in my transition from student to chemist. I want to acknowledge my committee members (Drs. Taylor, White, Frech, and Moore-Furneaux) for their support and patience throughout my graduate career.

I would like to thank members of the Ashby research group, in particular Drs. Bheki “Alex” Xulu and Peter Nagy, with whom I became good friends as we worked side by side for the majority of my time at OU. Alex was my graduate “buddy,” encouraging and helping me through the tough times when research was not going well.

Other members of the OU faculty and staff have also had an influence on my success. Drs. Susan Nimmo and Steven Foster helped with special projects by providing expertise in NMR and MS, respectively. Dr. Glazhofer offered me a summer internship position in 2001 and 2002, which aided in my desire to attend OU. Drs. Yip and Frech, who were my internship mentors, helped me understand the basics of research and encouraged me to continue my education beyond a Bachelor’s degree.

Special thanks go to Jamie Huntley, a fellow analytical graduate student, who also understood the pressures and difficulties of graduate student life. We helped each other get through the first two years of graduate school.

I also would like to thank my newly found coworkers at ODAFF (Oklahoma Department of Agriculture, Food, and Forestry) for their support in my transition from an ABD (all but dissertation) student to a career chemist.

Lastly, but most importantly, I want to thank my family (Gutshall/Crawford, Beal/Garber, and Yandell/Burton) for all their love, support, and encouragement, without which I could not have made it. To Jody, my husband and best friend; Dobbie, my kitty (who was always close by to cheer me up when times got stressful), Roadkill, my puppy, William Gutshall (my proud father), and brother Mikey, all of whom I think of as my biggest supporters: thank you for never giving up on me, and for never letting me give up on myself. I want to also thank Mom (Sue) Beal, Grandma Wert, and Grandma Yandell, all of whom believed in me, but left this world before they could see me graduate. Thanks for everything.



Table of Contents

Acknowledgements iv

Table of Contents vi

List of Tables xiii

List of Figures xv

List of Abbreviations xxv

Abstract xxvi

Chapter 1: Introduction: Production of Reactive Oxygen Species by the Human Immune System

1.1 Immune System 1

1.1.1 Innate immune system 1

1.2 Leukocytes 2

1.2.1 Neutrophils 3

1.3 Phagocytosis 4

1.4 Respiratory burst 5

1.5 Peroxidases and the production of ROS 6

1.5.1 Reactive oxygen species 7

1.6 Antioxidants 8

1.7 Summary of chapters 9

1.8 References 13

Chapter 2: Inhibitory Titrations: Development of a Method for Measuring Rate Constants of Fast Reactions

2.1 Introduction 17

2.1.1 Rate law 17

2.1.2 Fast reaction detection techniques 19

2.1.3 Methods used to change $t_{1/2}$ of a second-order reaction 24

2.1.4 Competition reactions 27

2.1.5 Development of the inhibitory titration method 28

2.2 Experimental methods 30

2.2.1 Materials 30

2.2.2 Sample preparation 31

2.2.2.1 DCPIP dye 31

2.2.2.2 Thiocyanate 31

2.2.2.3 Monochlorodimedone 31

2.2.2.4 Hypochlorous acid 31

2.2.2.5 Human serum albumin 32

2.2.3 Standardization of commercial bleach (hypochlorite) 32

2.2.3.1 Titration of $Na_2S_2O_3$ 32

2.2.3.2 Titration of bleach 34

2.2.4 pH measurements 34

2.2.5 UV-vis spectroscopy 34

2.2.6 Turbulent mixing of samples 35

2.2.7 Biologic instrument 35
2.2.7.1 General information 35
2.2.7.2 Quench-flow mode 36
2.2.7.3 Aging methods for quench-flow 38
2.2.7.3.1 Interrupted flow 38
2.2.7.3.2 Continuous flow 39
2.2.7.3.3 Pulsed flow 40
2.3 Results and discussion 42
2.3.1 MCD/SCN^- competition reaction with HOCl 42
2.3.2 MCD/HSA competition reaction with HOCl 49
2.4 Summary and conclusions 56
2.5 Future experiments 58
2.6 References 60

Chapter 3: Oxidation of Methionine by Hypochlorous Acid, Search for an Intermediate

3.1 Introduction 62
3.1.1 Methionine 62
3.1.2 Oxidation of methionine 63
3.1.3 Mechanism of oxidation 66
3.1.4 Methionine sulfoxide reductase 68
3.2 Experimental methods 69
3.2.1 Materials 69

3.2.2 Sample preparation 70
3.2.2.1 Hypochlorous acid 70
3.2.2.2 Synthesis of DNPMet 71
3.2.2.3 Synthesis of TNBMe 71
3.2.2.4 Methionine studies 72
3.2.2.5 TNBMe titration and molar absorptivity 72
3.2.3 High performance liquid chromatography (HPLC) 73
3.2.4 Ion chromatography (IC) 73
3.2.5 Biologic instrument 74
3.2.6 Intermediate production 75
3.3 Results and discussion 76
3.3.1 Oxidation of methionine by HOCl 77
3.3.2 Oxidation of methionine sulfoxide by HOCl 81
3.3.3 Oxidation of DNPMet 84
3.3.4 Oxidation of TNBMe 87
3.4 Summary and conclusions 93
3.5 Future experiments 94
3.6 References 96

Chapter 4: Oxidation of Methionine by Halogens to Produce the Potential Biomarker Dehydromethionine

4.1 Introduction 102
4.1.1 Oxidation of proteins 102

4.1.2 Biomarkers of oxidation by halogenating agents 107
4.1.3 Dehydromethionine 109
4.2 Experimental methods 115
4.2.1 Materials 115
4.2.2 Sample preparation 116
4.2.2.1 Preparation of oxidant stock solutions 116
4.2.2.2 Reaction of free methionine with oxidants 118
4.2.2.3 Reaction of antiflammin-1 and Ub1-6 with oxidants 118
4.2.2.4 Reactions and digestion of ubiquitin 119
4.2.3 pH measurements 120
4.2.4 UV-vis spectroscopy 120
4.2.5 ^{1}H NMR measurements 120
4.2.6 HSQC NMR measurements 121
4.2.7 LC-MS of tryptic digested ubiquitin 122
4.3 Results and discussion 123
4.3.1 Oxidation of free methionine 123
4.3.2 Oxidation of methionine containing peptides 127
4.3.3 Oxidation of Met-1 in ubiquitin 133
4.3.3.1 HSQC of oxidized ubiquitin 133
4.3.3.2 LC-UV and LC-MS of tryptic digested ubiquitin 144

4.4 Summary and conclusions 154

4.5 Future experiments 156

4.6 References 157

Chapter 5: Concluding Remarks and Future Experiments

5.1 Summary of findings 165

5.2 Recommended future studies 166

Appendices:

Appendix A: Complete data set for the competition reaction of SCN^- and MCD with HOCl 168

Appendix B: C++ code for computing rate constants using experimental data from the reaction of HOCl with MCD/SCN^- 170

Appendix C: C++ code used to fit experimental data for the reaction of HOCl with MCD/SCN^- with and without consideration of stoichiometry 173

Appendix D: Results of program code listed in appendix C when used to fit experimental data 176

Appendix E: Complete data set of the competition reaction of HSA and MCD with HOCl 179

Appendix F: C++ code for computing the rate constant for the reaction of HOCl with MCD/HSA 181

Appendix G: C++ code used to simulate the data for the competition reaction of MCD/Sulfite with HOCl 184

Appendix H: Simulated data for the competition reaction of MCD/Sulfite with HOCl, effect of varying the initial concentration of MCD 185

List of Tables

Table 1.1: Properties of leukocytes 2

Table 2.1**:** Program output which includes the data point number (i), the experimental [SCN], the experimental %MCD, the %MCD the program calculated, and the rate constant the program calculated 45

Table 2.2: Second-order rate constants for the reactions of HOCl with amino acids and lipid components; SCN^- added for comparison 49

Table 2.3: Program output which includes the data point number (i), the experimental [HSA], the experimental %MCD, the %MCD the program calculated, and the rate constant the program calculated 52

Table 4.1: Product distribution (%) for the reaction of various oxidants with Met to give MetO and DHM[a]. Conditions: 25 mM oxidant and 30 mM Met at pH = 7.4 (0.2 M PBS) and 20 ℃. [a]The oxidant was added to Met dropwise while vortexing. [b]Prior to its addition to Met, HOBr was generated *in situ* by addition of HOCl to Br^- or by addition of Br_2 to base, followed by neutralization. [c]I^- was added to Met prior to the addition of chloramine-T 125

Table 4.2: Comparison of ratio MetO:DHM and rate constants for oxidation of Met by various oxidants (pH = 7, 20 ℃) 126

Table 4.3: Rate constants for reaction of HOCl with amino acid residues in Ub 141

Table 4.4: Peptides of Ub after tryptic digestion 144

List of Figures

Figure 1.1:	Illustration of phagocytosis	4
Figure 1.2:	Production of ROS during neutrophillic oxidative bursts	6
Figure 2.1:	Time ranges of various kinetic methods. Time axis given in units of log of the first order rate constant (s^{-1})	20
Figure 2.2:	A plot of [A] or pH vs. k. X, Y, and Z for a generic reaction, used to point to particular conditions	24
Figure 2.3:	Schematic of SFM-400; DL = Delay line, used to vary aging time of samples	35
Figure 2.4:	Schematic of simple quench flow setup; M1 and M2 are mixers	37
Figure 2.5:	Reaction of HOCl (1 mM) with mixtures of MCD (1 mM) and SCN^- (0-4.6 mM) at pH 7.4 in 0.1 M phosphate and 0.1 M NaCl; percent MCD remaining at the end of the reaction (solid circles)	41
Figure 2.6:	Stoichiometry of the reaction of HOCl with SCN^-	41
Figure 2.7:	Flowchart of the iterative procedure that was employed to compute the rate constants, assuming parallel second-order reactions of HOCl with MCD and X (where X = inhibitor). The constant h is the incremental step for numerical integration and S is the experimental stoichiometry	43

Figure 2.8: Reaction of 1 mM HOCl with mixtures of 1 mM MCD and SCN^- (0-3.5 mM) at pH 7.4 (100 mM phosphate, 100 mM NaCl). Experimental percentage of MCD remaining at the end of the reaction (solid circles); the calculated percentages of MCD at the end of the reactions with (solid line) and without (dashed line) consideration of the stoichiometry 47

Figure 2.9: Reaction of 100 µM HOCl with mixtures of 100 µM MCD and HSA (0-61 µM) at pH 7.4 (100 mM phosphate, 100 mM NaCl). %MCD remaining (squares); stoichiometry of reaction (circles) 51

Figure 2.10: Reaction of 100 µM HOCl with 100 µM MCD and varying amounts of HSA (0-61 µM) at pH = 7.4 (100 mM phosphate and 100 mM NaCl). Experimental %MCD (circles); calculated %MCD using $k = 5.5x10^8\ M^{-1}s^{-1}$ with (triangles) and without (diamonds) consideration of stoichiometry; calculated %MCD using $k = 5.5x10^7\ M^{-1}s^{-1}$ without consideration of stoichiometry (squares); calculated %MCD using $k = 5.5x10^6\ M^{-1}s^{-1}$ without consideration of stoichiometry (crosses) 54

Figure 3.1: Molar absorptivity as a function of wavelength (in 100 mM PBS, pH = 7.4) of Met (circles), MetO (squares), and $MetO_2$ (diamonds). 77

Figure 3.2: Representative ion chromatography chromatogram for mixture of Met (C), MetO (A), and $MetO_2$ (B). Solutions were made up in 1 mM PBS, pH = 7.4 79

Figure 3.3: Reaction of Met (1.5 µM) with HOCl (1.5 µM) in 100 µM PBS, pH = 7.4, quenched with excess sodium sulfite (9 µM) after various delay times. Data was fit to second order reaction giving $k = 4x10^8\ M^{-1}s^{-1}$ 79

Figure 3.4: Reaction of Met (1.5 µM) with HOCl (1.5 µM) in 100 µM PBS, pH = 7.4, quenched with excess sodium sulfite (9 µM) after various delay times. Samples analyzed within 12 hours of collecting samples (circles), and samples analyzed > 24 hours after collecting samples (squares). Data points are averages with error bars of three samples 81

Figure 3.5: Reaction of MetO (500 µM) with HOCl (50 µM) in 5 mM PBS at pH = 7.4. Absorbance spectra (collected via biologic instrument) of reaction (dotted line) versus no reaction (solid line). Inset shows increase in peak at 252 nm 82

Figure 3.6: Reaction of MetO (500 µM) with HOCl (50 µM) in 5 mM PBS at pH = 7.4, kinetic trace followed at 254 nm and fit to first order reaction giving $k_{obs} = 280\ s^{-1}$ (calculated $k = 5.6x10^5\ M^{-1}s^{-1}$) 83

Figure 3.7: Absorbance spectra (0.1 cm cell; HP8452A diode array) of DNPMet (solid line, 0.01164 g in 100 mL 0.1 M PBS pH = 7.4), DNPMetO (long dashed line, 0.00664 g in 50 mL 0.1 M PBS pH = 7.4), $DNPMetO_2$ (dashed line, 0.00616 g in 50 mL 0.1 M PBS pH = 7.4); using Beer's law, molar absorptivities were calculated as DNPMet $\varepsilon_{358nm} = 1.55x10^4\ M^{-1}cm^{-1}$; DNPMetO $\varepsilon_{358nm} = 1.74x10^4\ M^{-1}cm^{-1}$; DNPMet $\varepsilon_{358nm} = 1.69x10^4\ M^{-1}cm^{-1}$ 85

Figure 3.8: Representative chromatogram of a mixture of DNPMetO (RT = 2.5 min) and DNPMet (RT = 7.5 min) 86

Figure 3.9: Reaction (100 µM PBS, pH = 7.4) of DNPMet (1.2 µM) with HOCl (1.2 µM), quenched with excess sodium sulfite (20 µM) after varying delay times, fit with rate constant of $5.5 \pm 0.3x10^6\ M^{-1}s^{-1}$ 87

Figure 3.10: Titration of 240 µM TNBMe with 0-500 µM HOCl (pH = 7.4, 0.05 M PBS, 0.1 M NaCl). Absorbance spectra taken using HP8452A diode array. From top to bottom (at 352 nm), stoichiometry TNBMe:HOCl, 1:0 (Δ), 1:0.3 (+), 1:0.6 (x), 1:0.8 (◊), 1:1(□), 1:2(○) 88

Figure 3.11: Plot of [TNBMe] (M, calculated by $[TNBMe]_0 - [HOCl]_0$) versus the A_{352} (circles) (using a 0.2 cm cell, data collected on HP8452A diode array), fit using linear equation y = 1.9735 x + 0.0336. Using Beer's law, $A = \varepsilon * b * c$, $\varepsilon = 9.8 \times 10^3\ M^{-1}cm^{-1}$ was determined 89

Figure 3.12: Reaction of 50 µM TNBMe with 10 µM HOCl (monitored at 352 nm). Data fit to first order reaction (solid line), trace from top to bottom (all done at pH = 7.4, top four traces (circles and squares) in 180 µM PBS (low buffer), bottom two traces (diamonds) in 50 mM PBS (high buffer), and solutions prepared with or without Cl^- added): (•)$k_{obs} = 0.68\ s^{-1}$ (TNBMe in low buffer, HOCl in water); (○)$k_{obs} = 0.91\ s^{-1}$ (TNBMe in low buffer, HOCl in water, 0.1 M Cl^-); (■)$k_{obs} = 0.68\ s^{-1}$ (TNBMe in low buffer, HOCl in low buffer); (□)$k_{obs} = 0.91\ s^{-1}$ (TNBMe in low buffer, HOCl in low buffer, 0.1 M Cl^-); (♦)$k_{obs} = 0.58\ s^{-1}$ (TNBMe in high buffer, HOCl made in water, 0.1 M Cl^-); (◊)$k_{obs} = 0.57\ s^{-1}$ (TNBMe in high buffer, HOCl made in high buffer, 0.1 M Cl^-). (Kinetic traces are offset by an absorbance of 0.01.) 90

Figure 3.13: Reaction of 50 µM TNBMe with 10 µM HOCl Data (180 µM PBS, pH = 7.4), reaction data collected within 5 min of preparation of reactants (squares, bottom) and after 2 h (circles, top), both fit to first order equation (solid line); bottom (t < 5 min) $k_{obs} = 0.68\ s^{-1}$; top (t > 2 h) $k_{obs} = 1.0\ s^{-1}$ 91

Figure 4.1: Representative ^{1}H NMR spectrum of the –S-CH_3 region of free Met derivatives obtained from the reaction of 30 mM Met with 25 mM halogenating agent in 0.2 M phosphate buffer, pH = 7.4-7.6. This spectrum was obtained from the oxidation of Met with HOCl at pH = 7.5, 20 ℃. The labeled resonances are S-CH_3 of Met (A), MetO (B), and DHM (C). Inset: expansion of chemical shift range from 2.74 to 2.86 ppm, showing the two peaks of the isomers of DHM 124

Figure 4.2: ^{1}H NMR spectra of antiflammin-1 (30 µM) in 0.1 M pD PBS (pH = 7.4): native (bottom), oxidized with 10% molar excess of H_2O_2 (middle), and oxidized with 10% molar excess I_3^- (top). Note that the triplet at 2.9 ppm is due to internal standard DSS. The labeled resonances are S-CH_3 of Met (A), MetO (B), and DHM (C) 129

Figure 4.3: (Expansion of Figure 4.2) ^{1}H NMR spectra of antiflammin-1 (30 µM) in 0.1 M pD PBS (pH = 7.4): peptide oxidized with 10% molar excess of H_2O_2 (bottom), and oxidized with 10% molar excess I_3^- (top). Note that the triplet at 2.9 ppm is due to internal standard DSS, used for normalization of chemical shifts 130

Figure 4.4: ^{1}H NMR spectra of hexapeptide Ub1-6 (40 µM) in 0.1M in PBS (pD 7.4): native peptide (bottom), oxidized with 10% molar excess of H_2O_2 (middle), and oxidized with 10% molar excess I_3^- (top). The labeled resonances are S-CH_3 of Met (A), MetO (B), and DHM (C). (Note that the triplet at 2.9 ppm is due to internal standard DSS, and that the middle spectrum, still shows the presence of unoxidized methionine, this is attributed to the slow oxidation of methionine by H_2O_2 and not allowing the sample to react long enough before collecting data.) 132

Figure 4.5: HSQC of 1 mM Ub in 0.1 M H_2PO_4 (pH = 7) 134

Figure 4.6: HSQC of Ub zoomed in on methyl region 135

Figure 4.7: HSQC overlay of Ub (black) and Ub + excess H_2O_2 (red); inset shows Met1 modification when Ub is oxidized with excess H_2O_2; Ub (black) integrates to 6 protons (assigned to A28 and M1) while Ub + excess H_2O_2 (red) integrates to 3 protons (assigned to A28) 137

Figure 4.8: HSQC overlay of Ub (black) and Ub + Chloramine-T/I^- (red); inset shows that Met1 remained unmodified; both Ub (black) and Ub + Chloramine-T/I^- (red) integrate to 6 protons (assigned to A28 and M1) 140

Figure 4.9: HSQC overlay of Ub (black) and Ub + 10 eq HOCl (red); inset shows Met1 modification when Ub is oxidized with excess HOCl; Ub (black) integrates to 6 protons (assigned to A28 and M1) while Ub + HOCl (red) integrates to 3 protons (assigned to A28) 143

Figure 4.10: Representative MS (solid) and UV (dotted) chromatograms of digested Ub. The scale of the MS chromatogram is shifted by 1.8 min to normalize the two chromatograms. The following peptides from the digested Ub have been assigned (based on observed m/z): A: Leu-Arg-Gly-Gly (73-76);
B: Thr-Leu-Thr-Gly-Lys (7-11);
C: Gln-Leu-Glu-Asp-Gly-Arg (49-54);
D: Thr-Leu-Ser-Asp-Tyr-Asn-Ile-Gln-Lys (55-63);
E: Leu-Ile-Phe-Ala-Gly-Lys (43-48);
F: Met-Gln-Ile-Phe-Val-Lys (1-6);
G: Glu-Ser-Thr-Leu-His-Leu-Val-Leu-Arg (64-72);
H: Thr-Ile-Thr-Leu-Glu-Val-Glu-Pro-Ser-Asp-Thr-Ile-Glu-Asn-Val-Lys (12-27). A-G were identified by m/z of $(M+H)^{1+}$ and H was identified as $(M+H)^{2+}$. Unidentified peaks may be due to autodigestion of trypsin. Inset: expansion of the chromatograms between 45 and 65 min 145

Figure 4.11: LC-MS-ESI$^+$ chromatogram of digested Ub. Inset: MS spectrum of native hexapeptide Ub1-6, eluted at 55 min. The theoretical monoisotopic mass is 764.4. The observed mass is 764.4 + H^+ 147

Figure 4.12: LC-MS-ESI$^+$ chromatogram of digested Ub that was oxidized with 10% molar excess of H_2O_2. Inset: MS spectrum of MetO derivative of the hexapeptide Ub1-6, eluted at 47.4 min. The theoretical monoisotopic mass is 780.4. The observed mass is 780.3 + H^+. 148

Figure 4.13: LC-MS-ESI$^+$ chromatogram of digested Ub that was oxidized with 10 molar equivalents of HOCl. Inset (left): MS of MetO derivative of the hexapeptide Ub1-6, eluted at 49.0 min. The theoretical monoisotopic mass is 780.4. The observed mass is 780.4 + H^+. Inset (right): MS of DHM derivative of the hexapeptide Ub1-6, eluted at 51.5 min. The theoretical monoisotopic mass is 762.4. The observed mass is 762.4 + H^+. 149

Figure 4.14: Comparison of MS spectra of the DHM derivative of the Ub1-6 hexapeptide top: prepared from addition of a small excess of I_3^- to Ub1-6 and directly injected into the mass spectrometer, and bottom: LC-MS of peak with retention time of 51.5 min from the tryptic digest of Ub oxidized with 10 molar equivalents of HOCl. The theoretical monoisotopic mass of DHM-Gln-Ile-Phe-Val-Lys is 762.4, observed mass is 762.4 + H^+. 151

Figure 4.15: LC-UV (205 nm) of Ub oxidized with 10 molar equivalents of HOCl and subsequently digested using trypsin (solid line). Same sample spiked with an authentic sample of the DHM derivative of Ub1-6 (prepared in 0.1 M phosphate buffer by adding a 10% molar excess of I_3^-; the product was characterized by ^{1}H NMR) in order to verify retention time 153

LIST OF ABBREVIATIONS

DCPIP	2,6-dichlorophenol indophenols sodium salt
TNB	5-thio-2-nitrobenzoic acid; thionitrobenzoate
ACS	American chemical society
Cys	cysteine
DHM	dehydromethionine
DHM-Ub	dehydromethionine derivative of ubiquitin
DNPMet	dinitrophenyl methionine
HSA	Human Serum Albumin
OCl^-	hypochlorite
HOCl	hypochlorous acid
$[X]_0$	initial concentration of X
IT	Inhibitory titration
LC	liquid chromatography
MS	mass spectrometry
Met	methionine
$MetO_2$	methionine sulfone
MetO	methionine sulfoxide
Msr	methionine sulfoxide reductase
TNBMe	methylated TNB (thioether of TNB)
MCD	monochlorodimedone
MPO	myeloperoxidase
NADPH	nicotinamide adenine dinucleotide phosphate
Ub1-6	*N*-terminal hexapeptide (NH_2-Met-Gln-Ile-Phe-Val-Lys-COOH) of ubiquitin
NMR	nuclear magnetic resonance
PO	peroxidase
PBS	phosphate buffer
k	rate constant
r	rate of reaction
ROS	reactive oxygen species
NaCl	sodium chloride
SCN^-	thiocyanate ion
Ub	ubiquitin
UV-vis	ultraviolet-visible spectroscopy

ABSTRACT

Hypochlorous acid (HOCl) is a neutrophil-derived oxidant that is used to kill invading pathogens. Since HOCl reacts indiscriminately with biological molecules, such as amino acids, excess or misplaced production of HOCl can cause host tissue damage. Methionine (Met), one of only two naturally occurring sulfur amino acids, reacts fast with HOCl making it one of the first targets. The mechanism for this reaction is not well known but is assumed to go through a chlorosulfonium intermediate to form methionine sulfoxide (MetO), and then methionine sulfone ($MetO_2$).

The first chapter of this dissertation introduces topics which will help the reader understand the significance of the research that is described herein. The second chapter presents the new method, which we called inhibitory titrations (IT). IT is an expansion of the competition method that is commonly used for measuring rate constants of fast reactions. IT tries to minimize assumptions that can create problems when indirectly measuring rate constants by: 1) making use of all the data collected (the rate constant measured using just the 50% inhibition point can underestimate the rate constant compared to that which fits all of the data); and 2) consideration of the stoichiometry of the reaction, which was important for accurately fitting data, especially when over-oxidation is possible. Our data shows that taking the stoichiometry of the reaction into consideration produces a better fit of the experimental data than assuming the reaction has a 1:1 stoichiometry. Without consideration of the rate law for the

reaction, one may derive a first order rate constant from a second order reaction, leading to a misrepresentative rate constant.

The third chapter examines thioether reactions with HOCl with the expectation that a chlorosulfonium intermediate could be characterized. In general, HOCl reacts with thioethers, at neutral pH, with a second order rate constant of 10^6-10^8 $M^{-1}s^{-1}$, consistent with those reported in literature. The reactions studied did not show definitive evidence for the formation of a chlorosulfonium ion intermediate. However, the observed product, dehydromethionine (DHM), formed in the reaction of Met with HOCl (studied in greater detail in the fourth chapter), gives insight into the identity of the intermediate. Due to the hypothesized method by which DHM is formed, from intramolecular attack followed by ring closure, a halosulfonium intermediate can account for the formation of the DHM product.

The fourth chapter describes an investigation of the reaction of free Met, peptide bound Met, and protein bound Met, by various two electron oxidants. Oxidation of Met, which has a free amine, can form either MetO or DHM, a potential biomarker of oxidative stress. Different oxidants form different percentages of DHM. Two electron oxidants that react through oxygen transfer do not produce DHM, while halogenating species (but not the pseudohypohalous acid HOSCN) that react through a halide cation (X^+, where X = I, Br, or Cl) transfer, produce a significant amount of DHM. The halogenating agents can be grouped by the yields of DHM they produce, where chlorinating agents produce around 43% DHM, brominating agents

approximately 75%, and iodinating agents close to 100% DHM. The percentage of DHM formed is related to the type of halosulfonium that is formed, whether it is a chlorosulfonium, bromosulfonium, or iodosulfonium species. Comparing analogous halosulfonium species, the stability towards hydrolysis is I > Br > Cl, reflecting the trend observed in the yields of DHM. The ease of formation along with the high kinetic stability of DHM at neutral pH, which in the absence of catalysts has a half life of over 600 days, shows the high potential for DHM as a biomarker of protein oxidation by halogenating agents.

The fifth chapter is a summary of important findings of this research along with recommended future experiments. Overall, the dissertation examines fast ($k = 10^6$-10^8 $M^{-1}s^{-1}$) reactions of HOCl and related oxidants with biologically relevant molecules.

Chapter 1: Introduction: Production of Reactive Oxygen Species by the Human Immune System

1.1 Immune system

The immune system protects the body from infection. It is comprised of two components, the innate (non-specific) immune system and the adaptive (specific) immune system. The innate response, the body's first defense, responds to pathogens generically (i.e. non-specific) (discussed in more detail below). If a pathogen evades the innate immune system, the body's second line of defense is the adaptive immune system. The adaptive immune system protects against re-exposure to the same pathogens by "remembering" what pathogens it has already been exposed to and how to combat them (1).

1.1.1 Innate immune system

The innate immune system provides defense against infection through a non-specific response to pathogens. The epithelial surface (i.e. skin) is one part of the innate immune system. It serves as the first line of defense by forming a physical barrier to prevent pathogens from entering the body. When a pathogen successfully enters the body, such as through a cut, the body's inflammatory response (inflammation) is activated. At the location of inflammation, chemicals, such as histamine, are released. These chemicals cause blood vessels to leak fluid into the infected area, causing swelling which helps in the isolation of the pathogen(s). In addition, these chemicals attract white blood cells (leukocytes).

Leukocytes, which normally are found in the blood, migrate to the inflamed tissue through a process known as chemotaxis (the directed movement of a cell along a chemical concentration gradient) (1).

Table 1.1: Properties of leukocytes

Type	Approx. % in adults	Main function
Neutrophil	54-62%	phagocytosis; destroy pathogenic bacteria
Eosinophil	1-3%	destroy parasitic worms; regulate allergic inflammatory responses
Basophil	<1%	release histamine during immune reactions to promote inflammation
Lymphocyte	25-33%	destroy virus-infected cells and tumor cells
Monocyte	3-7%	migrate from the bloodstream to other tissues in which they become macrophages (phagocytosis of cellular debris and pathogens)

1.2 Leukocytes

Leukocytes can be divided into two categories by looking for the presence of granules (defined as any structure barely visible by light microscopy). These two categories are granulocytes and agranulocytes (1-3). Granulocytes, which account for approximately 70% of all white blood cells, are characterized by the appearance of granules in their cytoplasm. Granules are membrane-bound enzymes that act primarily in the digestion of engulfed (phagocytized) foreign particles. The three types of granulocytes are neutrophils, basophils, and eosinophils. Agranulocytes, on the other hand, are

leukocytes which are characterized by what appears to be the absence of granules in their cytoplasm. Types of agranulocytes include lymphocytes and monocytes (also known as macrophages after they migrate from the bloodstream and enter tissue). Each leukocyte plays its own role in the human immune system and thus has different properties (table 1.1) (2-4).

1.2.1 Neutrophils

Neutrophils are the most abundant leukocyte in blood, accounting for 54-62% of all leukocytes (1,4-5). It is a small cell that has a diameter of approximately 9-10 µm. Neutrophils are often referred to as the first line of leukocyte defense since it is the first defensive cell type to be recruited to an infection site during the beginning stages of inflammation, usually arriving within the first hour of the onset of inflammation. A non-activated neutrophil circulates in the blood stream and once it is activated, it migrates out of the blood stream and into the infected tissue (chemotaxis). Activated neutrophils are phagocytes, whose primary function is to kill small microorganisms, such as fungi and bacteria (5).

Neutrophils have both nonoxidative and oxidative mechanisms for destroying pathogens (6). Specific granules (i.e. secondary granules), part of the nonoxidative antimicrobial mechanism, contain cytotoxic molecules, namely enzymes (e.g. lysozyme) and antimicrobial peptides (e.g. lactoferrin), which are released during a process called degranulation. These cytotoxic molecules help kill pathogens by inhibiting growth (lactoferrin aids in depriving bacteria of iron which is needed for cellular growth) and by solubilizing the bacteria’s cellular

wall thereby making it more accessible to the oxidative killing agents (5,7). The oxidative antimicrobial mechanism contains two key components, the NADPH (nicotinamide adenine dinucleotide phosphate) oxidase system and myeloperoxidase (MPO). The NADPH oxidase system (discussed in more detail below) is contained throughout the cytoplasm and plasma membrane of the neutrophil (8). MPO is found in azurophil granules. Azurophil (primary) granules play a role in killing and digesting pathogens through phagocytosis (5,9).

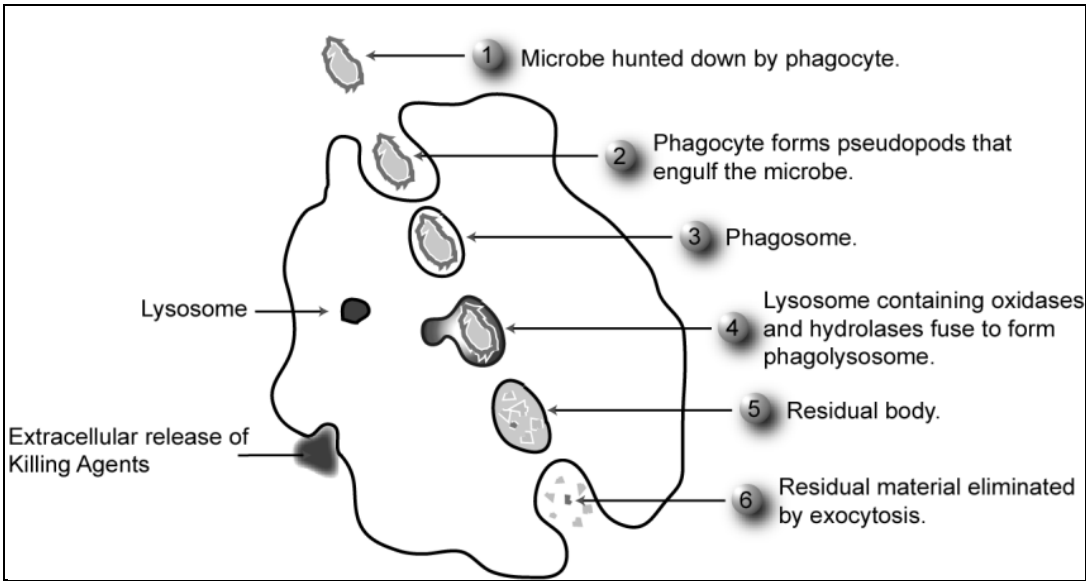


Figure 1.1: Illustration of phagocytosis

1.3 Phagocytosis

Phagocytes (e.g. neutrophils, macrophages) engulf foreign material (e.g. bacteria, viruses, and dead or damaged cells) through a process called phagocytosis (5). Phagocytosis involves several steps (figure 1.1), which includes the white blood cell (WBC) identifying and tracking down the foreign

material (through receptors on the surface which detect foreign material), engulfing it, digesting it, and eliminating the waste. A single WBC is capable of engulfing many microbes, with each of these phagocytic events resulting in the formation of a phagosome.

1.4 Respiratory burst

Prior to the phagocytosis of the particle, the phagocyte (e.g. neutrophils) begins to consume oxygen in a process called the respiratory burst (oxidative burst). During the respiratory burst, oxygen is consumed to form reduced oxygen which will be used to kill the microorganism(s). The respiratory burst involves the activation of the enzyme NADPH oxidase, which catalyzes the one electron reduction of oxygen (O_2), using NADPH as an electron donor, forming large quantities of superoxide (O_2^-) (figure 1.2). Superoxide, a reactive oxygen species (ROS), serves as the starting point in a cascade of reactive species that are derived from O_2^-. The superoxide can disproportionate to give hydrogen peroxide (H_2O_2) and oxygen (a reaction that is catalyzed by superoxide dismutase, SOD). H_2O_2 is a powerful oxidizer but kinetically stable. H_2O_2 can be converted into more reactive ROS such as hydroxyl radical (•OH) (10). In addition, H_2O_2 serves as a substrate for the peroxidase enzymes [e.g. MPO] (5-6,8-9,11-12).

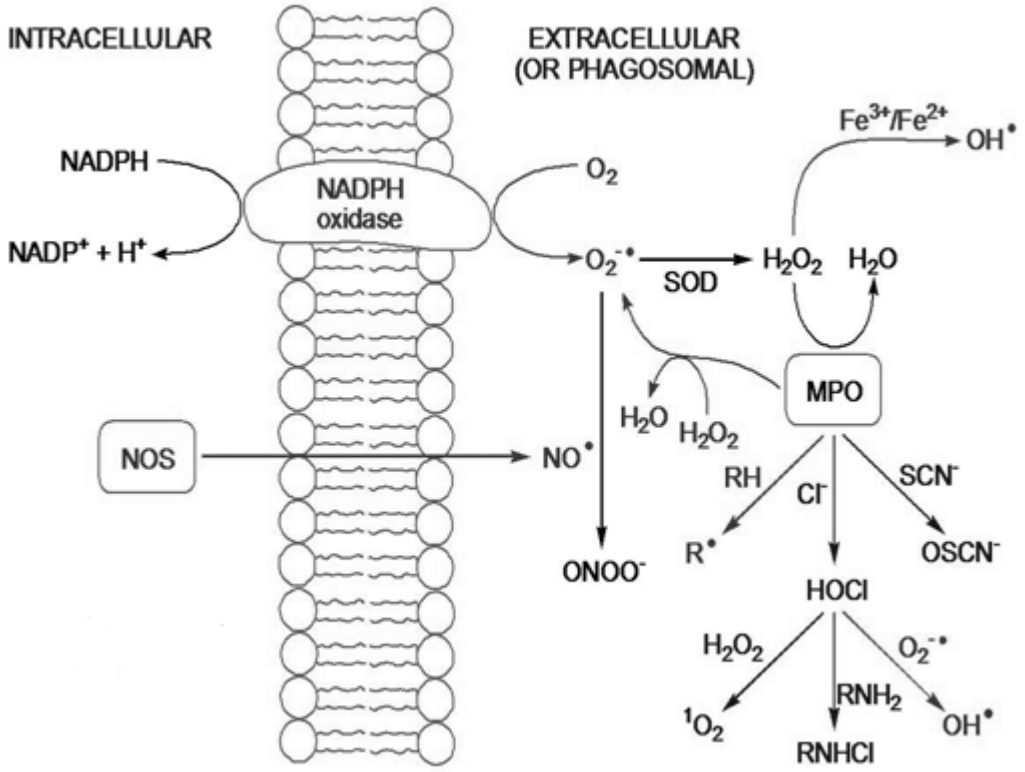


Figure 1.2: Production of ROS during neutrophillic oxidative bursts

1.5 Peroxidases and the production of ROS

Mammalian peroxidases (PO) are enzymes that catalyze the oxidation of halides (or pseudo halide SCN^-) by H_2O_2 (1.1).

$$X^- + H_2O_2 \xrightarrow{\text{Enzyme}} OX^- + H_2O \quad (X=Cl, Br, I, \text{ or } SCN) \qquad (1.1)$$

Eosinophil peroxidase (found in eosinophils), lactoperoxidase (found in breast milk, lung, and other mucosa), thyroid peroxidase (found in the thyroid), and MPO (found in neutrophils and macrophages) are examples of mammalian PO. The ability of a PO to catalyze the oxidation of halides depends on two factors, the bioavailability of the halide and the redox potential of the peroxidase (13). MPO is unique amongst other mammalian PO in that it is the only naturally

occurring enzyme capable of catalyzing (under physiological conditions) the oxidation of chloride by H_2O_2 to form hypochlorous acid (HOCl) (13-14). Chloride is accepted to be the major substrate for MPO due to the presence of high concentrations in the blood which ranges from 100-140 mM (iodide < 1 µM; bromide = 20-100 µM; thiocyanate = 20-120 µM) (14). HOCl is believed to play an important role in inflammation and has been linked to many inflammatory diseases such as atherosclerosis, arthritis, asthma, emphysema, cystic fibrosis, and periodontitis (15-18). HOCl is several orders of magnitude more cytotoxic than H_2O_2 and it is non-specific (it reacts with a large variety of functional groups). When left unchecked, HOCl can destroy host tissue as well as its pathogenic target (14,16-18).

1.5.1 Reactive oxygen species

Reactive oxygen species (ROS) that are produced by phagocytes are implicated in host tissue damage that occurs during both acute and chronic inflammation (19). A cascade of ROS begins with the production of superoxide ($O_2^{\cdot-}$) by NADPH oxidase, which is normally dormant in phagocytes but is activated during an oxidative burst (respiratory burst) (11,20). NADPH oxidase, a membrane bound enzyme complex found in the membrane of a phagosome, generates superoxide by transferring electrons from NADPH inside the cell across the membrane and coupling these to molecular oxygen to produce the superoxide (1.2) (20).

$$NADPH + 2O_2 \rightleftharpoons NADP^+ + 2O_2^- + H^+ \qquad (1.2)$$

A majority of the superoxide disproportionates to yield H_2O_2 and molecular oxygen in a reaction that is efficiently catalyzed by superoxide dismutase (SOD) (1.3) (21-22).

$$2O_2^{-}\bullet + 2H_2O \rightarrow O_2 + H_2O_2 + 2OH^{-} \qquad (1.3)$$

H_2O_2, though being kinetically inert, is a powerful oxidant (13) which phagocytes use, with the assistance of peroxidases (23), to produce more effective killing agents (24).

ROS oxidize both proteins and lipid components of low-density lipoprotein (LDL). Superoxide is relatively nonreactive with respect to protein components, but instead is highly reactive towards lipids (25). In contrast, the hypohalous acids [e.g. HOCl and hypobromous acid (HOBr)] are more reactive towards proteins and less reactive towards lipids (13,26-27). The pseudo-hypohalite, hypothiocyanite ($OSCN^-$), in contrast to these other ROS mentioned, is a mild oxidant that appears to react selectively with sulfhydryl groups, such as cysteine and its derivatives (13,28).

1.6 Antioxidants

Despite the apparent correlation between oxidative stress and inflammatory diseases, antioxidant strategies, both dietary (29) and pharmaceutical (18), have exhibited poor performance in limiting atherosclerosis in humans (30). Most antioxidants that have been investigated in great detail, for example vitamin E, have been chosen because it inhibits the oxidation of LDL by one electron oxidants *in vitro*. One electron oxidants are

typically radical species. There is also evidence that two electron oxidants, such as the ROS HOCl and reactive nitrogen species (RNS) peroxynitrite, play a significant role in LDL damage (31). Since there are a variety of different oxidants, including ROS, RNS, and reactive sulfur species (RSS), which play a role in oxidation of LDL, possibly contributing to atherosclerosis, there is considerable interest in determining the role that endogenous antioxidants (scavengers) play in moderating these oxidants (13,32). For HOCl and HOBr, the most effective scavengers are organosulfur compounds, in particular, methionine (Met) (33) and cysteine (Cys) (18,34) derivatives. These derivatives include glutathione (GSH), a small tripeptide which exhibits millimolar concentration in human cells (35), as well as the macromolecule human serum albumin (HSA), a protein bearing a single Cys group on its surface and six Met groups, which in blood plasma has a concentration around 600 μM (13).

1.7 Summary of chapters

This dissertation is comprised of several projects that have been progressively built off one another. Though the chapters follow a general theme, they are written to be independent of each other and as such each chapter contains its own introduction of relevant concepts, experimental design, interpretation, and conclusions.

Chapter one has been a general introduction to some of the basic concepts that will aid the reader in understanding the research presented later and its importance. The goal of this chapter was to help the reader understand

where the oxidants studied in these research projects are derived from and the importance of their study.

Chapter two presents the development of a method we call inhibitory titration, which we have used to measure the rate constants of fast reactions in solution. Ideally, rate constants should be measured under conditions of interest; however, this is not always practical. Historically, measuring rate constants of fast reactions has been problematic. Difficulties include the fact that the time required to get complete mixing of the reactants is often longer than the reaction time, so turbulent (i.e. complete) mixing does not occur. In addition, the instrumentation needed to monitor fast reactions is not always available (e.g. it is not possible to monitor a reaction with a half-life of μs when instrumental time resolution is on the order of ms). Techniques used in the past for fast reactions in solution include the competition reaction method and pH extrapolation. The competition reaction method uses the rate constant of a known reaction to obtain the rate constant for other reactions if competition conditions can be arranged. By measuring the proportions of competition reactants and/or products that remain after reaction, the rate constant can be found for the reaction of interest. For reactions which are pH dependent, changing the pH may slow down the reaction enough to use concentrations in which the rates are measurable, and then the rate constant at the pH of interest can be computed by extrapolation. Anytime the rate constant is measured under conditions other than that of interest, whether it is through competition reactions, pH extrapolation, etc., experimental assumptions are needed which

may cause inaccuracy in the computed rate constant (*e.g.* when using pH extrapolation to compute the rate constant, one assumes that the rate law at the pH of interest is the same as it is at the pH of the measurement). Using the reaction of thiocyanate with HOCl, for example, the rates that were extrapolated from measurements under alkaline conditions (pH extrapolation) (36) and those from competition reactions (18,37) were not self-consistent, pointing to a potential problem with one or both of these techniques. The inhibitory titration method that is described herein offers insight into these inconsistencies.

Chapter three examines the oxidation of four thioethers [methionine (Met), methionine sulfoxide (MetO), dinitrophenyl-methionine (DNPMet), and TNBMe (thioether derivative of 5-thio-2-nitrobenzoic acid, TNB)]. Oxidation of thioethers by HOCl is believed to occur through a Cl^+ transfer from the O of HOCl to the sulfur of the thioether, forming a chlorosulfonium ion intermediate (CH_3-S^+(Cl)-R). Though there is no direct evidence for the formation of the chlorosulfonium intermediate, it is still widely accepted that oxidation of thioethers first forms the chlorosulfonium intermediate which subsequently hydrolyzes to form the observed sulfoxide. Studying the reaction of these four thioethers with HOCl was done to help understand the mechanism by which thioethers are oxidized.

Chapter four examines the oxidation of Met by two-electron oxidants, forming varying amounts of dehydromethionine (DHM) and MetO. In 1945, Lavine (38) identified a Met derivative which he called DHM. He found that oxidation of Met with iodine causes Met to form a cyclic (a sulfur-nitrogen bond)

derivative that differs from Met (in mass) by a loss of two hydrogens. Due to the ease of production and stability at neutral pH, Lavine suggested that DHM has biological importance (38). Young *et al.* (39) later proposed a mechanism by which iodine (I_2) oxidizes Met through a I^+ transfer that ring closes forming DHM. Since I_2 has limited biological relevance (40), we wanted to investigate whether other halogenating agents such as HOCl and HOBr, two biologically relevant oxidants, oxidize Met through an analogous mechanism (since HOCl has been proposed to occur through a Cl^+ transfer (36)) to form DHM. In addition, we studied the formation of DHM in peptides and proteins (containing an *N*-terminus Met), in hopes of finding a potential biomarker for hypohalous acids. If DHM is formed only by certain oxidants, or particular groups of oxidants, identifying DHM would help in understanding which oxidant(s) caused damage in hopes of developing preventative measures against destructive oxidants.

Chapter five is a summary of the important findings of the dissertation including suggested future experiments. This chapter helps connect the dissertation together in a broad view and bring focus to the importance of the work.

1.8 References

(1) Kaufmann, S. H. E.; Rouse, B.; Sacks, D. *The immune response to infection*; Amer Soc Microbiology, 1752 N Street Nw, Washington, Dc 20036-2904 USA, 2011.

(2) Desai, A.; Grolleau-Julius, A.; Yung, R. "Leukocyte function in the aging immune system." *Journal of Leukocyte Biology* **2010**, *87*, 1001-1009.

(3) Alberts, B.; Bray, D.; Lewis, J.; Raff, M.; Roberts, K.; Watson, J. D. *Molecular biology of the cell*, 1986.

(4) Normal adult laboratory values. Chicago, IL: National Board of Osteopathic Medical Examiners, Inc.; 2010 [updated 2010; cited 2011 July]; Available from: http://www.nbome.org/comvexcbt/html/LabValues.htm.

(5) Miyasaki, K. Phagocytes-neutrophils.[cited March 2009]; Available from: http://www.dent.ucla.edu/pic/members/neutrophils/neutrophils.html

(6) Miyasaki, K. T.; Wilson, M. E.; Brunetti, A. J.; Genco, R. J. "Oxidative and nonoxidative killing of actinobacillus-actinomycetemcomitans by human-neutrophils." *Infection and Immunity* **1986**, *53*, 154-160.

(7) Maallem, H.; Sheppard, K.; Fletcher, J. "The discharge of primary and secondary granules during immune phagocytosis by normal and chronic granulocytic-leukemia polymorphonuclear neutrophils." *British Journal of Haematology* **1982**, *51*, 201-208.

(8) Van Heerebeek, L.; Meischl, C.; Stooker, W.; Meijer, C.; Niessen, H. W. M.; Roos, D. "Nadph oxidase(s): New source(s) of reactive oxygen species in the vascular system?" *Journal of Clinical Pathology* **2002**, *55*, 561-568.

(9) Segal, A. W. "How neutrophils kill microbes." *Annual Review of Immunology* **2005**, *23*, 197-223.

(10) Forman, H. J. *Hydrogen peroxide: The good, the bad, and the ugly*; Springer, Po Box 17, 3300 Aa Dordrecht, Netherlands, 2008.

(11) Rossi, F. "The o-2(-)-forming nadph oxidase of the phagocytes - nature, mechanisms of activation and function." *Biochimica Et Biophysica Acta* **1986**, *853*, 65-89.

(12) John, R. "Reactive oxygen species in phagocytic leukocytes." *Histochemistry and Cell Biology* **2008**, *130*, 281-297.

(13) Nagy, P.; Beal, J. L.; Ashby, M. T. "Thiocyanate is an efficient endogenous scavenger of the phagocytic killing agent hypobromous acid." *Chemical Research in Toxicology* **2006**, *19*, 587-593.

(14) Vandalen, C. J.; Whitehouse, M. W.; Winterbourn, C. C.; Kettle, A. J. "Thiocyanate and chloride as competing substrates for myeloperoxidase." *Biochemical Journal* **1997**, *327*, 487-492.

(15) Fialkow, L.; Wang, Y.; Downey, G. P. "Reactive oxygen and nitrogen species as signaling molecules regulating neutrophil function." *Free Radical Biology and Medicine* **2007**, *42*, 153-164.

(16) Beal Jennifer, L.; Foster Steven, B.; Ashby Michael, T. "Hypochlorous acid reacts with the n-terminal methionines of proteins to give dehydromethionine, a potential biomarker for neutrophil-induced oxidative stress." *Biochemistry* **2009**, *48*, 11142-8.

(17) Ashby Michael, T.; Carlson Amy, C.; Scott, M. J. "Redox buffering of hypochlorous acid by thiocyanate in physiologic fluids." *Journal of the American Chemical Society* **2004**, *126*, 15976-7.

(18) Pattison, D. I.; Davies, M. J. "Absolute rate constants for the reaction of hypochlorous acid with protein side chains and peptide bonds." *Chemical Research in Toxicology* **2001**, *14*, 1453-1464.

(19) Kehrer, J. P. "Free-radicals as mediators of tissue injury and disease." *Critical Reviews in Toxicology* **1993**, *23*, 21-48.

(20) Pourova, J.; Kottova, M.; Voprsalova, M.; Pour, M. "Reactive oxygen and nitrogen species in normal physiological processes." *Acta Physiologica* **2010**, *198*, 15-35.

(21) Xia, Y.; Zweier, J. L. "Superoxide and peroxynitrite generation from inducible nitric oxide synthase in macrophages." *Proceedings of the National Academy of Sciences of the United States of America* **1997**, *94*, 6954-6958.

(22) Desideri, A.; Falconi, M. "Prokaryotic Cu,Zn superoxidies dismutases." *Biochemical Society Transactions* **2003**, *31*, 1322-1325.

(23) O'brien, P. J. "Peroxidases." *Chemico-Biological Interactions* **2000**, *129*, 113-139.

(24) Henderson, J. P.; Heinecke, J. W. In *Natural production of organohalogen compounds*; Springer-Verlag Berlin: Berlin, 2003; Vol. 3, p 201-214.

(25) Girotti, A. W. "Mechanisms of lipid peroxidation." *J Free Radic Biol Med* **1985**, *1*, 87-95.

(26) Pattison, D. I.; Davies, M. J. "Kinetic analysis of the reactions of hypobromous acid with protein components: Implications for cellular damage and use of 3-bromotyrosine as a marker of oxidative stress." *Biochemistry* **2004**, *43*, 4799-4809.

(27) Pattison, D. I.; Hawkins, C. L.; Davies, M. J. "Hypochlorous acid-mediated oxidation of lipid components and antioxidants present in low-density lipoproteins: Absolute rate constants, product analysis, and computational modeling." *Chemical Research in Toxicology* **2003**, *16*, 439-449.

(28) Ashby, M. T.; Aneetha, H. "Reactive sulfur species: Aqueous chemistry of sulfenyl thiocyanates." *Journal of the American Chemical Society* **2004**, *126*, 10216-10217.

(29) Aviram, M. "Review of human studies on oxidative damage and antioxidant protection related to cardiovascular diseases." *Free Radical Research* **2000**, *33*, S85-S97.

(30) Nagy, P.; Ashby, M. T. "Reactive sulfur species: Kinetics and mechanism of the oxidation of cystine by hypochlorous acid to give n,n'-dichlorocystine." *Chemical Research in Toxicology* **2005**, *18*, 919-923.

(31) Stocker, R.; Keaney, J. F. "Role of oxidative modifications in atherosclerosis." *Physiological Reviews* **2004**, *84*, 1381-1478.

(32) Buettner, G. R. "The pecking order of free radicals and antioxidants: Lipid peroxidation, alpha-tocopherol, and ascorbate." *Archives of Biochemistry and Biophysics* **1993**, *300*, 535-543.

(33) Davies, M. J. "The oxidative environment and protein damage." *Biochimica Et Biophysica Acta-Proteins and Proteomics* **2005**, *1703*, 93-109.

(34) Hawkins, C. L.; Pattison, D. I.; Davies, M. J. "Hypochlorite-induced oxidation of amino acids, peptides and proteins." *Amino Acids* **2003**, *25*, 259-274.

(35) Srivasta.Sk; Beutler, E. "Transport of oxidized glutathione from erythrocytes of various species in presence of chromate." *Biochemical Journal* **1969**, *114*, 833-&.

(36) Armesto, X. L.; Canle L, M.; Fernandez, M. I.; Garcia, M. V.; Santaballa, J. A. "First steps in the oxidation of sulfur-containing amino acids by hypohalogenation: Very fast generation of intermediate sulfenyl halides and halosulfonium cations." *Tetrahedron* **2000**, *56*, 1103-1109.

(37) Winterbourn, C. C. "Comparative reactivities of various biological compounds with myeloperoxidase-hydrogen peroxide-chloride, and similarity of the oxidant to hypochlorite." *Biochimica et Biophysica Acta* **1985**, *840*, 204-10.

(38) Lavine, T. F. "Dehydromethionine, a new methionine derivative." *Federation Proceedings* **1945**, *4*, 96-96.

(39) Young, P. R.; Hsieh, L. S. "General base catalysis and evidence for a sulfurane intermediate in iodine oxidation of methionine." *Journal of the American Chemical Society* **1978**, *100*, 7121-7122.

(40) Smyth, P. P. A. "Role of iodine in antioxidant defence in thyroid and breast disease." *Biofactors* **2003**, *19*, 121-130.

Chapter 2: Inhibitory Titrations: Development of a Method for Measuring Rate Constants of Fast Reactions

2.1 Introduction

2.1.1 Rate law

Studying the kinetics of a chemical reaction aids in understanding the mechanism by which a reaction occurs. Investigation of the kinetics includes examining how different experimental conditions affect the rate of a chemical reaction, thereby helping to understand the intimate chemical mechanism though development of a rate law. The rate law describes the disappearance of reactants and/or the appearance of products as a function of experimental parameters (e.g., pH, temperature, physical state of the reactants, concentrations, ionic strength) that influence the rate. For a generic chemical reaction $aA + bB \rightarrow yY + zZ$, the rate is mathematically expressed by (2.1), where r is the rate, k is the rate constant, and m and n are the reaction orders (determined experimentally and dependent on the reaction mechanism).

$$r = \frac{1}{a} \times \left(-\frac{d[A]}{dt} \right) = \frac{1}{b} \times \left(-\frac{d[B]}{dt} \right) = \frac{1}{y} \times \left(\frac{d[Y]}{dt} \right) = \frac{1}{z} \times \left(\frac{d[Z}{dt} \right) = k[A]^m[B]^n \qquad (2.1)$$

Elementary reactions can be unimolecular (e.g. $A \rightarrow C$) or bimolecular (e.g., homogenous $A + A \rightarrow C$ or heterogeneous $A + B \rightarrow C$); higher orders are improbable. This chapter describes the development of a method to measure rate constants for fast bimolecular reactions. Bimolecular reactions involve the homogenous or heterogeneous reaction of two components, with their rate laws expressed in (2.2) and (2.3), respectively.

$$-\frac{d[A]}{dt} = 2 \times k[A]^2 \quad (2.2)$$

$$-\frac{d[A]}{dt} = -\frac{d[B]}{dt} = k[A][B] \quad (2.3)$$

For equations (2.2) and (2.3), k is the second-order rate constant with units of inverse concentration inverse time (usually $M^{-1}s^{-1}$). The rate of a homogenous second-order reaction can only be measured if the reactant, A, can be produced faster than it reacts with itself. This chapter discusses near diffusion controlled ($k = 10^9$-10^{10} $M^{-1}s^{-1}$) irreversible heterogeneous reactions. To accurately measure the rate, the solution (of A and B) must be homogenous (i.e. completely mixed). Heterogeneous second-order reactions can be measured under second-order conditions ([A] and [B] are of comparable value) or pseudo first-order conditions ([A] >> [B] or [A] << [B]). Pseudo first-order conditions are unique to heterogeneous systems, and not available for homogenous systems. While it is necessary to know the initial concentration of A ($[A]_0$) for homogenous systems and heterogeneous systems when $[A]_0 = [B]_0$, it is not necessary to know $[A]_0$ under pseudo first-order conditions when $[A]_0 << [B]_0$ (or $[B]_0$ when $[A]_0 >> [B]_0$), although it is necessary to know the concentration of the reagent in excess. To follow a reaction under pseudo first-order conditions, there needs to be enough reaction remaining after mixing to measure a change in concentration (directly or indirectly, e.g., though change in absorbance).

2.1.2 Fast reaction detection techniques

Though the term “fast reaction” is subjective, for the following discussion a fast reaction is one for which the half-life is less than one second. A problem occurs when measuring rates of fast reactions when the time it takes to mix the reactants is comparable or less than the half-life of the reactants ($t_{1/2}$, the time it takes for half of the reactant(s) to be depleted), so that the initial half of the reaction cannot be measured accurately. Another potential problem is the time resolution of the method that is used to monitor the reaction. For reactants that are consumed in a matter of seconds, a technique which can only take data on the order of minutes is not appropriate. The faster the reaction, the faster the data collection capabilities of the instrument used needs to be in order to follow the reaction. Different time domains can be accessed using the available fast kinetic techniques (figure 2.1). Figure 2.1 compares some of the kinetic methods used for fast reactions, comparing the first order rate constants ($k = \frac{\ln 2}{t_{1/2}}$). Choice of which kinetic method to use depends on the type of reaction as well as expected time frame of the reaction.

Depending on the type of reaction under investigation and the rate constant anticipated, it can be useful to compare techniques. Unfortunately, a majority of the techniques are for specific applications. For example, if there is no fluorescent compound in the reaction being studied, then fluorescent decay is not applicable (1).

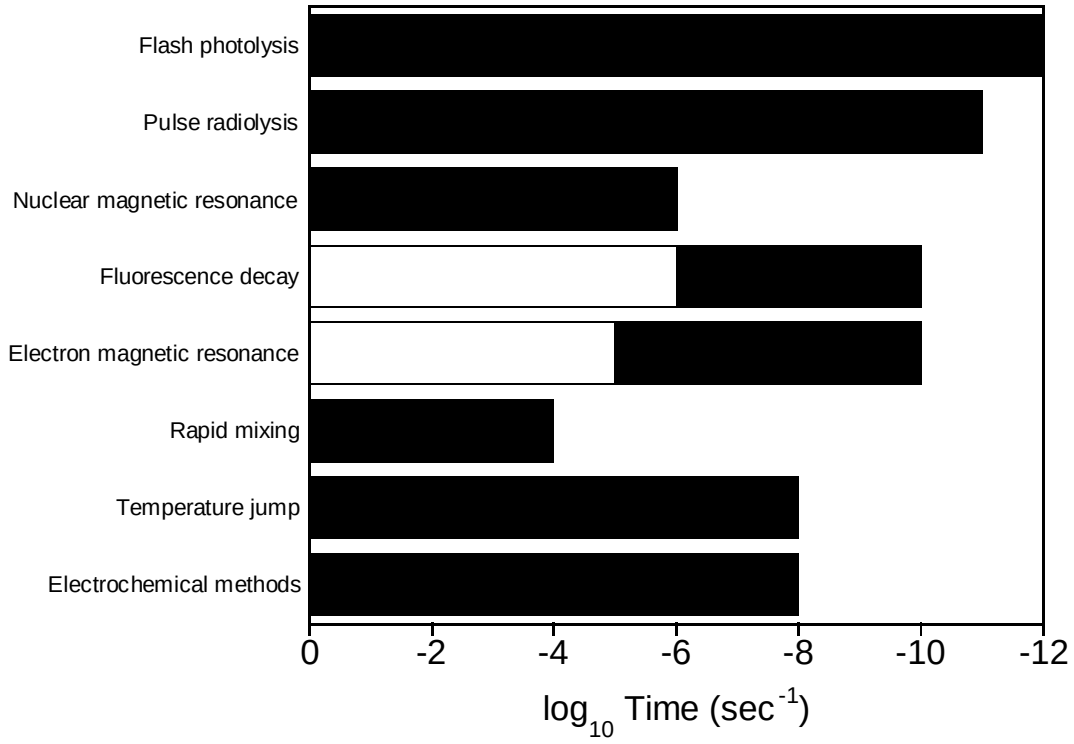


Figure 2.1: Time ranges of various kinetic methods. Time axis given in units of log of the first order rate constant (s^{-1}) (1).

Flow techniques (referred to in figure 2.1 as rapid mixing) are the most commonly used method for measuring fast reactions and involve rapidly delivering two or more solutions (or gases) into a mixing vessel. Stopped-flow is a commonly used method that involves using syringes to rapidly mix two (or more) reactants, the flow is abruptly stopped (time = zero), and some physical property is measured (e.g., absorbance through spectroscopic instrumentation). Since stopped-flow methods are limited by the time it takes to homogenously mix the solutions (about one millisecond), they are applicable for reactions with half-lives on the order of milliseconds or greater (figure 2.1) (1).

Relaxation methods are applicable to reactions that come to equilibrium. For reactions which do not reach equilibrium, e.g., oxidation/reductions reactions, relaxation methods are not appropriate. Relaxation methods work when the reaction equilibrium is disturbed by some external parameter. After the disturbance to the equilibrium, there is a time period before the system returns to equilibrium, a parameter which is measured. An example of a relaxation method is temperature jump (T-jump) in which a sudden change in the temperature causes the reaction to reach a new equilibrium; data are collected as the reaction reaches a new equilibrium (the rate at which the reaction reaches the new equilibrium will dictate which kind of instrument can be used to measure the reaction by this method). Half-lives accessible for relaxation methods are about 10^{-9} s to over 1 s (figure 2.1) (1).

Flash methods use an intense flash of light to photochemically initiate a reaction, which is subsequently measured. An example of a flash method is when the absorption of light electronically excites a molecule forming a free radical which subsequently reacts with other molecules in solution. Reactions that have half-lives as small as 10^{-5} s can be observed by this method (figure 2.1). Pulse radiolysis is a method similar to flash photolysis. In pulse radiolysis, however, instead of a light flash, a pulse of high energy radiation is used to initiate the reaction (1).

Fluorescence methods are applicable to reactions which contain a molecule which is capable of fluorescing. Fluorescence quenching is a common form of this method and involves studying the rate of reaction of a

photochemically excited molecule with another substance, which reduces the intensity of the fluorescence, called the quenching molecule. Typically, a molecule that is capable of fluorescing is excited by a light pulse lasting less than 10^{-9} s, and the observed intensity of the emitted light is measured. When a quenching molecule is added, this competes with the deactivation of the fluorescent molecule by other mechanisms that occur even in the absence of quencher, such as loss of energy to a solvent. The half-quenching times (i.e. the half-life of the reaction between the fluorescent molecule and the quenching molecule) are on the order of 10^{-8} s (figure 2.1), allowing for diffusion controlled reactions to be studied by this method, assuming one of the reagents are capable of fluorescence (1).

Electrochemical methods require that one of the species involved in the reaction of interest be redox active so that the reaction can be coupled to an electrode reaction. This method measures current, which is typically controlled by the rate of diffusion of a redox active species to the electrode, but is also controlled by the rate at which that species is produced by a chemical reaction in solution. Polarography is an example of this method, which measures the current that flows in solution as a function of an applied voltage. Since the current depends on the diffusion of the electrochemical species through solution towards the electrode, the diffusion controlled rate of reaction in which reactants meet by diffusion to react with each other cannot be greater than the diffusion rate constant ($k = 10^{9}$-10^{10} $M^{-1}s^{-1}$) (figure 2.1) (1).

Electron-spin resonance (ESR), also known as or paramagnetic resonance (EPR), is a process observed with free radicals possessing an unpaired electron. In a strong magnetic field the electron aligns with this field, either parallel or anti-parallel to the field, both of which differ in energy. If a second magnetic field is applied, the electrons can be made to pass from one orientation to the other, leading to a peak in the power absorbed. The position, structure, and width of the line observed depend on the lifetime of the radical; if a reaction occurs which destroys the free radical, thereby changing the lifetime, the spectrum is altered. From the observed spectral changes, the rate of the reaction can be determined. Rate constants up to about 10^{10} s^{-1} have been determined (figure 2.1, electron magnetic resonance) (1).

Nuclear magnetic resonance (NMR) may be exhibited by any compound whose molecule contains a nucleus with a spin. The most common nuclei include protons (^{1}H and ^{2}H), the common isotopes of nitrogen (^{14}N) and fluorine (^{19}F), and also less common isotopes of carbon (^{13}C) and oxygen (^{17}O). NMR is analogous to ESR described previously; the spinning nucleus has a magnetic moment and a spin orientation associated with it. By applying and modifying a second magnetic field the structure of the absorption spectrum and width are modified, both of which depend on the lifetime of the nucleus. When the environment of the nucleus is altered, such as when the compound undergoes a reaction, the spectrum changes. Half-lives accessible are as fast as 10^{-7} s (figure 2.1) (1).

2.1.3 Methods used to change $t_{1/2}$ of a second-order reaction

Ideally, having the capabilities to measure the rate of a reaction under the conditions of interest is ideal but unfortunately desirable conditions may not be practical for analysis. Instrumentation to measure fast reactions in solution is not commonly found in a majority of laboratories, however, changing experimental conditions in order to modify the rate constant can be done. Common experimental conditions chosen to vary, which affect the rate, include concentration of the reactants, pH, and temperature. Each method chosen has its own limitations.

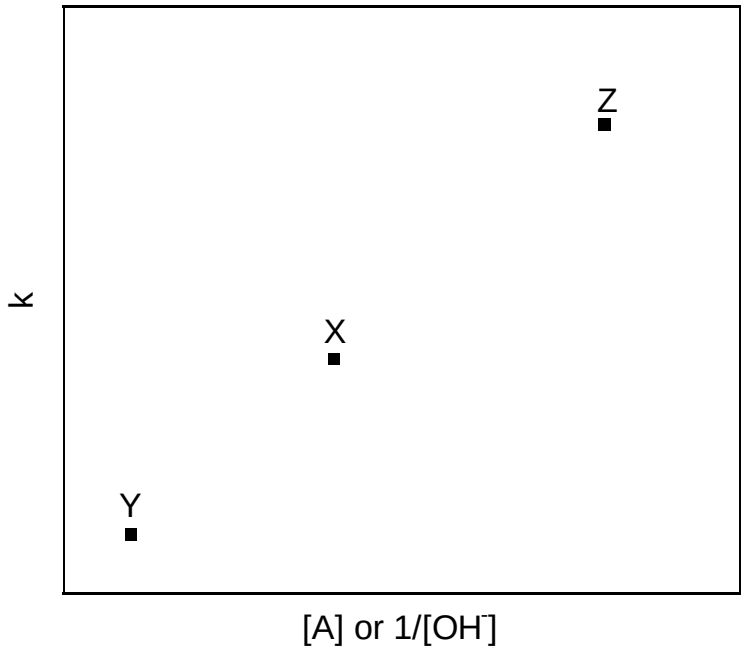


Figure 2.2: A plot of [A] or pH vs. k. X, Y, and Z points for a generic reaction used to point to particular conditions.

Varying the concentration of the reactant(s) is the most common method used to change the rate constant. Take the generic example given in Figure 2.2. In this example, the [A] of interest is at point Y, and gives a certain k. Unfortunately, it is not possible to observe the reaction under these conditions because [A] is too small to give a change in absorbance which is large enough to measure by commonly used instrumentation. By increasing the [A], the rate constant also increases, say to point marked with an X. Under these conditions suppose the change in absorbance is large enough to observe a change in reaction and the rate constant is not too large to measure, making these the conditions chosen for analysis. If the [A] is increased to point Z, the rate constant also increases. By increasing the [A], there will be a larger change in concentration over the course of the reaction, however, the larger the rate constant, the more difficult it may be to find an instrument capable of collecting the data. Though we were interested in conditions marked by point Y, for practical reasons we had to measure the reaction under conditions at point X. This is often the situation faced; the conditions under which a reaction is wanted to be studied is not practical, and therefore other conditions must be chosen. Anytime conditions other than those of interest are studied, there is possible error when extrapolating the data.

For reactions that are pH dependent, changing the pH may slow down the reaction enough to use conditions in which the rates are measurable. Using extrapolation techniques, it may be possible to estimate the rate constant at the pH of interest. Typically, for first-order pH-dependent reactions, every pH unit

will change the rate of reaction by an order of magnitude. Using the following generic reaction:

$$HA \rightleftharpoons H^+ + A^- \qquad pK_a=X$$

and

$$B + HA \rightarrow C$$

In this reaction, B reacts with HA, but depending on the pH, there is equilibrium between HA and A^-. When the pH > X, there is more A^- (nonreactive form) and therefore less HA is present, which slows down the reaction. Say, for example, we want to measure the reaction of B + HA under conditions at point Z (figure 2.2), however, the rate of the reaction is too fast. Fortunately, the reaction is not too fast to measure around point Y. By measuring the rate (and calculating the rate constant) under conditions around point Y and plotting $1/[OH^-]$ vs. k, using extrapolation we can estimate what the rate constant will be at point Z. Extrapolation, while it has been shown to be a good estimator, can be problematic. This method often requires extrapolation of the effects of $[H^+]$ by many orders of magnitude in order to estimate the rates at conditions of interest. Also, this method is not practical for measuring all reaction rates if one or more of the reactants are unstable under conditions which are suitable for measuring the rate. Finally, when one or more reactants have multiple pKa's, changing the pH can complicate the interpretation and extrapolation.

Another method of changing the rate is by varying the temperature at which the reaction is measured at. Generally, by decreasing the temperature of the reaction, the rate of the reaction decreases. Temperature also has its own

limitations, especially for aqueous solutions in which the minimum temperature must be above the freezing point. Also, many instruments are not capable of low temperature control. Temperature tends to not have as large of an effect on the rate when compared to changing the concentration and/or pH, but is another method which can be used to slow down the rate if needed. As when changing concentration and pH, by changing the temperature to modify the rate to conditions which are observable, those conditions may not be the conditions of interest.

2.1.4 Competition reactions

When the rate constant is known for a reaction, it can be used to obtain the rate constant for other reactions if competition conditions can be arranged. Take the following generic reactions:

$$A + X \xrightarrow{k_A} P_a$$

and

$$B + X \xrightarrow{k_B} P_b$$

If k_A is known, then by employing conditions in which B is competitive for X, k_B can be calculated (by measuring the proportions of A, B, P_a, and/or P_b). Historically, competition reactions have not been used for fast reactions, although there is no reason why they cannot, as long as conditions are chosen in which complete mixing can be achieved. Competition reactions can possibly have the same issue as others mentioned previously in that conditions in which competition is successful might not be conditions of interest. Referring again to

figure 2.2, point Y is the conditions of interest for our inhibitor (C), however, we need to run the competition reactions under conditions of point Z in order to achieve competitive conditions, again facing the potential problem of running the experiment under conditions other than what is desired (1).

Winterbourn has used competition reactions to measure the relative rates of reactions of small biological molecules, such as amino acids, with HOCl at physiological pH (2). By determining the concentration of the competitive biological molecule that inhibits the reaction of HOCl with monochlorodimedone (MCD) (chosen as the competing substance) by 50%, a point at which the rates of the reaction of HOCl with MCD and the inhibitor are presumably equal, Winterbourn was able to measure the relative rates of reactions of biological molecules with HOCl (2). Using data collected by Winterbourn (2) along with the rate of reaction of HOCl with MCD, Pattison and Davies tried to derive the rate constants of the reactions of HOCl with biological molecules (3). However, the rates that were extrapolated from measurements made under alkaline conditions (4) and those that were derived from the MCD data (2-3) were not self-consistent, pointing to a potential problem with one or both of these techniques.

2.1.5 Development of the inhibitory titration method

It is desirable to develop a method to measure the rate of the reaction under conditions of interest which utilizes commonly found instrumentation

(such as UV-vis or stopped-flow instrumentation), as this would allow research groups to investigate reactions which had previously been out of reach.

Our approach is an extension of the commonly used method of competition reactions, with an overall aim to develop a method of measuring rates of fast reactions that can be applied to any type of reaction, though our particular interest is in biologically relevant reactions. For competition reactions used by Winterbourn, for example, the concentration of competitor that is required to inhibit the reaction of MCD by HOCl by 50% is used to calculate the rates of reaction of HOCl with competitor. Competition reactions typically use just this 50% inhibition point, while the rest of the data set remains unused. Our method, which is named inhibitory titration (IT), goes one step further and uses the whole data set (not just the 50% inhibition point) to fit the data and obtain the rate constant. We believe that all of the data is important in accurately calculating the rate constant. This is especially important when conditions the reaction is being studied under are different from those desired.

Though our overall goal was to develop a generic method for measuring fast reactions, we wanted to investigate a reaction we were interested in to validate the IT method. Thus, we used the reaction of SCN^- with HOCl. The developed method was subsequently used to investigate a new reaction, HSA with HOCl. These particular reactions are of interest since members of the Ashby research group have demonstrated that HOCl reacts rapidly with thiocyanate (SCN^-) to give the RSS hypothiocyanite ($OSCN^-$) (5), an antimicrobial agent (6). Human plasma contains substantial amounts of SCN^-

(33±26 µM for non-smokers and 158±51 µM for smokers) (7), an environment in which HSA is believed to be the main target of HOCl (5). We believe that in a plasma environment, SCN^- may be competitive with HSA for HOCl. Having accurate rate constants for these reactions may help in modeling the partitioning of HOCl in human plasma.

2.2 Experimental methods

2.2.1 Materials

All chemicals were A.C.S certified grade or better and were used without further purification unless stated otherwise. Water was doubly-distilled in glass. Unless otherwise noted, all solutions contain 0.1 M NaCl in 0.1 M phosphate buffer at pH 7.4, prepared from Na_2HPO_4 (used as received from Mallinckrodt). Sodium chloride (NaCl) and potassium iodide (KI) were obtained from EMD Chemicals. 2-chloro-5,5-dimethyl-1,3-cyclohexanedione (monochlorodimedone, MCD), sodium thiosulfate (anhydrous, >98%), sodium thiocyanate (98%), potassium dichromate (>99.0%), 2,6-dichlorophenol indophenols sodium salt (DCPIP), and Human Serum Albumin (lyophilized powder essentially fatty acid free) were all obtained from Sigma-Aldrich. Sodium phosphate dibasic anhydrous Na_2HPO_4 was used as received from Mallinckrodt. Stock solutions of hypochlorite (OCl^-) were prepared from dilution of commercial bleach (Clorox) which had been periodically standardized prior to use.

2.2.2 Sample preparation

2.2.2.1 DCPIP dye

Stock solutions of DCPIP were prepared from the sodium salt in 0.1 M PBS, pH=7.4, [NaCl] = 0.1 M. The concentration of DCPIP was determined spectrophotometrically at 600 nm (ε_{600} = 2.06x10^4 M^{-1}cm^{-1}) (8).

2.2.2.2 Thiocyanate

Stock solutions of thiocyanate were prepared from the sodium salt (dried in oven for a minimum of 2 hours, then cooled at room temperature in a desiccator prior to weighing) in 0.1 M PBS, pH = 7.4, [NaCl] = 0.1 M. Concentrations of thiocyanate were determined based on mass of sample, MW NaSCN = 81.07 g/mol, and volume of water added (either in volumetric flask or with volumetric pipettes).

2.2.2.3 Monochlorodimedone (MCD)

Stock solutions of MCD were prepared from its salt in 0.1 M PBS, pH=7.4, [NaCl] = 0.1 M. The concentration of MCD was determined spectrophotometrically at 290 nm (ε_{290} = 1.99x10^4 M^{-1}cm^{-1}) (9).

2.2.2.4 Hypochlorous acid

Stock solutions of HOCl were prepared from dilution of standardized commercial bleach into 0.1 M PBS, pH=7.4, [NaCl] = 0.1 M. Approximate concentrations of HOCl were determined spectrophotometrically at 292 nm

(OCl^- ε_{292} = 350 $M^{-1}cm^{-1}$) (10), at pH=7.4 there is approximately 50% OCl^- and 50% HOCl). For accurate concentrations, HOCl solutions were titrated with MCD (1:1 stoichiometry) spectrophotometrically, observing the disappearance of the MCD at 290 nm (ε_{290} = 1.99x10^4 $M^{-1}cm^{-1}$).

2.2.2.5 Human serum albumin (HSA)

Stock solutions of HSA were prepared from its lyophilized powder into 0.1 M PBS, pH=7.4, [NaCl] = 0.1 M. Concentrations were determined from sample mass (monomer MW = 66,478 g/mol) and known volumes.

2.2.3 Standardization of commercial bleach (hypochlorite)

The procedure used to standardize hypochlorite stock solutions was adapted from a book published by Daniel Harris (11), which consists of first standardizing a sodium thiosulfate ($Na_2S_2O_3$) solution that has been freshly prepared, and then using that to standardize the OCl^- stock solution. (The following uses conditions based on the titration of a stock solution of bleach which is 0.4-0.6 M, for concentrations which are higher or lower, the concentration of $Na_2S_2O_3$ (as well as the amount of $K_2Cr_2O_7$ used to titrate the $Na_2S_2O_3$) needs to be adjusted.

2.2.3.1 Titration of $Na_2S_2O_3$

The following solutions were prepared prior to the standardization of $Na_2S_2O_3$: 40 mL of 2.0 M KI (in water, prepared fresh every four hours), 50 mL

of a 1:1 (v/v) HCl solution (50% dilution of concentrated HCl into water), and 50 mL of starch indicator (mix approximately 0.5 g of soluble starch with 2-3 mL of water to create a paste, then transfer into 50 mL of boiling water and heat 2-3 mins until solution is clear, and cool to room temperature). A stock solution of approximately 0.1 M $Na_2S_2O_3$ (0.5-1 L) is prepared from addition of the appropriate mass of the salt to water (to prevent bacteria growth, it is important to clean the bottle with soap and water, rinsing bottle at least 3 times to rid it of residual soap) that is essentially bacteria and CO_2 free (achieved by boiling for 5-10 min., capping, and letting cool to room temperature). Prepare 3-5 Erlenmeyer flasks with 0.20-0.23 g of $K_2Cr_2O_7$ (dried in oven for approximately 2 hours, then cooled at room temperature in a desiccator prior to weighing), add approximately 50 mL of water to each sample to dissolve the $K_2Cr_2O_7$. Prepare a burette with the $Na_2S_2O_3$ solution. To the first $K_2Cr_2O_7$ sample, add 8 mL of 2.0 M KI, 10 mL of 1:1 HCl, and titrate immediately with $S_2O_3^{2-}$ until the dark red-brown color of I_2 has faded to an olive green color. At this time, add 2-3 mL of the starch indicator solutions and continue to titrate with $S_2O_3^{2-}$ until the purple-black color turns to a pure green, indicating the end point of the titration. Repeat for each of the remaining $K_2Cr_2O_7$ samples. The mechanism for this reaction is in (2.4) and (2.5), giving a stoichiometry of 1 $Cr_2O_7^{2-}$: 6 $S_2O_3^{2-}$.

$$Cr_2O_7^{2-} + 14H^+ + 6I^- \rightarrow 3I_2 + 2Cr^{3+} + 7H_2O \qquad (2.4)$$

$$I_2 + 2S_2O_3^{2-} \rightarrow S_4O_6^{2-} + 2I^- \qquad (2.5)$$

2.2.3.2 Titration of bleach

A diluted bleach solution was prepared by taking 15.0 mL of stock bleach and diluting up to 250 mL with water in a volumetric flask (giving a concentration of approximately 60 mM, or one around one third of your $Na_2S_2O_3$ stock solution). To the Erlenmeyer flasks which contain 50.0 mL bleach sample, 10 mL glacial acetic acid was added followed by addition of 8 mL of 2.0 M KI. The resulting solutions were titrated immediately with the primary standard of $Na_2S_2O_3$ until color fades to a pale yellow. Next add 2 mL of starch solution and continue titrating until the sample just becomes colorless. The reaction is occurring through the mechanism in (2.6) and (2.7), giving a stoichiometry of 1 OCl^-: 2 $S_2O_3^{2-}$.

$$OCl^- + 2H^+ + 2I^- \rightarrow I_2 + Cl^- + H_2O \quad (2.6)$$

$$I_2 + 2S_2O_3^{2-} \rightarrow S_4O_6^{2-} + 2I^- \quad (2.7)$$

2.2.4 pH measurements

The $[H^+]$ of the buffered solutions were determined with an Orion Ion Analyzer EA920 using an Ag/AgCl combination pH electrode. pH was adjusted with NaOH or HCl (made from pellets or concentrated solution, respectively) as required.

2.2.5 UV-vis spectroscopy

Electronic spectra were measured using a HP 8452A diode array spectrophotometer with quartz cells calibrated for 1 mm, 2 mm, 1 cm, and 10 cm path lengths, at 20 $^{\circ}$C.

2.2.6 Turbulent mixing of samples

HOCl was added drop wise to samples of SCN^-/MCD while vortexing.

2.2.7 Biologic instrument

2.2.7.1 General information

A Biologic SFM-400 MOS 450 (stopped-flow spectrometer equipped with a Xe arc lamp and a PMT detector) was employed for some experiments. This system contains two delay lines that allow for a variation in the sample ageing time. It has the capability of single, double, or triple mixing. Unlike most stopped-flow instruments, this instrument drives its syringes individually using stepper motors, which allow mixing of solutions to occur in two ways, either by continuous flow or interrupted flow (discussed in more detail later). This instrument is designed to be used in either stopped-flow (SF) or quench-flow (QF) mode (figure 2.3) (12).

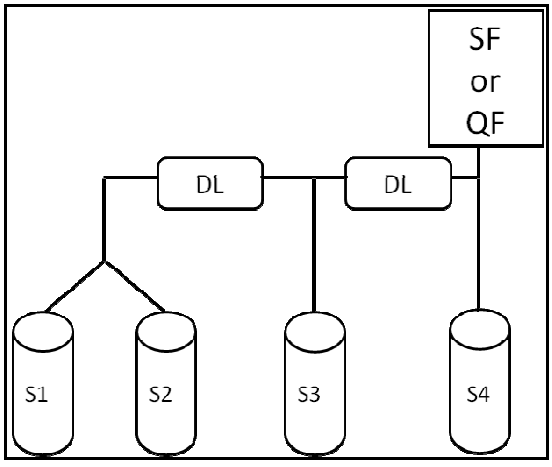


Figure 2.3: Schematic of SFM-400; DL = Delay line, used to vary aging time of samples

The instrument contains four syringes (S1-4, figure 2.3), of which two, three, or all four can be used. If all four syringes are used, syringes 1 and 2 are pushed simultaneously through a DL (delay line). The delay line can be modified to create either longer or shorter delay times depending on desired aging time of the reaction. The solutions resulting from syringes 1 and 2 is mixed with syringe 3 through a second delay line, and finally with syringe 4. In stopped-flow configuration, samples are rapidly mixed and pushed through an observation cell which allows for direct analysis of absorbance, transmittance, or fluorescence on the instrument using the MOS 450. In quench-flow configuration, samples are rapidly mixed and collected for analysis by a technique which is independent of the SFM-400. A water circulator bath is attached, set to 20ºC, encapsulating all SFM syringes, valves, delay lines, and cuvettes allowing temperature regulation (12).

2.2.7.2 Quench-flow mode

A quench-flow experiment designed for a simple reaction of $A + B \xrightarrow{Q} C$ where the reaction is stopped by the addition of a quencher, Q. This simple reaction consists of three steps (figure 2.4): a mixing step, an aging step, and a quenching step (complex experiments can consist of more steps, however, to simplify this discussion, only a three-step setup, the simplest quench-flow experiment, will be described) (12).

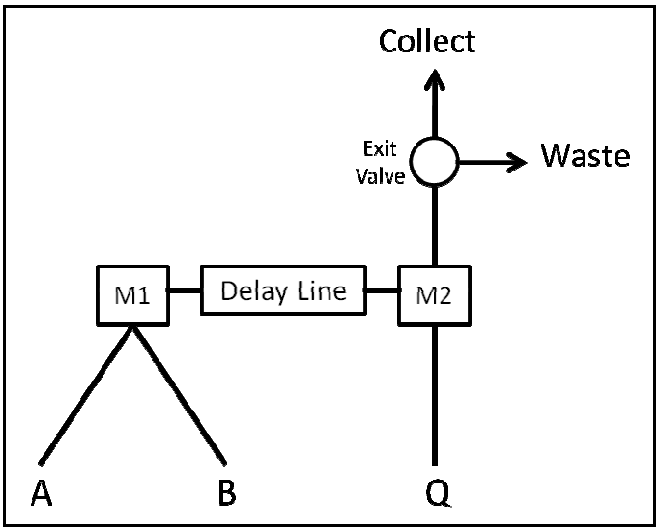


Figure 2.4: Schematic of simple quench flow setup; M1 and M2 are mixers

The first step is the mixing step, in which A and B are pushed through the mixer, by the stepper motors of the syringes, where they are mixed and allowed to react to start producing the product C. The second step is the aging step which occurs as the syringes continue to push A and B through the mixer and into the delay line. As the samples travel through the delay line, the sample ages (i.e. reacts) until it reaches the second mixer. As the sample moves through the second mixer it is mixed with the reactant Q, the quencher, which quenches (i.e. stops) the reaction. The sample is then collected and can be analyzed for amount of C produced, or amount of A or B remaining. The amount of time allowed for A and B to react, referred to as the ageing time (t_{age}, defined as total time between the start of the reaction at which A and B combine and the quenching of the reaction), depends on both the speed at which syringes are pushed (i.e. flow rate) as well as length of delay line. The t_{age} could

also depend on the pause time if using interrupted flow. By plotting t_{age} versus the results of each sample analyzed, a kinetic trace of the reaction can be determined (12).

2.2.7.3 Aging methods for quench-flow

In quench-flow mode, samples can be aged by one of three means: interrupted flow, continuous flow, or pulsed flow. (For stopped-flow experiments, the continuous flow method is adopted.)

2.2.7.3.1 Interrupted flow

When using interrupted flow as the aging method, the flow of the samples is paused for a certain time period, incubating the samples before mixing with the quencher. With this type of aging, t_{age} is determined by the intermixer volume (delay line volume), the flow rate of the sample into and out of the intermixer volume, and the incubation time that the sample waits in the intermixer volume (2.8).

$$t_{age} = \frac{\text{intermixer volume}}{\text{flow rate through intermixer volume}} + \text{incubation time} \qquad (2.8)$$

This method of aging is typically used for samples which need to be aged longer than can be achieved with continuous flow, typically several hundreds of ms to several seconds, or longer. With interrupted flow, higher amounts of sample are typically needed than in continuous flow, due to the inability of recovering the entire sample without contamination. The contamination is due to diffusion; though the flow of the samples is stopped during the incubation

time, the solution in the delay line is not isolated, it is in contact with solutions A, B, and Q, which as the incubation time increases, allows for more time for these solutions to diffuse into the intermixer volume, causing unwanted reaction and quenching near the mixer interfaces. To try and avoid collection of contaminated samples, the leading and ending edge of the intermixer volume are thrown out (i.e. partial sample collection). Long delay lines (i.e. delay lines that have a higher volume requirement to fill) are used for aging and multiple shots are taken in order to collect enough sample for analysis, all of which leads to more sample required for the experiment. The longer the incubation time, the higher the risk of contamination due to diffusion, causing the need for more sample to be discarded (12).

2.2.7.3.2 Continuous flow

In continuous flow method, just as the name implies, there is no interruption in the flow of the sample (no pause from the start of the reaction through the sample collection) so t_{age} is determined only by the intermixer volume and the total flow rate (2.9).

$$t_{age} = \frac{\text{intermixer volume}}{\text{flow rate through intermixer volume}} \qquad (2.9)$$

The time the sample is allowed to age can be adjusted by using a delay line which has a larger volume or by changing the flow rate by programming the syringes in the driving sequence to either push the solution faster or slower. As mentioned previously, the Biologic instrument drives solutions using a stepping motor, which unlike the commonly used pneumatic based system, allows for a

larger range of flow rates since flow rates are independent of the viscosity and temperature of the solutions. Continuous flow is typically used for reactions that have a t_{age} from 1 ms up to approximately 200 ms. Unlike interrupted flow, all of the sample can be collected and analyzed with minimal risk of contamination due to diffusion, since the time period between reaction and quenching is small therefore allowing less time for diffusion to occur (12).

2.2.7.3.3 Pulsed flow

Pulsed flow mode is a special aging method that is unique to the Biologic instrument, due to the use of stepper motors to drive syringes versus the use of pneumatics such as that used in Hi-Tech stopped flow instruments. By making a few pulses to fill the delay line (mixing a small volume of solution A and B at a time instead of pushing a larger volume all at one time as in continuous flow), solutions are turbulently mixed. (Each pulse is essentially a small volume, a "plug," of solution A and B that get pushed through the intermixer volume by the next pulse of solution, and as the plug gets pulsed through the delay line it ages.) The pulses are followed by a short incubation time and then mixed with a quencher. Using this method, t_{age} is determined by the number of pulses used to fill the delay line, the flow rate, and the incubation time (2.10).

$$t_{age} = \left(\frac{n \times V_{pulse}}{\text{flow DL}} \right) + \left[t_{inc} \times (n-1) \right] \qquad (2.10)$$

In (2.10), n = number of pulses; V_{pulse}= volume of pulse; flow DL = flow rate in the delay line; and t_{inc} = incubation time. An advantage of pulsed-flow aging

method is in order to achieve a different aging time, only the incubation time needs to be modified, the other parameters remain unchanged making varying aging times from one sample to the next a quick change.

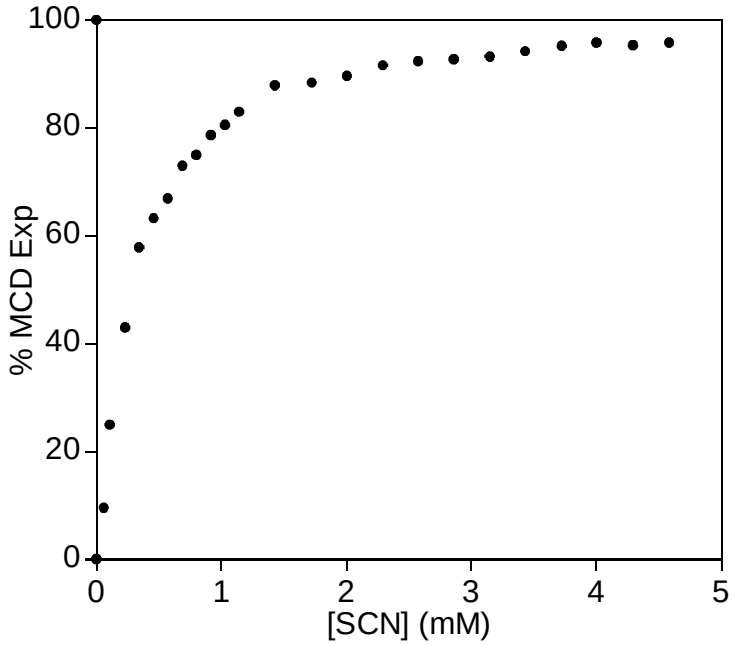


Figure 2.5: Reaction of HOCl (1 mM) with mixtures of MCD (1 mM) and SCN^- (0-4.6 mM) at pH 7.4 in 0.1 M phosphate and 0.1 M NaCl; percent MCD remaining at the end of the reaction (solid circles)

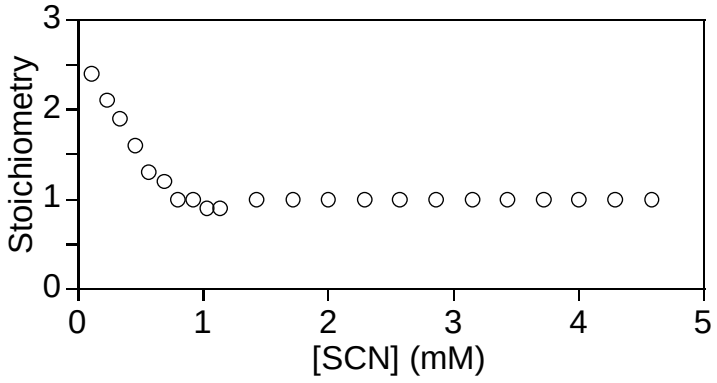


Figure 2.6: Stoichiometry of the reaction of HOCl with SCN^-

2.3 Results and discussion

2.3.1 MCD/SCN^- competition reaction with HOCl

Representative data that was collected for the reaction of HOCl with MCD in the presence of varying amounts of SCN^- are given in figure 2.5. From independent experiments we know that SCN^- reacts with up to three molar equivalents of HOCl. Figure 2.6, a plot of the stoichiometry for the reaction of HOCl with SCN^- that was calculated from the data, is consistent with the 3:1 stoichiometry. As can be seen, when the concentration of SCN^- is less than the concentration of HOCl, more than one molar equivalent of HOCl is consumed. However, when $[SCN^-] >> [HOCl]$, a stoichiometry of 1:1 is observed.

A mathematical program was developed to calculate the absolute rate constant for the reaction of HOCl with SCN^-. This model makes use of the experimental data (see appendix A for complete data set) and our measured rate constant for the reaction of MCD with HOCl, $4x10^6$ $M^{-1}s^{-1}$, a value that is comparable to that previously reported (3). To fit the data, we decided on a simple model of two parallel second-order reactions, one between HOCl and MCD, and one between HOCl with the inhibitor. Since there is no closed solution for the simultaneous differential equations that define the reaction mechanism of our system, we used Euler's method to fit the data (13). Using a known initial value, Euler's method takes small steps and integrates them using the differential equations in order to produce a numerical value. Figure 2.7 is a flowchart of the iterative procedure we used in our program to compute the rate constants.

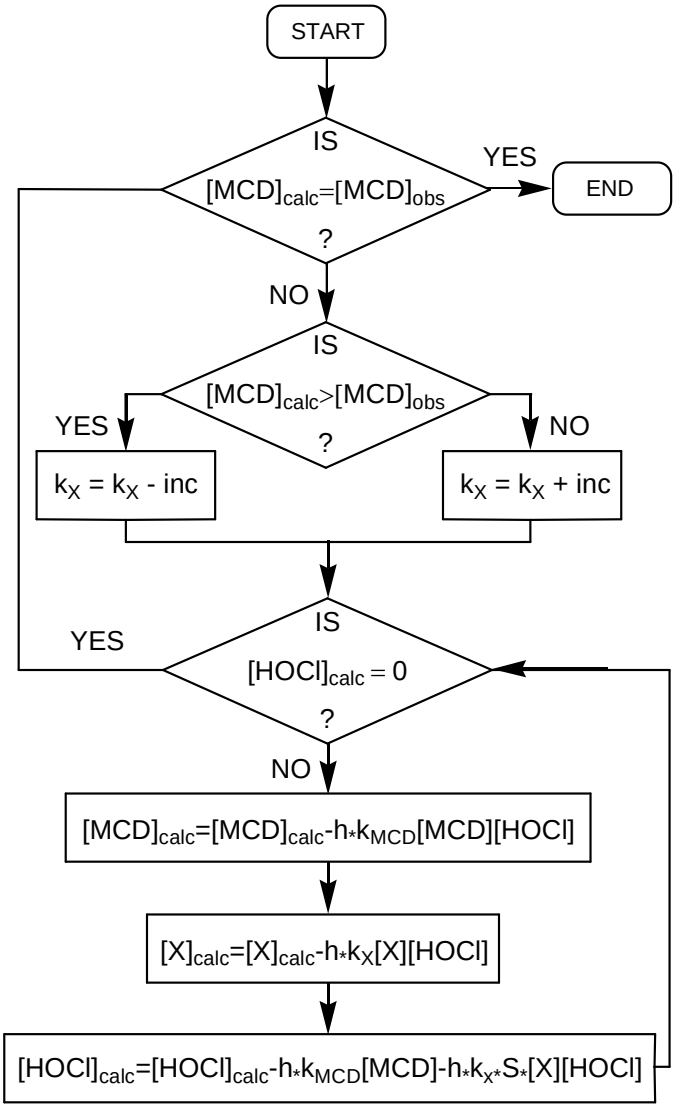


Figure 2.7: Flowchart of the iterative procedure that was employed to compute the rate constants, assuming parallel second-order reactions of HOCl with MCD and X (where X = inhibitor). The constant h is the incremental step for numerical integration and S is the experimental stoichiometry.

To explain, the program (see appendix B for program code) starts by taking the calculated MCD (MCD_{calc}) value (arbitrarily chosen as twice the experimental MCD (MCD_{obs}) value for starting the program) and compares it to the experimental MCD value. If they are not the same, the program will take the rate constant for X and increase it if MCD_{calc} is greater than MCD_{obs}, or decrease the rate constant by the increment if MCD_{calc} is less than MCD_{obs}. This incremental amount is calculated by the percent difference in MCD_{calc} and MCD_{obs}, which allows for smaller steps to be taken as the calculated MCD value approaches the experimental MCD value. The program enters an inside loop in which it takes the amount of HOCl and runs through the loop, calculating a new MCD value each time, until there is no HOCl left. Once all the HOCl is consumed, it takes the MCD_{calc} and repeats the program, comparing that value to the MCD_{obs}. To summarize, the program takes a calculated MCD amount, if it is not the same as the experimental MCD amount, it changes the rate constant for HOCl + X (X = SCN^- for these experiments) and goes through and recalculates another MCD_{calc}, until $MCD_{calc} = MCD_{exp}$ (uses the experimentally found amount of MCD to calculate the k for the inhibitor, SCN^-). Table 2.1 gives the results of the program.

Table 2.1: Program output which includes the data point number (i), the experimental [SCN], the experimental %MCD, the %MCD the program calculated, and the rate constant the program calculated (does not take stoichiometry into account, calculated based on one data point, using $[SCN]_{exp}$ and $\%MCD_{calc}$).

i	$[SCN]_{exp}$	$\%MCD_{exp}$	$\%MCD_{calc}$	$k_{SCN\ calc}$
0	6.00E-05	9.6	9.6	1.07E+07
1	1.10E-04	25.0	25.0	3.29E+07
2	2.30E-04	43.0	43.0	3.99E+07
3	3.40E-04	57.8	57.7	5.70E+07
4	4.60E-04	63.3	63.2	5.08E+07
5	5.70E-04	67.0	66.9	5.51E+07
6	6.90E-04	73.0	72.9	5.89E+07
7	8.00E-04	75.0	75.0	6.71E+07
8	9.20E-04	78.7	78.6	5.81E+07
9	1.03E-03	80.6	80.5	6.03E+07
10	1.14E-03	83.0	82.9	5.73E+07
11	1.43E-03	88.0	87.9	5.43E+07
12	1.72E-03	88.5	88.4	4.38E+07
13	2.00E-03	89.7	89.6	4.06E+07
14	2.29E-03	91.6	91.5	4.28E+07
15	2.57E-03	92.4	92.3	4.15E+07
16	2.86E-03	92.7	92.6	3.82E+07
17	3.15E-03	93.3	93.2	3.74E+07
18	3.43E-03	94.2	94.1	3.93E+07
19	3.72E-03	95.2	95.1	4.30E+07
20	4.00E-03	95.8	95.7	4.50E+07
21	4.29E-03	95.4	95.3	3.86E+07
22	4.58E-03	95.8	95.7	3.92E+07

The next step was to develop code which uses a given rate constant to calculate a %MCD remaining (see appendix C for full code), and that %MCD can be used to fit the experimental data. The code developed has two parts; it calculates the %MCD without any consideration of stoichiometry, so assumes HOCl reacts with either MCD or SCN^-. The code also calculates the %MCD with consideration of the possibility of over-oxidation of the SCN^- (i.e. HOCl reacts with either MCD or SCN^-, then HOCl can react with $OSCN^-$, the product of HOCl and SCN^-, and likewise HOCl can further react with O_2SCN^-, the product of HOCl and $OSCN^-$). Figure 2.8 is a plot of the resulting program output (complete data set in appendix D) plotted along with experimental data points and stoichiometry.

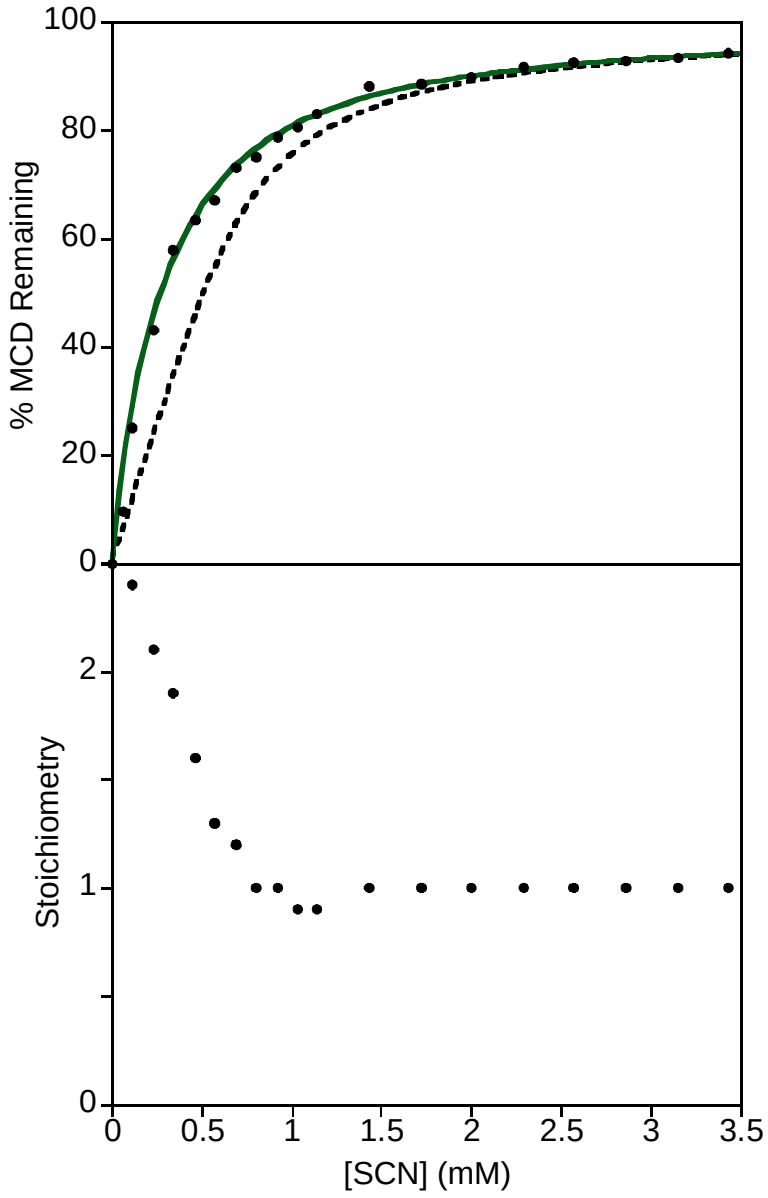


Figure 2.8: Reaction of 1 mM HOCl with mixtures of 1 mM MCD and SCN^- (0 - 3.5 mM) at pH 7.4 (100 mM phosphate, 100 mM NaCl). Experimental percentage of MCD remaining at the end of the reaction (solid circles); the calculated percentages of MCD at the end of the reactions with (solid line) and without (dashed line) consideration of the stoichiometry.

As can be seen in figure 2.8, at [SCN^-] > 1.5 mM, where a stoichiometry of 1:1 is observed, the simple model in which no stoichiometry is considered (dashed line) suffices in the fitting of the data. However, at lower concentrations of SCN^-, this simple model is not appropriate, but a model which considers three (but not two) sequential reaction steps fit all of the data (solid line). From independent stopped-flow experiments performed at higher pH, it is known that these three sequential reaction steps that SCN^- undergoes when oxidized by HOCl are of the same order of magnitude. Keeping this in mind, it was found that $k_X : k_{XO} : k_{XO2} = 1.0 : 0.1 : 0.4$ and $k_{SCN} = k_X = 1.9 \times 10^7\ M^{-1}s^{-1}$ satisfactorily fit the data. The agreement in the rate constants calculated by our two program methods is remarkable. Using our experimental MCD values (first program), we found a $k_{scn} = 4.5 \times 10^7\ M^{-1}s^{-1}$. Using a k_{scn} of $1.9 \times 10^7\ M^{-1}s^{-1}$, along with values of $k_X : k_{XO} : k_{XO2} = 1.0 : 0.1 : 0.4$, we were successfully able to fit our experimental data (program two). If you compare these two rate constants to $k_{SCN} = 2.34(9) \times 10^7\ M^{-1}s^{-1}$, extrapolated from the rate constants between HOCl and SCN^- that was measured between pH 10.5-13.8 and extrapolated to pH 7.4 (5), there is even more room for excitement. Given that this extrapolation involved a 10^3 change in [H^+], there is a remarkable agreement in the rate constant. Also worth mentioning is a possible problem in the traditionally used competition reaction method (e.g. Winterbourn (2)) which assumes that the pseudo-rate constants are equal at the point of 50% inhibition; examining figure 2.8, the 50% inhibition point does not correspond to a stoichiometry of 1:1, which was shown to be essential in correctly fitting the data.

2.3.2 MCD/HSA competition reaction with HOCl

We studied the reaction of HOCl with the inhibitor HSA. HSA, being a protein, has multiple sites of possible reaction with HOCl along with some sites being capable of being over-oxidized (i.e. Met groups). Table 2.2 lists some of the amino acid residues found in HSA and their (free amino acid) rate constants with HOCl; SCN^- is added to the table for comparison (3,5,14-16).

Table 2.2: Second-order rate constants for the reactions of HOCl with amino acids and lipid components; SCN^- added for comparison; *estimated values.

Moiety	# residues in HSA	k_{HOCl} ($M^{-1}s^{-1}$)
His	16	$1.0x10^5$
Lys	59	$5.0x10^3$
Arg	24	$1.8x10^3$
Asn	17	0.03
Gln	20	0.03
Cys*	1	$3.0x10^7$
Met*	6	$3.8x10^7$
Cystine	17	$1.6x10^5$
Tyr	18	44
Trp	1	$1.1x10^4$
RNH_2	1	$1.0x10^5$
Amide	583	10
SCN^{-*}	0	$2.3x10^7$

As can be seen in table 2.2, the most reactive residues are the 6 Met and 1 Cys residues. Unlike SCN^-, which reacts with HOCl through three sequential reactions, HSA is capable of undergoing multiple parallel reactions. In addition, each subsequent reaction can undergo sequential reactions, possibly complicating the analysis of the data and interpretation. The procedures that were employed for HSA were done similar to those for SCN^-. A plot of the data along with calculated stoichiometry is in figure 2.9 (complete table of data in appendix E).

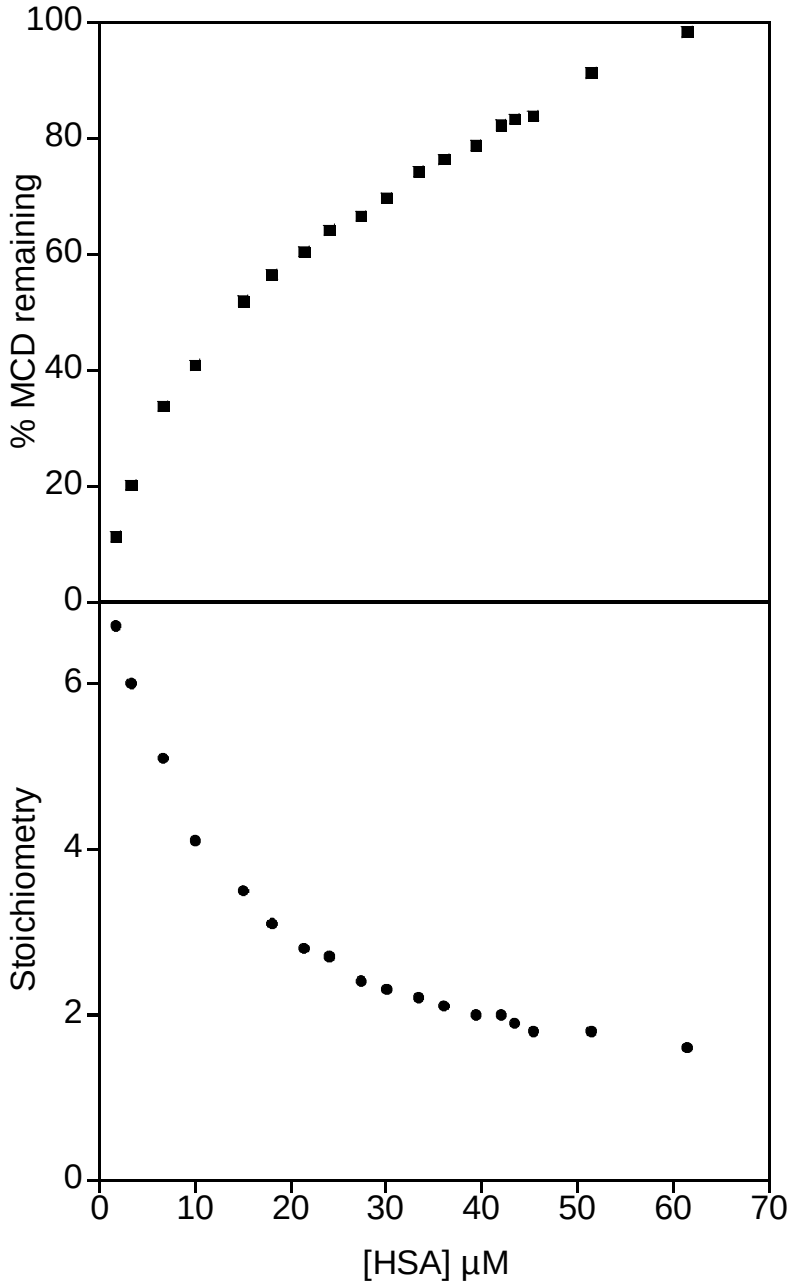


Figure 2.9: Reaction of 100 µM HOCl with mixtures of 100 µM MCD and HSA (0-61 µM) at pH 7.4 (100 mM phosphate, 100 mM NaCl). %MCD remaining (squares), stoichiometry of reaction (circles)

Table 2.3: Program output which includes the data point number (i), the experimental [HSA], the experimental %MCD, the %MCD the program calculated, and the rate constant the program calculated (does not take stoichiometry into account, calculated based on one data point, using $[HSA]_{exp}$ and $\%MCD_{calc}$)

i	X_{exp} (M)	$\%MCD_{exp}$	$\%MCD_{Calc}$	kXcalc ($M^{-1}s^{-1}$)
0	1.67E-06	11.1	11.1	5.65E+07
1	3.34E-06	20.1	20.1	9.08E+07
2	6.68E-06	33.7	33.7	1.19E+08
3	1.00E-05	40.8	40.8	1.28E+08
4	1.50E-05	51.9	51.8	1.47E+08
5	1.80E-05	56.4	56.3	2.07E+08
6	2.14E-05	60.4	60.3	2.05E+08
7	2.40E-05	64.1	64	1.74E+08
8	2.74E-05	66.4	66.3	2.34E+08
9	3.01E-05	69.7	69.6	2.40E+08
10	3.34E-05	74.1	74	2.95E+08
11	3.61E-05	76.3	76.2	2.98E+08
12	3.94E-05	78.7	78.6	2.77E+08
13	4.21E-05	82.2	82.1	2.66E+08
14	4.54E-05	83.8	82.8	3.60E+09
15	4.34E-05	83.3	83.2	4.76E+08
16	5.14E-05	91.2	91.1	5.52E+08
17	6.15E-05	98.3	98.2	2.52E+09

As seen in figure 2.9, stoichiometry of up to 7:1 were observed, which is consistent with the prediction that Cys-34 and the six Met groups of HSA should be the most reactive. Similar to SCN^-, the experimental data was fit using the first program (no consideration of stoichiometry) (code in appendix F), resulting in a rate constant for the reaction of HOCl with HSA, table 2.3.

Comparing this rate constant to that by SCN^- (k_{SCN} = 4.5(9)x10^7 $M^{-1}s^{-1}$), this is about an order of magnitude faster. The second program (consideration of stoichiometry) was used to calculate %MCD remaining in an attempt to obtain a better fit of the experimental data, but difficulties were encountered. We could not successfully find a model which gave a good fit of the data. We started by trying to fit the data using 7 parallel reactions, all with similar rate constants, however, there were several run-time errors in the program code, which we did not investigate further. Though the SCN^- model is not appropriate (three consecutive reactions), we were able to successfully get the program to run, and so it is included here for discussion. Figure 2.10 gives a plot of the experimental data along with some results from fitting the data using the SCN^- model, which shows how the fit changes with the program conditions.

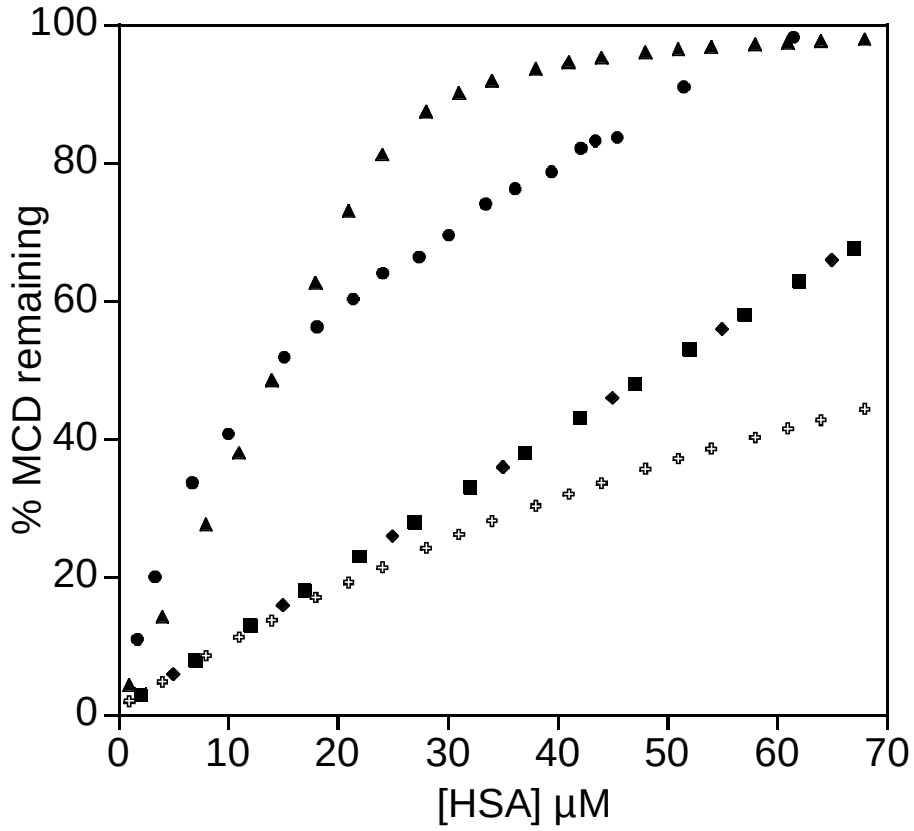


Figure 2.10: Reaction of 100 µM HOCl with 100 µM MCD and varying amounts of HSA (0-61 µM) at pH = 7.4 (100 mM phosphate and 100 mM NaCl). Experimental %MCD (circles); calculated %MCD using $k = 5.5 \times 10^8$ $M^{-1}s^{-1}$ with (triangles) and without (diamonds) consideration of stoichiometry; calculated %MCD using $k = 5.5 \times 10^7$ $M^{-1}s^{-1}$ without consideration of stoichiometry (squares); calculated %MCD using $k = 5.5 \times 10^6$ $M^{-1}s^{-1}$ without consideration of stoichiometry (crosses)

In figure 2.10, the circles are the experimental data. Looking at a fit with (triangles, figure 2.10) and without (diamonds, figure 2.10) stoichiometry taken into account, when stoichiometry is considered, the calculated data more closely resembles the experimental. When comparing how changing the rate constant affects the fit, we need to compare the $k = 5.5x10^{8}\ M^{-1}s^{-1}$ (diamonds, figure 2.10), $k = 5.5x10^{7}\ M^{-1}s^{-1}$ (squares, figure 2.10), and $k = 5.5x10^{6}\ M^{-1}s^{-1}$ (crosses, figure 2.10). Changing the rate constant from 10^{6} to $10^{8}\ M^{-1}s^{-1}$ did not make any depreciable difference (we observed similar behavior when using a mathematical program (appendix G and H) to model the kinetics when using sulfite as the inhibitor). This shows that by increasing the rate constant between HSA and HOCl, the data does not fit better. However, taking stoichiometry into account is needed to improve the fit of the data, although HSA is not believed to go through subsequent reactions like SCN^{-}. We were unable to successfully find a good fit for the data, however it does show the importance of including stoichiometry in accurately fitting the data.

We note there were problems with the reproducibility in this system. Depending on the technique used for mixing (slowly pouring reactants together, using a hand-mixer, vortexing sample while adding oxidant dropwise, or using the quench-flow instrument), results were not reproducible between methods (i.e. data obtained from using the hand-mixer gave different results than when mixed using quench-flow instrument). Use of the quench-flow instrument to mix the reactants gave the most consistent results from one experiment to the next. Studying the reaction using different mixing techniques helped us understand

the importance of turbulent (or complete) mixing for these very fast reactions. When the reactants react faster than they are mixed, a heterogeneous (not homogenous) reaction may occur. For larger molecules, like proteins, which are capable of reacting with multiple equivalents of HOCl, incomplete mixing will affect results.

2.4 Summary and conclusions

Measuring rate constants directly under conditions of interest (e.g. concentration, pH, and temperature) is ideal, however, sometimes not practical due to experimental and instrumental limitations. Researchers have used methods such as pH extrapolation (for reactions which are pH dependent, changing the pH may slow down the reaction enough to use conditions at which the rate constant is measurable, and then use extrapolation to estimate the rate constant at the pH of interest) and competition reactions (when the rate constant is known for a particular reaction, it can be used to obtain rate constant for another reaction if competitive conditions can be employed) to indirectly measure rate constants under conditions of interest (1), thus avoiding these limitations. Comparison of rate constants from pH extrapolation and competition reactions has shown inconstancies (2-4) which needed investigating. Our inhibitory titration method has given insight into these inconsistencies.

Competition reactions typically use the 50% inhibition point for measuring rate constant of the competition reaction, while the rest of the data set remains unused (i.e. rate constant is calculated from one data point). In addition, reactions are typically assumed to be measured under pseudo first order conditions (independent of initial concentration), though the rate laws for the two competition reactions are sometimes not understood.

The method that is developed here, inhibitory titration (IT), tries to minimize assumptions that can create problems when indirectly measuring rate constant. Firstly, IT makes use of all the data collected, not just the 50% inhibition point; fitting the complete data set to obtain the rate constant. We show that the rate constant measured using just the 50% inhibition point underestimates the rate constant compared to that which fits all of the data. In addition, consideration of the stoichiometry of the reaction is important for accurately fitting data, especially when over-oxidation is possible. Our data shows that taking the stoichiometry of the reaction into consideration produces a better fit than assuming the reaction has a 1:1 stoichiometry. Without consideration of the rate law for the reaction, one may derive a first order rate constant from a second order reaction, leading to a misrepresentative rate constant.

2.5 Future experiments

- Validation of IT method: A simple system needs to be chosen to validate the IT method. We investigated complex systems (biomolecules which react with multiple stoichiometry and possible over-oxidation) that were of particular interest to us. To show the overall general use of the IT method for measuring rate constants of fast reactions, a simple system needs to be used.
    - Take the simple system of $A + O \xrightarrow{kA} X$ and $B + O \xrightarrow{kB} Y$, where k_A (a known value) and k_B are the rate constants of the reactions, respectively. Both reactions need to be non-complex reactions. The products X and Y cannot be reactive (so a stoichiometry between A or B and O is a 1:1) and no reactive intermediates can be formed. Also, the mechanisms for the reactions needs to be the same under the experimental conditions where the competition reaction occurs as well as the conditions at which k_A and k_B are measured independently. The best option is to validate the method under the same conditions as k_A and k_B can be independently measured. In addition, k_A and k_B must be of similar orders of magnitude.
- Additional experiments need to be performed with HOCl and HSA to aid in the development of a mathematical program that can fit the data and obtain a more accurate rate constant for this reaction. Also, additional experiments may help provide insight into the complex reaction which is

occurring including how many equivalents of HOCl that HSA is able to scavenger. In addition, studying larger biological molecule may help understand turbulent mixing issues.

2.6 References:

(1) Caldin, E. F.; Blackwell Scientific Publications: Great Britain, **1964**.

(2) Winterbourn, C. C. "Comparative reactivities of various biological compounds with myeloperoxidase-hydrogen peroxide-chloride, and similarity of the oxidant to hypochlorite." *Biochimica et Biophysica Acta* **1985**, *840*, 204-10.

(3) Pattison, D. I.; Davies, M. J. "Absolute rate constants for the reaction of hypochlorous acid with protein side chains and peptide bonds." *Chemical Research in Toxicology* **2001**, *14*, 1453-1464.

(4) Armesto, X. L.; Canle L, M.; Fernandez, M. I.; Garcia, M. V.; Santaballa, J. A. "First steps in the oxidation of sulfur-containing amino acids by hypohalogenation: Very fast generation of intermediate sulfenyl halides and halosulfonium cations." *Tetrahedron* **2000**, *56*, 1103-1109.

(5) Ashby Michael, T.; Carlson Amy, C.; Scott, M. J. "Redox buffering of hypochlorous acid by thiocyanate in physiologic fluids." *Journal of the American Chemical Society* **2004**, *126*, 15976-7.

(6) Ashby, M. T.; Aneetha, H. "Reactive sulfur species: Aqueous chemistry of sulfenyl thiocyanates." *Journal of the American Chemical Society* **2004**, *126*, 10216-10217.

(7) Jacob, P.; Savanapridi, C.; Yu, L.; Wilson, M.; Shulgin, A. T.; Benowitz, N. L.; Eliasbaker, B. A.; Hall, S. M.; Herning, R. I.; Jones, R. T.; Sachs, D. P. L. "Ion-pair extraction of thiocyanate from plasma and its gas-chromatographic determination using on-column alkylation." *Analytical Chemistry* **1984**, *56*, 1692-1695.

(8) Laskey, J. G.; Patterson, P.; Bilyeu, K.; Morris, R. O. "Rate enhancement of cytokinin oxidase/dehydrogenase using 2,6-dichloroindophenol as an electron acceptor." *Plant Growth Regulation* **2003**, *40*, 189-196.

(9) Kettle, A. J.; Winterbourn, C. C. "The mechanism of myeloperoxidase-dependent chlorination of monochlorodimedon." *Biochimica et Biophysica Acta* **1988**, *957*, 185-91.

(10) Anbar, M.; Dostrovsky, I. "Ultra-violet absorption spectra of some organic hypohalites." *Journal of the Chemical Society* **1954**, 1105-1108.

(11) Harris, D. C. *Quantitative chemical analysis*; 5th ed.; W.H. Freeman & Company: New York, NY, 1998.

(12) *Sfm-300/400 user's manual*; Ver. 2.2 ed.; Bio-Logic SA: France, 2005.

(13) Coe, D. A. "Numerical-solutions of kinetic-equations on a spreadsheet." *Journal of Chemical Education* **1987**, *64*, 496-497.

(14) Pattison, D. I.; Davies, M. J. "Kinetic analysis of the reactions of hypobromous acid with protein components: Implications for cellular damage and use of 3-bromotyrosine as a marker of oxidative stress." *Biochemistry* **2004**, *43*, 4799-4809.

(15) Nagy, P.; Beal, J. L.; Ashby, M. T. "Thiocyanate is an efficient endogenous scavenger of the phagocytic killing agent hypobromous acid." *Chemical Research in Toxicology* **2006**, *19*, 587-593.

(16) Nagy, P.; Ashby, M. T. "Reactive sulfur species: Kinetics and mechanism of the oxidation of cystine by hypochlorous acid to give n,n'-dichlorocystine." *Chemical Research in Toxicology* **2005**, *18*, 919-923.

Chapter 3: Oxidation of Methionine by Hypochlorous Acid, Search for an Intermediate

3.1 Introduction

3.1.1 Methionine

Methionine (Met) is one of only two sulfur containing amino acids, with Cys being the other. It is an essential amino acid that humans are unable to synthesize, so it must be obtained from dietary sources (e.g. nuts, fish, and meats). Met can be found as the free amino acid or within proteins. Like Cys, Met has several functions including antioxidant defense (1), regulation of cellular function through reversible oxidation and reduction (2-5), and functioning as a methyl donor, a process which is necessary for the synthesis of proteins (6).

Free Met reacts with adenosine triphosphate (ATP) in a reaction catalyzed by methionine adenosyltransferase. The reaction forms S-Adenosyl methionine (SAM), a compound which serves as a methyl donor in biochemical pathways such as the synthesis of epinephrine and coline (7-8). The majority of Met, however, is found within proteins. Met serves as an initiator in protein synthesis and is encoded into the *N*-terminal position of all eukaryotic proteins (*N*-formylmethionine, a Met derivative is encoded at the *N*-terminal in bacterial proteins), though it is sometimes removed by post-translational modification (2).

3.1.2 Oxidation of methionine

Met is oxidized by a host of oxidants, both one and two electron ROS (*i.e.* H_2O_2, hypohalous acids, ozone, peroxynitrite, superoxide, and chloramines) (9). Oxidation occurs over a broad pH range (2). Due to the ease of oxidation, Met is believed to play an important role in defending proteins against high levels of ROS during times of oxidative stress (9). MPO, the heme containing enzyme found in mammalian neutrophils, which catalyzes the oxidation of chloride by hydrogen peroxide to form HOCl, contains 36 methionine residues (10-12). These Mets may offer protection to the MPO, which is often in an environment that has a high concentration of oxidants.

Oxidation of Met forms a mixture of *S* and *R* isomers of methionine sulfoxide (MetO) (13); further oxidation produces methionine sulfone ($MetO_2$). Formation of MetO can be biologically reversed while that to the sulfone is not. While free Met can be used as a methyl donor, formation of the sulfoxide deprives it of that ability. Protein Met oxidation can have varying consequences depending on the location and the extent of oxidation, but Met oxidation is mostly thought of as decreasing or inhibiting the activity of the protein. In some cases, however, oxidation of protein Met has lead to the activation of the protein (*i.e.* cell signaling) (5).

Most proteins have Met that is capable of being oxidized. The amount of MetO present in protein is believed to be directly related to the severity and duration of oxidative stress in diseases. High levels of sulfoxide have been found in cataract lens (about 2/3 of total Met is oxidized) as well as rheumatoid

arthritis fluid (13-14). In addition, studies have shown a correlation between levels of MetO and age-related illnesses such as Alzheimer disease (13-15). Oxidation of protein Met to the sulfoxide influences the biological activity of the protein and has been proposed to cause protein aggregation and dysfunction (16-18). Lavine *et al.* have compiled a list of proteins and peptides in which the activity is altered as a result of Met oxidation (2). Met, when located near the active sites of enzymes (e.g. glutamine synthase), acts as a protector during times of increased levels of oxidant (14). *In vitro* experiments have shown that oxidation of Met-36 and Met 48 of human stem cell factor (SCF, a protein that plays a role in formation of blood cells) alters the tertiary structure and ultimately decreases the biological activity (18-19). Studies have been performed on the oxidation of α-1-proteinase inhibitor, a serum protein that is known to regulate elastase (an enzyme that breaks down elastin, a protein in connective tissue) activity and play a role in emphysema of smokers. Oxidation of the Met-358 inactivates the protein. Fortunately, activity is restored when the oxidized protein is incubated with methionine sulfoxide reductase (Msr) in the presence of thioredoxin (20).

The oxidation of Met to MetO does not always lead to loss of activity. α-2-macroglobulin, a protease inhibitor (inhibits proteases from breaking down proteins) that functions at sites of inflammation where high levels of damaging ROS exist, has been shown to scavenge at least 10 equivalents of ROS (21). Continuous exposure to oxidants eventually leads to the oxidation of α-2-macroglobulin's one tryptophan, causing inactivation (21). Luo *et al.* stated that

Met residues appeared to act as molecular bodyguards, protecting the important tryptophan residue (21). Similar results were found with a study of glutamine synthetase (an enzyme that plays a role in metabolism of nitrogen by catalyzing the formation of glutamine) (22). Levine *et al.* oxidized glutamine synthase with H_2O_2 and found that 8 of the 16 Met residues in the protein were oxidized to MetO. These eight oxidized Mets were located near the surface of the protein, lining the entrance to the active site, while the eight unmodified Mets were buried (oxidation of the active site is known to cause inactivation of glutamine synthetase) (1,22). As with α-2-macroglobulin, activity was preserved. Luo *et al.* suggested that the ability of Met to scavenge oxidizing equivalents without loss of activity along with their placement in the protein(s) that protects important functional groups helps show the ability of Met to defend against oxidants. Furthermore, since oxidation of Met to its sulfoxide can be reversed (20), it shows the effective scavenging of more reactive species by proteins such as these two mentioned.

Oxidation of Met residues in proteins tends to increase the surface hydrophobicity of the protein (2). Considering that MetO is less hydrophobic than Met, this is contrary to what would be predicted. When Met is oxidized to MetO, the oxygen perturbs the folding pattern of the protein, exposing more hydrophobic resides, causing the hydrophobicity to increase. The more extensive the oxidation damage becomes, the more likely the protein will go through proteolysis (digestion of proteins by enzymes called proteases) (2, 20-21).

3.1.3 Mechanism of oxidation

The thioether group of Met is readily oxidized by a large number of oxidants. A selected list of oxidants that react with Met appears in a review by M.J. Davies (23), and includes hydroxyl radical, ozone, H_2O_2, HOCl, HOBr, chloramines, and peroxynitrite. As previously mentioned, the major product from the oxidation of Met, whether it be protein bound or not, has been reported as MetO, rarely has sulfone been found in a biological system (5,23).

The mechanism by which Met is oxidized by oxidants to form its sulfoxide is not completely understood. Oxidation of Met by radicals such as hydroxyl radical ($^{\bullet}OH$) is believed to occur with an addition at the sulfur atom to form R-$^{\bullet}$S(OH)-R adduct, which goes through a series of fast reactions to eventually form the sulfoxide (15,24). The exact mechanism is not known but it is believed that multiple pathways can lead to the sulfoxide product. One theory is that the initial adduct reacts with itself forming a dimeric radical cation that contains a two centered three-electron bond, a compound believed to be stabilized by neighboring resides (24-25). Similarly, a three electron intramolecular S-N bond has been proposed, one in which the sulfur and amide nitrogen form a 5 member ring (25). It has also been proposed that the adduct reacts with other radicals, such as superoxide to give the sulfoxide (23,26). Met reacting with two electron oxidants is also believed to form a short-lived adduct, though there is no direct evidence (23). Reaction of Met with H_2O_2 and other peroxides is believed to initially form an R-S^+(OH)-R species which is rapidly deprotonated to give the sulfoxide (23). The reaction of Met with H_2O_2 is a

rather slow reaction ($k = 6x10^{-3}\ M^{-1}s^{-1}$) (23) but can be catalyzed by both copper and iron, two biologically relevant metals (although very little free metal ion is found *in vivo*). In the presence of these metals, H_2O_2 reacts to form $^{\bullet}OH$ (5) which oxidizes Met ($k = 8x10^{9}\ M^{-1}s^{-1}$) (23). Similar to the uncatalyzed reaction of Met with H_2O_2, reaction with hypohalous acids (e.g. HOCl and HOBr) are likely to produce the analogous $R\text{-}S^{+}(Cl/Br)\text{-}R$ intermediate which rapidly hydrolyzes to the sulfoxide (23,27-28).

Sulfenyl halides (R-S(Cl/Br)] and halosulfonium cations [$R\text{-}S^{+}(Cl/Br)\text{-}R$] are often suggested to be the intermediates in the oxidation of Cys and Met, respectively, though there is little kinetic and mechanistic evidence for their involvement (27,29-33). Armesto *et al.* performed a mechanistic study of the reaction of Met (and Cys) with HOCl. Though they were not able to find direct evidence of an intermediate, they were able to develop a mechanism, supported by their experimental results, in which Met is chlorinated through an effective Cl^{+} transfer from the oxygen of HOCl to the sulfur of Met, forming a chlorosulfonium cation. The chlorosulfonium cation then hydrolyzes to form MetO. Armesto *et al.* conclude that a detailed mechanistic study is still needed (27). Though discussed in more detail in chapter four, it is worth mentioning a study by Hong *et al.* who examined the iron catalyzed reaction of Met by H_2O_2 and found evidence for an azasulfonium intermediate. The azasulfonium of Met, referred to in other publications as dehydromethionine (DHM), slowly hydrolyzes to the sulfoxide at neutral pH (26,34).

3.1.4 Methionine sulfoxide reductase

Most organisms, whether they are human or bacteria, have methionine sulfoxide reductase (Msr), a family of enzymes that catalyze the reduction of MetO to Met (3). Since oxidation of Met in proteins can lead to either activation or inactivation of their biological activities, Msr serves to repair oxidative damage of some proteins. It also plays an important role in the regulation of protein activities by facilitating the interconversion of Met residues between oxidized and reduced forms. Oxidation of Met forms a mixture of *S* and *R* isomers of MetO (3.1). MsrA catalyzes the reduction of *S*-MetO and MsrB the reduction of *R*-MetO. Both MsrA and MsrB catalyze the thioredoxin [$Th(SH)_2$] dependent reduction of MetO to Met (3.2). In addition, oxidized thioredoxin (THS-S) can be reduced back to thioredoxin by Nicotinamide adenine dinucleotide phosphate (NADPH) (3.3). The net reaction is the consumption of ROS by NADPH (3.4) (1-3,13,21).

$$\mathrm{Met} + \mathrm{ROS} \rightarrow \mathrm{MetO} + \mathrm{ROS}_{\mathrm{inactive}} \tag{3.1}$$

$$\mathrm{MetO} + \mathrm{Th(SH)_2} \xrightarrow{\mathrm{Msr}} \mathrm{Met} + (\mathrm{ThS-S}) \tag{3.2}$$

$$(\mathrm{ThS-S}) + \mathrm{NADPH} + \mathrm{H^+} \rightarrow \mathrm{Th(SH)_2} + \mathrm{NADP^+} \tag{3.3}$$

$$\mathrm{ROS} + \mathrm{NADPH} + \mathrm{H^+} \rightarrow \mathrm{NADP^+} + \mathrm{ROS}_{\mathrm{inactive}} \tag{3.4}$$

Msr is believed to play a vital role in protection against oxidative stress. In studies conducted on mutant strains (modified to remove the Msr gene) of mice (35), bacteria (36-38), and yeast (39), lack of the Msr gene made the organism more sensitive to oxidative stress versus the wild-type strains (13). In addition, over-expression of the Msr gene in human T cells (40), yeast (40), and

fruit flies (41), leads to an increase in the resistance in oxidative stress (13). Studies have shown a correlation between age-related diseases and the amount of Msr present. Stadtman *et al.* wrote a review article which has shown that MsrA in rat tissue declines with age (13). Levels of Msr are lower in patients (vs. healthy patients) whom have age-related disease such as Alzheimer's disease (42), emphysema (especially in smokers) (5,43), and Parkinson's disease (44-45). In addition, lower levels of MsrA activity in mice led to a 40 % decrease in the life span (13,35), while over-expression lead to an almost doubling of the life span (41).

3.2 Experimental methods

3.2.1 Materials

All chemicals were A.C.S certified grade or better and were used without further purification unless stated otherwise. 18.2 MΩ•cm water, obtained from a Millipore Milli-Q A10 ultrapure water purification system, was used for all experiments. Unless otherwise noted, all solutions contain 0.1 M NaCl in 0.1 M phosphate buffer at pH 7.4, prepared from $NaH_2PO_4•3H_2O$ and Na_2HPO_4 (used as received from Mallinckrodt). Sodium chloride (NaCl), sodium hydroxide pellets (NaOH), and potassium iodide (KI) were all obtained from EMD Chemicals. 2-chloro-5,5-dimethyl-1,3-cyclohexanedione (monochlorodimedone, MCD), sodium thiosulfate (anhydrous, > 98%), potassium dichromate (> 99.0%), 5,5'-dithiobis-(2-nitrobenzoic acid) (DTNB, 99%), sodium sulfite (> 98%), DL-methionine (> 99%), DL-methionine sulfoxide (> 99%), DL-methionine

sulfone (> 99%), DNP-DL-methionine sulfoxide (95%), DNP-DL-methionine sulfone (95%), 1-fluoro-2,4-dinitrobenzene (FDNB, > 99%), and iodomethane (99%) were all obtained from Sigma-Aldrich. Sodium phosphate dibasic anhydrous Na_2HPO_4 was used as received from Mallinckrodt. Sodium hydroxide solution (50% certified) used for preparation of chromatography eluents was obtained from fisher chemical.

3.2.2 Sample preparation

3.2.2.1 Hypochlorous acid

Stock solutions of NaOCl were prepared by sparging Cl_2 into a 0.3 M solution of NaOH. The sparging was stopped when the [OCl^-] was approximately 0.1 M, as determined spectrophotometrically at 292 nm (OCl^- ε_{292} = 350 $M^{-1}cm^{-1}$) (46). Solutions prepared by dilution of stock solution into water or buffer were further standardized prior to experimental use. Approximate concentrations of HOCl were determined spectrophotometrically at 292 nm (OCl^- ε_{292} = 350 $M^{-1}cm^{-1}$) for solutions with pH > 10 (a drop of concentrated sodium hydroxide was added to raise pH if needed) (46). For a more accurate measurement of concentration, HOCl solutions were titrated with MCD (1:1 stoichiometry), spectrophotometrically observing the disappearance of the MCD at 290 nm (ε_{290} = 1.99x10^4 $M^{-1}cm^{-1}$) (47) or titrated with $Na_2S_2O_3$ as described in chapter 2. All HOCl stock solutions were titrated prior to reaction. To avoid possible issues with reaction of HOCl and buffer (discussed in chapter 2), all HOCl solutions with concentrations < 25 µM were prepared in water.

3.2.2.2 Synthesis of DNPMet

Dinitrophenyl-methionine was synthesized similar to the method used by Levy *et al.* (48). In 40 mL (at 40 ºC) of DI water, 2 g DL-Met and 2.5 g Na_2CO_3 (pH = 9-10) were added and stirred until mostly dissolved. To the solution, 2.5 g 1-fluoro-2,4-dinitrobenzene (FDNB) was added. The reaction was allowed to continue until there was no more unreacted FDNB, after which the solution was acidified with 6 M HCl until yellow. The solution was put in the refrigerator (~ 2 ºC) overnight. Precipitate was collected and recrystalized twice with ether/pentane (dissolve in minimum amount of ether with 4x amount of pentane, put on ice, filtered to collect yellow ppt). Yellow precipitate was dried under vacuum overnight and then stored in freezer (at -20 ºC). Neither percent yield nor purity was determined (NMR data looked free of unreacted Met).

3.2.2.3 Synthesis of TNBMe

TNB (5-thio-2-nitrobenzoic acid) was synthesized from dissolving 1 g DTNB (Ellman's reagent) and 0.64 g sodium sulfite (dried in oven overnight) in 50 mL water. The solution was stirred for about an hour and then acidified with HCl and extracted twice with petroleum ether. The organic layer was collected and dried over $CaCl_2$. After gravity filtering the organic layer, it was kept in refrigerator (~2 ºC) overnight, and the crystals were collected and dried under vacuum. TNB was refluxed with CH_3I (in about 50mL water) overnight, acidified with HCl, and the resulting yellow precipitate was collected by filtration. Neither

percent yield nor purity was determined (NMR spectrum looked free of unreacted TNB).

3.2.2.4. Methionine studies

A 550 µM Met solution (in 100 mM PBS, pH = 7.4) was made by 10.3 mg Met in 25 mL buffer, 1:5 dilution with buffer. A 610 µM MetO solution was prepared by dissolving 0.0126 g in 25 mL buffer, followed by a 1:5 dilution in buffer. A 305 µM $MetO_2$ was prepared by dissolving 0.0138 g in 25 mL buffer, followed by a 1:5 dilution in buffer. Absorbance spectra collected using HP diode array and 1 cm cell to determine approximate molar absorptivities.

3.2.2.5. TNBMe titration and molar absorptivity

A stock solution of TNBMe was prepared by 10.3 mg in 100 mL buffer (0.05 M PBS, 0.1 M NaCl, pH = 7.4). The UV-vis spectral data were collected using HP8452. Molar absorptivity of the TNBMe was calculated using Beer's law (known concentration, path length, and measured absorbance) as well as from the titration experiments. A stock solution of 485 µM gave an absorbance of 0.493 (0.1 cm cell), giving a calculated value of ε = 10,165 $M^{-1}cm^{-1}$. For titration experiments, HOCl (stock made in 0.1 M NaOH) solutions were standardized with sodium thiosulfate, and then diluted into buffer. Various aliquots were added to TNBMe solutions and spectra were taken using UV-vis diode array (190-820 nm).

3.2.3 High performance liquid chromatography (HPLC)

A Gilson HPLC was equipped with a 156 UV-vis (dual wavelength), 805 manometric module, 811b dynamic mixer (1.5 mL mixing chamber), and two 305 pumps. Eighty microliters of sample was manually injected into a 20 µL loop. The data was monochromatically collected at 358 nm, using Gilson Unipoint 5.11 software. DNP-Mets were separated on a varian microsorb 100-5, C18, 250 x 4.6 mm column using an isocratic gradient of 1.30 mL/min flow rate with 80% A (1% acetic acid in water), 20% B (acetonitrile). All eluents were prepared using HPLC grade solvents, 18.2 MΩ•cm water, and degassed under vacuum (while stirring) for about 30 minutes prior to using.

3.2.4 Ion chromatography (IC)

Ion chromatography experiments were performed using a Dionex ICS 3000. The instrument was equipped with a single pump, electrochemical detector with pH/Ag/AgCl reference electrode and gold working electrode (either disposable or non-disposable), and an AS autosampler. Samples containing mixtures of Met, MetO, and $MetO_2$ were separated on aminopac PA10 amino acid column (2 x 250 mm), equipped with a guard column (2 x 50 mm), and analyzed using Dionex's Chromeleon chromatography management software. The instrumental method used was a modification of Dionex's standard amino acid analysis method for separation of "oxidation products of methionine, cysteine, and cystine," document number 031481-12. All eluents used were prepared with 18.2 MΩ•cm water that was degassed by bubbling

ultra high purity helium through for 30 minutes prior to using. Sodium hydroxide solutions were prepared by diluting a 50% sodium hydroxide solution with previously degassed water. To avoid excess carbonate formation, all eluents were kept under a blanket of nitrogen. In addition, 50% sodium hydroxide stock solutions were discarded every 6 months or when 1/4 of the stock solution remained (sodium hydroxide has a high potential of being contaminated with carbon dioxide, forming carbonate which increases the noise level).

3.2.5 Biologic instrument

The biologic instrument is described in more detail in chapter 2. Briefly, experiments were performed in either stopped-flow or quench-flow mode. Stopped-flow mode (single mixing) was used for the reactions of MetO with HOCl and TNBMe with HOCl. In stopped-flow mode the instrument can either be used to observe the kinetic traces (as a function of time) or scan a sample to obtain a complete absorbance spectrum (parascan mode). The experiments involving reaction of Met or DNPMet with HOCl used quench-flow mode. The quench-flow experiments were similar for both reactions and occurred in double-mixing mode using a combination of continuous flow (for delay times <200 ms) and pulsed flow (delay times > 200 ms). Met (or DNPMet) was mixed with HOCl and after a set delay time, the sample was quenched with excess sodium sulfite [reacts with HOCl with a $k = 10^9\ M^{-1}s^{-1}$ (49)]. Met and DNPMet were prepared in 200 µM PBS (pH = 7.4) (100 µM after mixing 1:1 with HOCl). HOCl was prepared in water instead of buffer [diluted from its initial stock

solution (0.1 M OCl^- in 0.1 M NaOH)] to avoid possible interaction between phosphate and HOCl at these low concentrations (micromolar) (discussed in chapter 2). The pH of reacted solution was measured for every other sample to ensure that the pH of the sample after reaction was 7.4±0.4. Sulfite, used as the quenching agent for the reaction, was prepared fresh (sulfite air oxidizes to sulfate, resulting in a loss of its quenching ability) in water. The sulfite used to quench the reaction was no more than five times the concentration of HOCl used (a large excess of sulfite corrodes the gold electrode and decreases sensitivity over time).

3.2.6 Intermediate production

Our experiments focus on pseudo-first order conditions. For a simple reaction in which no intermediate is formed, we would expect the data to fit to a simple first order plot. Any deviation from first order kinetics may be evidence for an intermediate being formed. Unfortunately, depending on the experimental conditions and properties of the intermediate, non-deviation from first order plot does not necessarily mean an intermediate is not being formed. Take the following generic reaction:

$$A + O \xrightarrow{k_A} I$$

$$I \xrightarrow{k_I} B$$

To get significant deviation from a first order fit of the data, the second reaction needs to be significantly slow with respect to the first reaction (i.e. $k_A >> k_I$, causing a buildup of I to occur). If k_A and k_I are similar, then an overall first order

plot is observed (as fast as the reaction can produce I, it disappears forming B, so no buildup of an intermediate is observed). If $k_A > k_I$ or $k_I > k_A$, either first or second order overall may occur. We are hoping for biphasic kinetics (combination of two first order plots), which would indicate multiple reactions are occurring. Unfortunately, only under a narrow range of experimental conditions are biphasic kinetics observed (need approximately a tenfold difference in rate constants to see any buildup of an intermediate). Observing biphasic kinetics is dependent not just on the rates of reactions, but also on the molar absorptivities of the reactants and products, since we are monitoring the reaction by either the disappearance of reactant (A) or appearance of product (B). If both A and B have distinctive molar absorptivities (ε_A and ε_B), we will see A disappear and B appear, forming one or more “tight” isosbestic points (the wavelength at which the absorptivities of A and B are equal). To observe an intermediate form, ε_A and ε_I (or ε_B and ε_I) need to be different enough so that their spectra can be differentiated. Depending on how different the molar absorptivities are (between A, I, and B), determines how “tight” the isosbestic point is. The less “tight” the isosbestic point is, the more indication that multiple species are being formed (50).

3.3 Results and discussion

Several reactions were investigated in hopes of finding evidence for a chlorosulfonium (or sulfenyl chloride) intermediate buildup.

3.3.1 Oxidation of methionine by HOCl

Figure 3.1 shows the calculated (from Beer's law) molar absorptivities of Met, MetO, and $MetO_2$. The molar absorptivities are relatively low and unfortunately do not produce distinct absorbance spectra (several compounds absorb in this region of the spectrum).

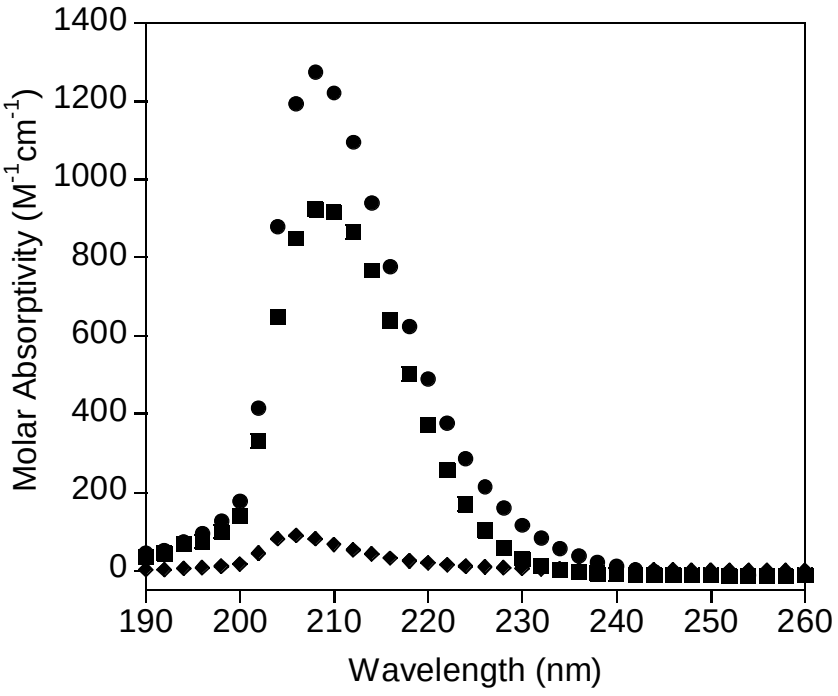


Figure 3.1: Molar absorptivity as a function of wavelength (in 100 mM PBS, pH = 7.4) of Met (circles), MetO (squares), and $MetO_2$ (diamonds).

In addition, the rate constant of the reaction of Met with HOCl at pH = 7 has been estimated to be around $3x10^7$ $M^{-1}s^{-1}$ (28). Due to the low molar absorptivity and large rate constant (at neutral pH), it is difficult to directly follow the kinetics of a reaction using conventional equipment (i.e. stopped-flow instrument which

has a mixing time on the order of ms). Under pseudo-first order conditions, a reaction with a half-life of 20 ms (a reasonable half-life for a reaction studied using stopped-flow instrument) and rate constant of $3x10^7$ $M^{-1}s^{-1}$ would need a reactant concentration of about 1 µM to be measurable by stopped-flow. A 1 µM solution of Met would give a maximum change in absorbance of 2 mAU, too small to measure accurately. Increasing the concentration would help increase the absorbance change; however, it also speeds up the rate of the reaction. A similar situation would be observed for a reaction under second-order conditions, giving concentration of each reactant as 1.6 µM. Since direct observation of the reaction was not feasible, we utilized the quench flow method, quenching the reaction after varying delay times with a reductant. Sodium sulfite was chosen as the quenching agent, a compound that reacts with HOCl and is presumed to not react with MetO, $MetO_2$, and any intermediate that may form. Representative data are shown in figure 3.2 (IC chromatogram).

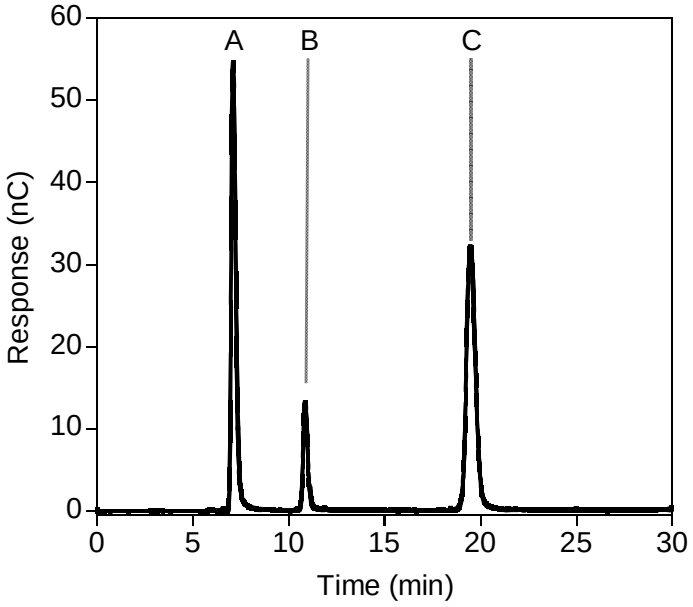


Figure 3.2: Representative ion chromatography chromatogram for mixture of Met (C), MetO (A), and $MetO_2$ (B). Solutions were made up in 1 mM PBS, pH = 7.4.

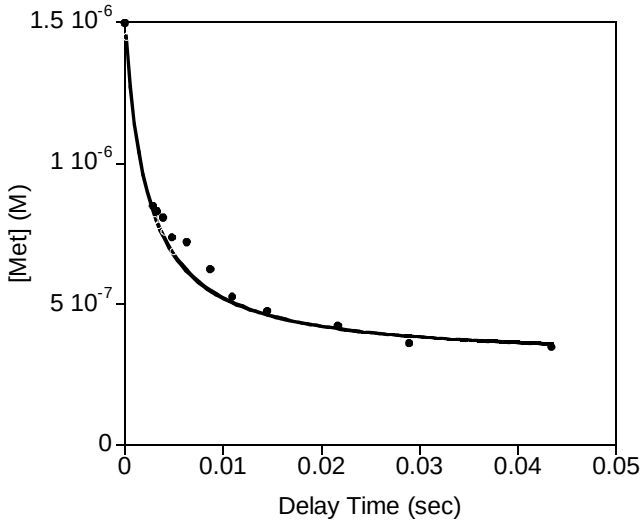


Figure 3.3: Reaction of Met (1.5 µM) with HOCl (1.5 µM) in 100 µM PBS, pH = 7.4, quenched with excess sodium sulfite (9 µM) after various delay times. Data was fit to a second order reaction giving $k = 4x10^8\ M^{-1}s^{-1}$.

Figure 3.3 is a representative trace of the reaction of Met with HOCl. The trace fits to a second order reaction and gives a $k = 4x10^8\ M^{-1}s^{-1}$, which is a larger than had been previously estimated (55). This difference could be due to several factors including different experimental conditions (buffer concentration, ionic strength, etc.) and also lack of sufficient data points. As can be seen in figure 3.3, under these conditions the reaction is over half way completed before our first data point is collected. Ideally, data should be collected so that there are more data points near the beginning of the reaction and less towards the end, however, the instrument has a limitation as to how fast it can mechanically mix solutions. To increase the $t_{1/2}$, a smaller concentration of reactants could be used, however, this is nearing the limits of detection of the IC instrument. Although it may be worth investigating further to get a more accurate rate constant, this is all a moot point in relation to an intermediate formation. Though the reaction does not fit perfectly to a first order reaction, it does not appear to be biphasic (biphasic is a combination of two first order reactions and can indicate multiple reactions are occurring such as would be observed if there was a buildup of an intermediate which subsequently underwent a reaction). From the experiments performed, there does not appear to be definitive evidence for a buildup of an intermediate. That being said, it is worth pointing out that during these studies, we were never able to recover all of our oxidizing equivalents. Since equal amounts of HOCl and Met were reacted, we would expect all Met to be consumed. In addition, the longer the samples aged after collecting, the more Met was detected (figure 3.4). Though

this issue of lack of recovering all oxidizing equivalents is worth pursuing (discussed further in chapter 4), it does not give conclusive evidence for presence of an intermediate.

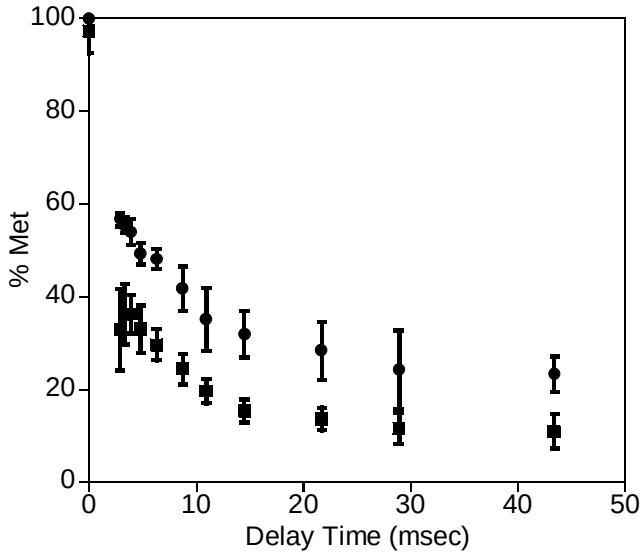


Figure 3.4: Reaction of Met (1.5 µM) with HOCl (1.5 µM) in 100 µM PBS, pH = 7.4, quenched with excess sodium sulfite (9 µM) after various delay times. Samples analyzed within 12 hours of collecting samples (circles), and samples analyzed > 24 hours after collecting samples (squares). Data points are averages with error bars of three samples.

3.3.2 Oxidation of methionine sulfoxide by HOCl

The reaction of MetO with HOCl was investigated. Figure 3.5 shows a portion of the absorbance spectrum collected for the reaction of MetO with HOCl. As shown, there is an increase in the absorbance at about 252 nm, characteristic of chloramine formation (51).

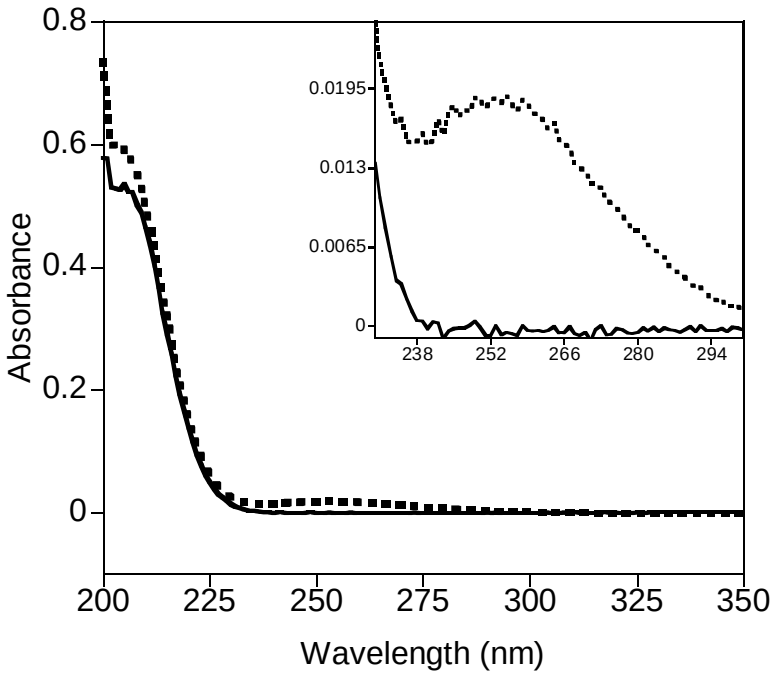


Figure 3.5: Reaction of MetO (500 µM) with HOCl (50 µM) in 5 mM PBS at pH = 7.4. Absorbance spectra (collected via biologic instrument) of reaction (dotted line) versus no reaction (solid line). Inset shows an increase in peak at 252 nm.

Neither MetO nor $MetO_2$ have a significant molar absorptivity at 252 nm (figure 3.1). Therefore, if the oxidation of MetO formed $MetO_2$, there should not be a peak at 252 nm; however a peak is clearly present (figure 3.5). The absorbance max for HOCl is 230 nm (292 nm for OCl^-), so this does not appear to be unreacted oxidant. Additionally, the new species at 252 nm is stable (no significant decrease in absorbance after 8 hour period) so it is not likely an intermediate. A typical kinetic trace is shown in figure 3.6.

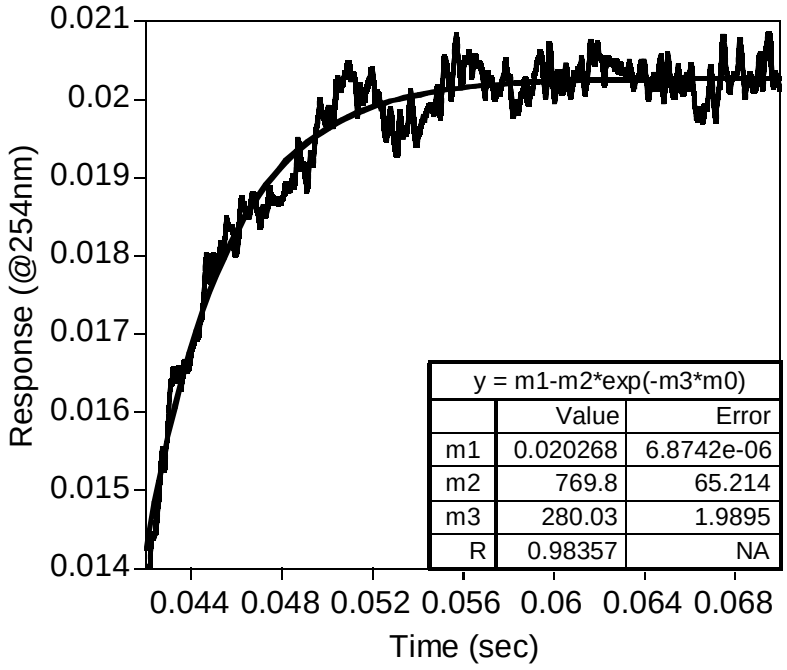


Figure 3.6: Reaction of MetO (500 µM) with HOCl (50 µM) in 5 mM PBS at pH = 7.4, kinetic trace followed at 254 nm and fit to first order equation giving k_{obs} = 280 s^{-1} (calculated k = 5.6x10^5 $M^{-1}s^{-1}$).

Though these particular reaction conditions are pushing the limits of the instrument (change in absorbance and rate of reaction), the trace clearly fits a first order reaction, giving a k_{obs} = 280 s^{-1} (second order k = 5.6x10^5 $M^{-1}s^1$, calculated using concentration of MetO); similar results were determined under second-order conditions (k = 8.4x10^5 $M^{-1}s^{-1}$). Experimental studies of MetO + HOCl shows no evidence for any intermediate buildup. A somewhat surprising result is evidence for the formation of a chloramine, not $MetO_2$, when MetO is oxidized by HOCl (the amino group of MetO reacts faster than the sulfoxide group). This can help explain why $MetO_2$ is rarely found in a biological system (5,23). MetO can be reduced back to Met by use of the enzyme Msr and

chloramines can transfer its oxidizing equivalents to another compound (forming MetO). $MetO_2$, on the other hand, is a “dead” form of Met, with no practical means of reverting back to Met. *In vivo*, however, this reaction may be irrelevant considering a vast majority of Met is protein bound and do not have free amino groups which are capable of forming chloramines (unless found at the *N*-terminus of a protein).

3.3.3 Oxidation of DNPMet

Dinitrophenyl-methionine (DNPMet), a derivative of Met which has the amino group blocked by the dinitrophenyl group, was synthesized. The addition of the dinitrophenyl group increases the molar absorptivity of the compound, relative to Met. With an increase in the molar absorptivity, it may be possible to directly observe the kinetics of the reaction, leaving out the need to quench the reaction (important if an intermediate reacts with the quenching agent). Figure 3.7 shows the absorbance spectra of DNPMet, DNPMetO, and $DNPMetO_2$.

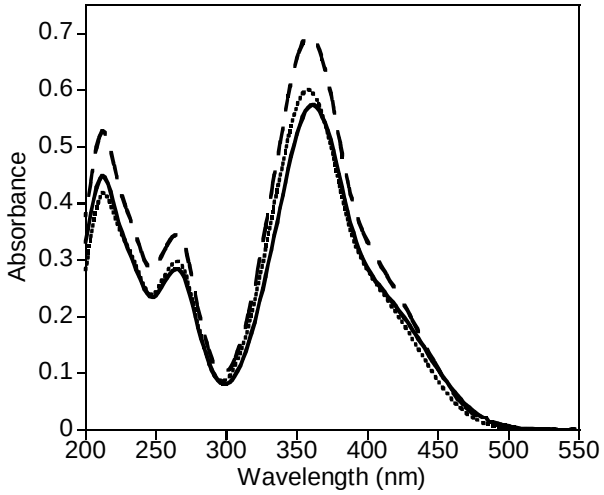


Figure 3.7: Absorbance spectra (0.1 cm cell; HP8452A diode array) of DNPMet (Solid line, 0.01164 g in 100 mL 0.1 M PBS pH = 7.4), DNPMetO (long dashed line, 0.00664 g in 50 mL 0.1 M PBS pH = 7.4), $DNPMetO_2$ (dashed line, 0.00616 g in 50 mL 0.1 M PBS pH = 7.4). Using Beer's law, molar absorptivities were calculated as DNPMet ε_{358nm} = $1.55x10^4$ $M^{-1}cm^{-1}$; DNPMetO ε_{358nm} = $1.74x10^4$ $M^{-1}cm^{-1}$; DNPMet ε_{358nm} = $1.69x10^4$ $M^{-1}cm^{-1}$.

As was expected, the addition of the DNP group to the Met increases the molar absorptivity, by a factor of around 10. Unfortunately though, the spectrum and molar absorptivities between the DNPMet's are very similar, which could still potentially be a problem for directly following the kinetics of the reaction, since we monitor the reaction by a change in absorbance. As with Met, our best option was to use quench-flow, thereby collecting the samples and analyzing offline using another instrument, in this case HPLC with UV-vis detection (since the compounds still do have large extinction coefficients). The DNPMet derivatives were successfully separated using HPLC (figure 3.8).

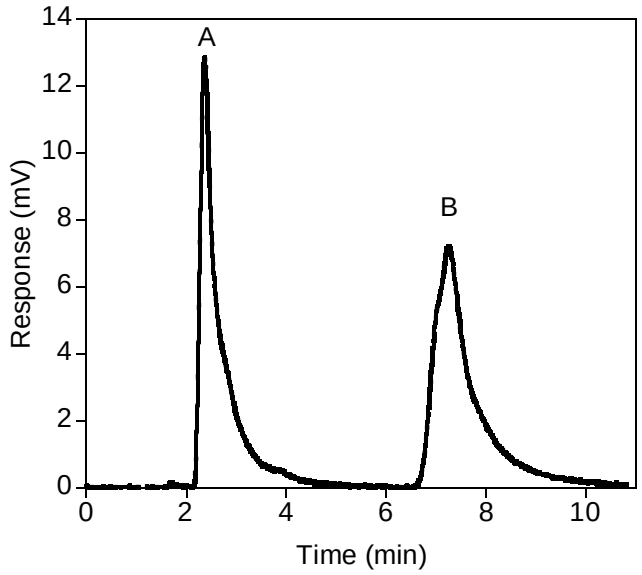


Figure 3.8: Representative chromatogram of a mixture of DNPMetO (RT = 2.5 min) and DNPMet (RT = 7.5 min).

The reaction between DNPMet and HOCl was done similarly to that with Met and HOCl. The reactants were mixed in equal amounts and then after a known delay time, the reaction was quenched with sulfite, collected, and analyzed for amounts of DNPMet and DNPMetO remaining. Figure 3.9 illustrates a representative plot of the kinetic trace of the reaction along with a fit to a second-order reaction, $k = 5x10^6\ M^{-1}s^{-1}$. Unlike what was observed with the oxidation of Met by HOCl, we were able to recover all of the HOCl in this reaction, but there still does not appear to be any intermediate (a stoichiometric conversion of DNPMet to DNPMetO is observed). Though we were not able to find any intermediates, this system was straight forward and to the best of the author's knowledge, had not been investigated before.

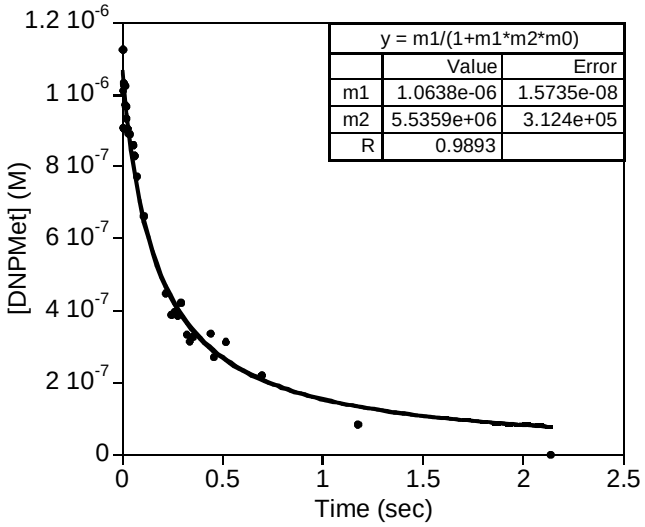
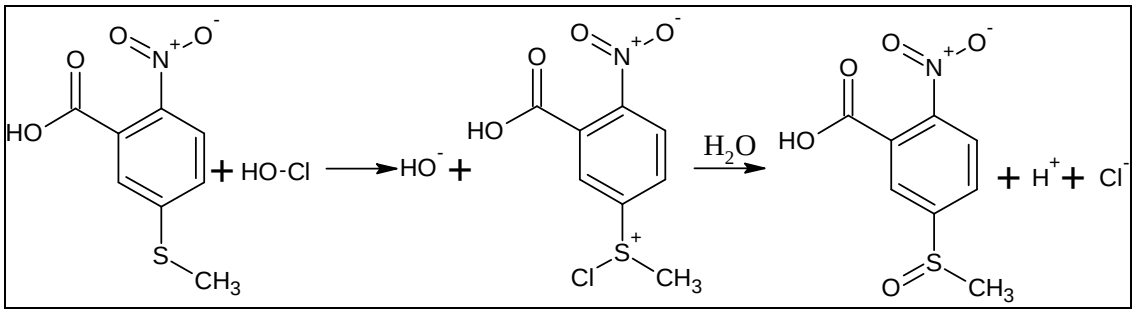


Figure 3.9: Reaction (100 µM PBS, pH = 7.4) of DNPMet (1.2 µM) with HOCl (1.2 µM), quenched with excess sodium sulfite (20 µM) after varying delay times, fit with rate constant of $5.5 \pm 0.3 \times 10^{6}\ M^{-1}s^{-1}$.

3.3.4 Oxidation of TNBMe

Still searching for an intermediate, we investigated the oxidation of TNBMe with HOCl (scheme 3.1), hoping that an intermediate would be longer lived in this system, increasing the chance of observing it.

Scheme 3.1: Proposed mechanism for the oxidation of TNBMe by HOCl, forming a chlorosulfonium ion intermediate.



TNBMe is a thioether derivative of TNB (5-thio-2-nitrobenzoic acid), a compound commonly used for redox titrations. Though TNBMe (and TNB) is not biological relevant, it has a distinct advantage over the Met system in that it has a large molar absorptivity, allowing for the possibility to directly observe the kinetics, instead of reacting and quenching, a process in which an intermediate has the possibility of also being quenched. Figure 3.10 shows the titration of TNBMe using varying amounts of HOCl. The TNBMe peak at 352 nm disappears with the addition of HOCl forming a new peak at 280 nm, which is presumed to be the TNBMeO (sulfoxide of TNBMe).

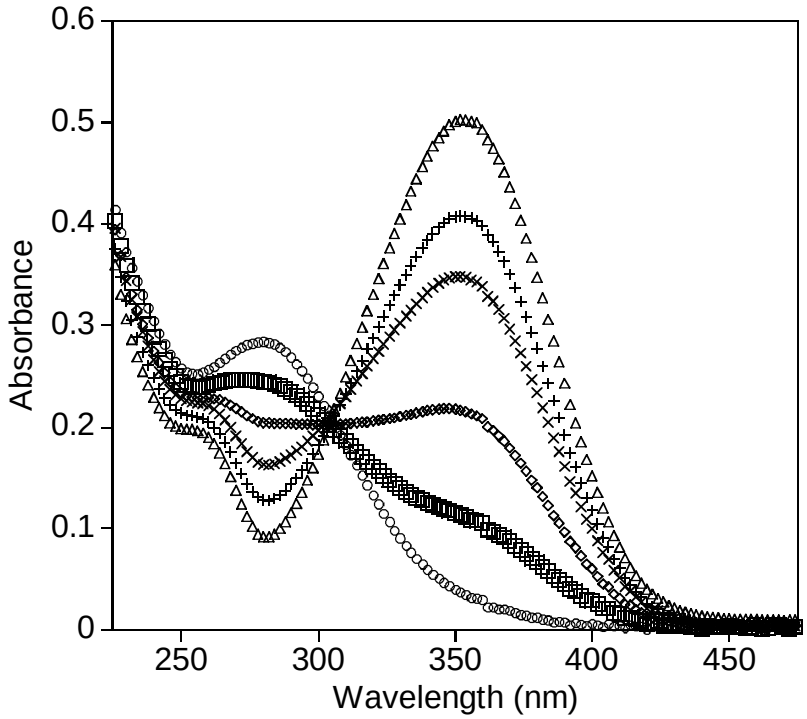


Figure 3.10: Titration of 240 µM TNBMe with 0-500 µM HOCl (pH = 7.4, 0.05 M PBS, 0.1 M NaCl). Absorbance spectra taken using HP8452A diode array. From top to bottom (at 350 nm), stoichiometry TNBMe:HOCl, 1:0 (Δ), 1:0.3 (+), 1:0.6 (x), 1:0.8 (◊), 1:1(□), 1:2(○).

A molar absorptivity, determined using Beer's law (known concentration and pathlength), was found to be $\varepsilon_{352} = 1.0 \times 10^4\ M^{-1}cm^{-1}$. The molar absorptivity was also determined by a plot of [TNBMe] versus absorbance, taken from the titration of TNBMe, giving a molar absorptivity of $9.8 \times 10^3\ M^{-1}cm^{-1}$ (figure 3.11).

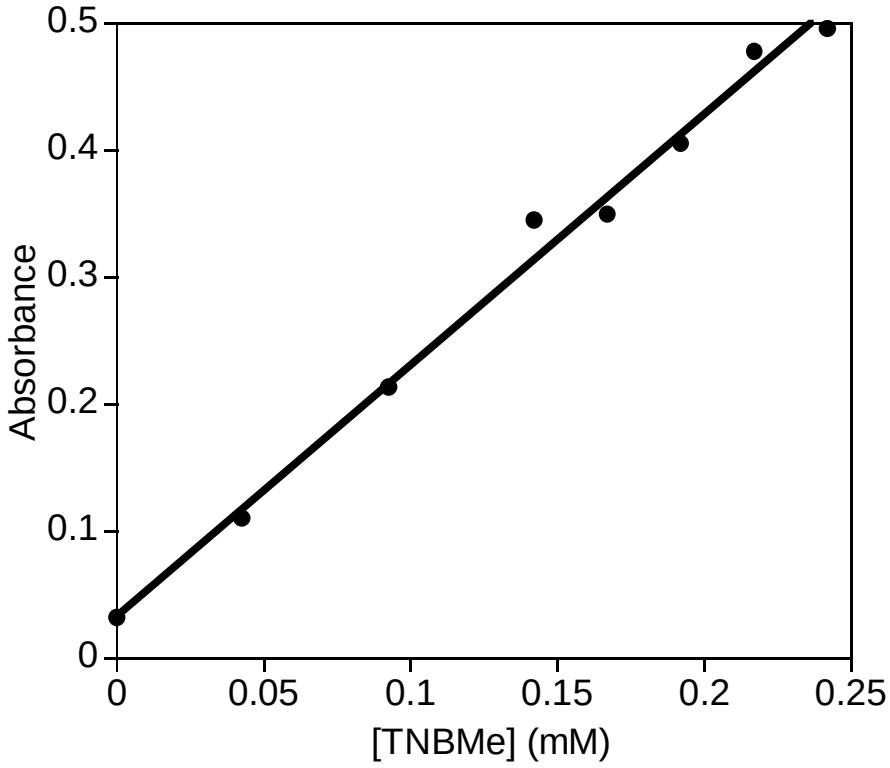


Figure 3.11: Plot of [TNBMe] (M, calculated by $[TNBMe]_0 - [HOCl]_0$) versus the A_{352} (circles) (using a 0.2 cm cell, data collected on HP8452A diode array), fit using linear equation y = 1.9735 x + 0.0336. Using Beer's law, A = ε*b*c, $\varepsilon = 9.8 \times 10^3\ M^{-1}cm^{-1}$ was determined.

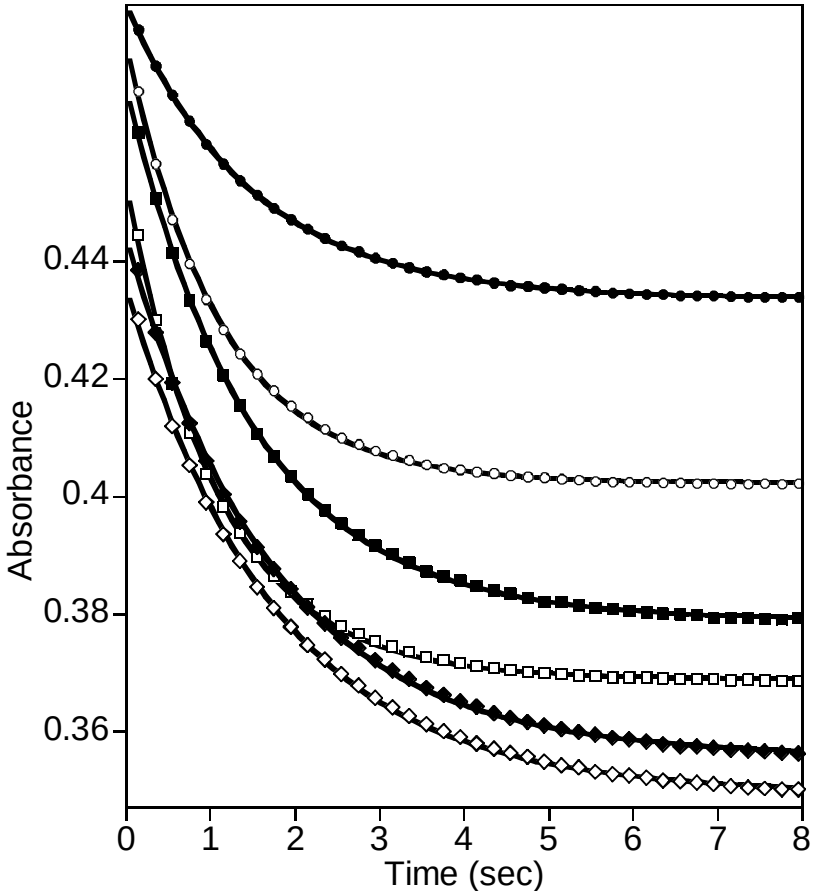


Figure 3.12: Reaction of 50 µM TNBMe with 10 µM HOCl (monitored at 352 nm). Data fit to first order reaction (solid line), trace from top to bottom (all done at pH = 7.4, top four traces (circles and squares) in 180 µM PBS (low buffer), bottom two traces (diamonds) in 50 mM PBS (high buffer), and solutions prepared with or without Cl^- added): (•)k_{obs} = 0.68 s^{-1} (TNBMe in low buffer, HOCl in water); (○)k_{obs} = 0.91 s^{-1} (TNBMe in low buffer, HOCl in water, 0.1 M Cl^-); (■)k_{obs} = 0.68 s^{-1} (TNBMe in low buffer, HOCl in low buffer); (□)k_{obs} = 0.91 s^{-1} (TNBMe in low buffer, HOCl in low buffer, 0.1 M Cl^-); (♦)k_{obs} = 0.58 s^{-1} (TNBMe in high buffer, HOCl made in water, 0.1 M Cl^-); (◊)k_{obs} = 0.57 s^{-1} (TNBMe in high buffer, HOCl made in high buffer, 0.1 M Cl^-). (Kinetic traces are offset by an absorbance of 0.01.)

Reaction of TNBMe with HOCl (under various experimental conditions), unfortunately turned up no evidence of formation of an intermediate. Figure 3.12 gives representative kinetic traces, all of which fit well to a first order reaction. As can be seen in figure 3.12, traces have subtle differences though all fit very well to a first order reaction. Sample conditions, such as chloride addition to modify the ionic strength, changes the rate slightly, but no evidence for any build up of an intermediate was obtained. From initial examination of the data, it did not appear to make a marked difference on the kinetics as to how HOCl was prepared (in buffer or water). Further examination of this, however, shows a possible effect of buffer on the reaction (figure 3.13).

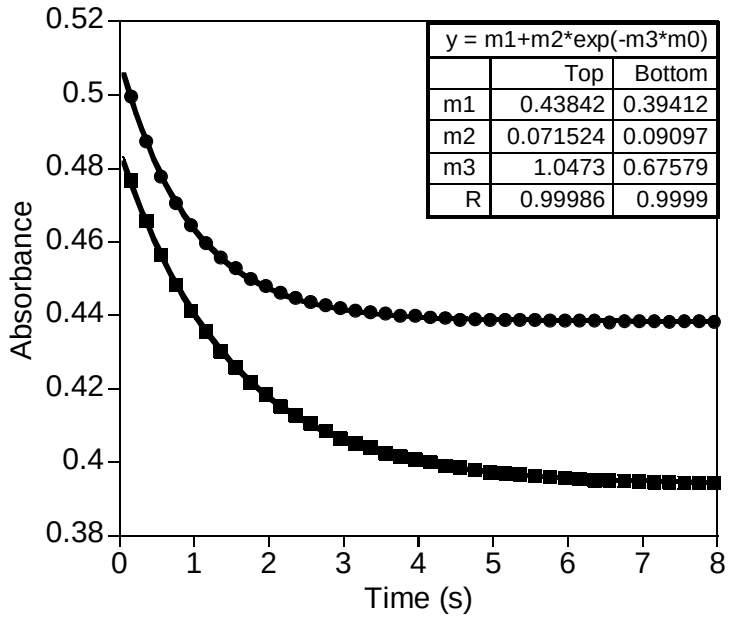


Figure 3.13: Reaction of 50 µM TNBMe with 10 µM HOCl Data (180 µM PBS, pH = 7.4), reaction data collected within 5 min of preparation of reactants (squares, bottom) and after 2 h (circles, top), both fit to first order equation (solid line); bottom ($t < 5$ min) $k_{obs} = 0.68\ s^{-1}$; top ($t > 2$ h) $k_{obs} = 1.0\ s^{-1}$.

Figure 3.13 compares reaction data for TNBMe + HOCl within five mins of preparation versus allowing the HOCl to age in buffer for around two hours, and then reacting with TNBMe. The reaction rate appears to increase as HOCl ages in the buffer (further experiments are needed to confirm that the difference in rates is more than experimental error). This observation can be explained as a slowly forming complex between HOCl and phosphate buffer; the longer the HOCl is stored in the buffer, the more complex could form (possibly forming an equilibrium although further investigation is necessary to confirm this). This HOCl-buffer complex and HOCl may react with TNBMe differently. Similar results were observed when both TNBMe and HOCl were prepared in buffer which contained chloride (180 µM PBS, 0.1 M Cl^-, at pH 7.4) ($t < 5$ min, $k_{obs} = 0.91$; $t > 2$ hours, $k_{obs} = 1.3$), but not observed when HOCl was prepared in water and reacted with TNBMe (in buffer).

Though not well represented in literature, inorganic phosphate is known to be oxidized by H_2O_2, forming a compound known as peroxymonophosphoric acid (52-53). It is conceivable that an analogous reaction occurs when phosphate is in the presence of HOCl. Though the possible formation of a new oxidant similar to peroxymonophosphoric acid is exciting and could play a role in reactions in which HOCl is stored in phosphate, we did not further investigate due to the unlikelihood of this reaction being biologically relevant (the reaction between inorganic phosphate and HOCl to form this compound is negligible in a biological setting compared to reactions of HOCl with other compounds).

3.4 Summary and conclusions

The rate constants for the reaction of HOCl with Met, MetO, DNPMet, and TNBMe have been measured. In general, HOCl reacts with thioethers, at neutral pH, with a second order rate constant of 10^{6}-10^{8} $M^{-1}s^{-1}$, consistent with those reported in literature (27,54-55). The reactions studied in this chapter unfortunately did not show conclusive evidence for the buildup of a chlorosulfonium intermediate. No biphasic kinetics was observed. In addition, polychromatic studies of the reaction of TNBMe with HOCl showed a “tight” isosbestic point, indicating a lack of detectable intermediate (50).

Taking the reaction of TNBMe with HOCl as an example, we can estimate the lifetime of the intermediate, though some assumptions are needed. An intermediate would likely have a similar absorbance spectrum to that of TNBMe (56). Since no buildup of an intermediate was observed, the rate constant for the intermediate must be at least 10 times faster than the reaction of TNBMe + HOCl, giving a half life of an intermediate less than 100 ms. With a half life of 100 ms at pH = 7, presumed to be the hydrolysis of the intermediate, the intermediate should be long enough lived to observe under stopped-flow conditions, if the intermediate has a distinguishable molar absorptivities. Though there is a lack of direct evidence for the reaction of HOCl with thioethers being able to produce a chlorosulfonium ion intermediate, estimated lifetimes should be sufficiently long enough to find conditions at which the intermediate can be observed.

3.5 Future experiments

- Find direct evidence for a chlorosulfonium intermediate
    - Study a simple thioether which has a distinctive spectrum for both the thioether and sulfoxide form of the compound. Vary experimental conditions to try and find evidence for an intermediate
        - Vary pH of reaction to try and find an intermediate
            - Lower pH should increase rate of reaction between thioether and HOCl and decrease rate of hydrolysis of an intermediate (biggest chance of finding an intermediate, however, one must consider solubility of the reactants; typically Met is not soluble at pH values that are less than its $pKa_{(COOH)}$
            - Higher pH should decrease rate of reaction between thioether and HOCl and increase rate of hydrolysis of an intermediate
        - Since rate constants for the reaction of HOCl with thioethers are 10^5-10^7 $M^{-1}s^{-1}$, a thioether which has a large extinction coefficient will aid in studying the reaction

- Study a system which produces the analogous sulfenyl chloride intermediate
    - Chlorosulfonium ($R\text{-}S^{+}(Cl)\text{-}CH_3$) intermediates carry a charge and may be shorter lived than their analogous sulfenyl chloride intermediates (R-S-Cl); studying sulfenyl chlorides may help in finding conditions in which chlorosulfonium ions are more stable
- Find a method of trapping the chlorosulfonium intermediate allowing it to be isolated and characterized
    - Search for chlorosulfonium intermediates *in vivo* as way of identifying which type of oxidant it originated from
- Determine if the analogous bromosulfonium or iodosulfonium intermediates can be formed and isolated
- Investigate the possible formation of a phosphate-HOCl complex, since a large number of studies are performed with HOCl in a buffered system; determine if this complex causes any interference in reactions of interest

3.6 References

(1) Levine, R. L.; Mosoni, L.; Berlett, B. S.; Stadtman, E. R. "Methionine residues as endogenous antioxidants in proteins." *Proceedings of the National Academy of Sciences of the United States of America* **1996**, *93*, 15036-15040.

(2) Levine, R. L.; Moskovitz, J.; Stadtman, E. R. "Oxidation of methionine in proteins: Roles in antioxidant defense and cellular regulation." *Iubmb Life* **2000**, *50*, 301-307.

(3) Brot, N.; Weissbach, H. "Biochemistry and physiological-role of methionine sulfoxide residues in proteins." *Archives of Biochemistry and Biophysics* **1983**, *223*, 271-281.

(4) Gonias, S. L.; Swaim, M. W.; Massey, M. F.; Pizzo, S. V. "Cis-dichlorodiammineplatinum(ii) as a selective modifier of the oxidation-sensitive reactive-center methionine in alpha-1-antitrypsin." *Journal of Biological Chemistry* **1988**, *263*, 393-397.

(5) Vogt, W. "Oxidation of methionyl residues in proteins - tools, targets, and reversal." *Free Radical Biology and Medicine* **1995**, *18*, 93-105.

(6) Atmaca, G. "Antioxidant effects of sulfur-containing amino acids." *Yonsei Medical Journal* **2004**, *45*, 776-788.

(7) Sistla, S.; Rao, D. N. "S-adenosyl-l-methionine-dependent restriction enzyme." *Critical Reviews in Biochemistry and Molecular Biology* **2004**, *39*, 1-19.

(8) Bentley, R. "Methionine and derivatives - exploring chirality at sulfur." *Biochemistry and Molecular Biology Education* **2005**, *33*, 274-276.

(9) Savige, W. E.; Fontana, A. "Interconversion of methionine and methionine sulfoxide." *Methods Enzymol* **1977**, *47*, 453-9.

(10) Fiedler, T. J.; Davey, C. A.; Fenna, R. E. "X-ray crystal structure and characterization of halide-binding sites of human myeloperoxidase at 1.8 angstrom resolution." *Journal of Biological Chemistry* **2000**, *275*, 11964-11971.

(11) Zeng, J.; Fenna, R. E. "X-ray crystal-structure of canine myeloperoxidase at 3 angstrom resolution." *Journal of Molecular Biology* **1992**, *226*, 185-207.

(12) Carpena, X.; Vidossich, P.; Schroettner, K.; Calisto, B. M.; Banerjee, S.; Stampler, J.; Soudi, M.; Furtmuller, P. G.; Rovira, C.; Fita, I.; Obinger, C. "Essential role of proximal histidine-asparagine interaction in mammalian peroxidases." *Journal of Biological Chemistry* **2009**, *284*, 25929-25937.

(13) Stadtman, E. R. "Protein oxidation and aging." *Free Radical Research* **2006**, *40*, 1250-1258.

(14) Sochaski, M. A.; Jenkins, A. J.; Lyons, T. J.; Thorpe, S. R.; Baynes, J. W. "Isotope dilution gas chromatography/mass spectrometry method for the determination of methionine sulfoxide in protein." *Analytical Chemistry* **2001**, *73*, 4662-4667.

(15) Schöneich, C. "Methionine oxidation by reactive oxygen species: Reaction mechanisms and relevance to alzheimer's disease." *Biochimica et Biophysica Acta (BBA) - Proteins & Proteomics* **2005**, *1703*, 111-119.

(16) Szuchman-Sapir, A. J.; Pattison, D. I.; Ellis, N. A.; Hawkins, C. L.; Davies, M. J.; Witting, P. K. "Hypochlorous acid oxidizes methionine and tryptophan residues in myoglobin." *Free Radical Biology and Medicine* **2008**, *45*, 789-798.

(17) Chapman, A. L. P.; Winterbourn, C. C.; Brennan, S. O.; Jordan, T. W.; Kettle, A. J. "Characterization of non-covalent oligomers of proteins treated with hypochlorous acid." *Biochemical Journal* **2003**, *375*, 33-40.

(18) Grunert, T.; Pock, K.; Buchacher, A.; Allmaier, G. "Selective solid-phase isolation of methionine-containing peptides and subsequent matrix-assisted laser desorption/ionisation mass spectrometric detection of methionine- and of methionine-sulfoxide-containing peptides." *Rapid Communications in Mass Spectrometry* **2003**, *17*, 1815-1824.

(19) Hsu, Y. R.; Narhi, L. O.; Spahr, C.; Langley, K. E.; Lu, H. S. "In vitro methionine oxidation of escherichia coli-derived human stem cell factor: Effects on the molecular structure, biological activity, and dimerization." *Protein Science* **1996**, *5*, 1165-1173.

(20) Weissbach, H.; Resnick, L.; Brot, N. "Methionine sulfoxide reductases: History and cellular role in protecting against oxidative damage." *Biochimica et Biophysica Acta, Proteins and Proteomics* **2005**, *1703*, 203-212.

(21) Luo, S.; Levine, R. L. "Methionine in proteins defends against oxidative stress." *Faseb Journal* **2009**, *23*, 464-472.

(22) Farber, J. M.; Levine, R. L. "Sequence of a peptide susceptible to mixed-function oxidation - probable cation binding-site in glutamine-synthetase." *Journal of Biological Chemistry* **1986**, *261*, 4574-4578.

(23) Davies, M. J. "The oxidative environment and protein damage." *Biochimica Et Biophysica Acta-Proteins and Proteomics* **2005**, *1703*, 93-109.

(24) Schoneich, C.; Aced, A.; Asmus, K. D. "Mechanism of oxidation of aliphatic thioethers to sulfoxides by hydroxyl radicals - the importance of molecular-oxygen." *Journal of the American Chemical Society* **1993**, *115*, 11376-11383.

(25) Brunelle, P.; Schoneich, C.; Rauk, A. "One-electron oxidation of methionine peptides - stability of the three-electron s-n(amide) bond." *Canadian Journal of Chemistry-Revue Canadienne De Chimie* **2006**, *84*, 893-904.

(26) Miller, B. L.; Kuczera, K.; Schoneich, C. "One-electron photooxidation of n-methionyl peptides. Mechanism of sulfoxide and azasulfonium diastereomer formation through reaction of sulfide radical cation complexes with oxygen or superoxide." *Journal of the American Chemical Society* **1998**, *120*, 3345-3356.

(27) Armesto, X. L.; Canle L, M.; Fernandez, M. I.; Garcia, M. V.; Santaballa, J. A. "First steps in the oxidation of sulfur-containing amino acids by hypohalogenation: Very fast generation of intermediate sulfenyl halides and halosulfonium cations." *Tetrahedron* **2000**, *56*, 1103-1109.

(28) Hawkins, C. L.; Pattison, D. I.; Davies, M. J. "Hypochlorite-induced oxidation of amino acids, peptides and proteins." *Amino Acids* **2003**, *25*, 259-274.

(29) Wilson, G. E., Jr. "Fragmentations of halosulfonium salts and related reactions. Role of sulfenyl intermediates." *Quarterly Reports on Sulfur Chemistry* **1967**, *2*, 313-17.

(30) Choudhary, K.; Suri, D.; Kothari, S.; Banerji, K. K. "Kinetics and correlation analysis of reactivity in oxidation of organic sulfides by hexamethylenetetramine-bromine." *Journal of Physical Organic Chemistry* **2000**, *13*, 283-292.

(31) Wilson, G. E., Jr.; Huang, M. G. "Sulfonium salts. Iv. Cleavage--alpha -substitution competition of dibenzylhalosulfonium salts." *Journal of Organic Chemistry* **1970**, *35*, 3002-7.

(32) Wilson, G. E., Jr. "Structure and reactivity of halosulfonium salts." *Tetrahedron* **1982**, *38*, 2597-625.

(33) Allegra, G.; Wilson, G. E., Jr.; Benedetti, E.; Pedone, C.; Albert, R. "Structure of a halosulfonium salt. The 1:1 adduct of thiophane with bromine." *Journal of the American Chemical Society* **1970**, *92*, 4002-7.

(34) Beal Jennifer, L.; Foster Steven, B.; Ashby Michael, T. "Hypochlorous acid reacts with the n-terminal methionines of proteins to give dehydromethionine, a potential biomarker for neutrophil-induced oxidative stress." *Biochemistry* **2009**, *48*, 11142-8.

(35) Moskovitz, J.; Bar-Noy, S.; Williams, W. M.; Berlett, B. S.; Stadtman, E. R. "Methionine sulfoxide reductase (msra) is a regulator of antioxidant defense and lifespan in mammals." *Proceedings of the National Academy of Sciences of the United States of America* **2001**, *98*, 12920-12925.

(36) Moskovitz, J.; Rahman, M. A.; Strassman, J.; Yancey, S. O.; Kushner, S. R.; Brot, N.; Weissbach, H. "Escherichia-coli peptide methionine sulfoxide reductase gene - regulation of expression and role in protecting against oxidative damage." *Journal of Bacteriology* **1995**, *177*, 502-507.

(37) Douglas, T.; Daniel, D. S.; Parida, B. K.; Jagannath, C.; Dhandayuthapani, S. "Methionine sulfoxide reductase a (msra) deficiency affects the survival of mycobacterium smegmatis within macrophages." *Journal of Bacteriology* **2004**, *186*, 3590-3598.

(38) St John, G.; Brot, N.; Ruan, J.; Erdjument-Bromage, H.; Tempst, P.; Weissbach, H.; Nathan, C. "Peptide methionine sulfoxide reductase from escherichia coli and mycobacterium tuberculosis protects bacteria against oxidative damage from reactive nitrogen intermediates." *Proceedings of the National Academy of Sciences of the United States of America* **2001**, *98*, 9901-9906.

(39) Moskovitz, J.; Berlett, B. S.; Poston, J. M.; Stadtman, E. R. "The yeast peptide methionine sulfoxide reductase functions as an antioxidant in vivo." *Proceedings of the National Academy of Sciences of the United States of America* **1997**, *94*, 9585-9589.

(40) Moskovitz, J.; Flescher, E.; Berlett, B. S.; Azare, J.; Poston, J. M.; Stadtman, E. R. "Overexpression of peptide-methionine sulfoxide reductase in saccharomyces cerevisiae and human t cells provides them with high resistance to oxidative stress." *Proceedings of the National Academy of Sciences of the United States of America* **1998**, *95*, 14071-14075.

(41) Ruan, H.; Tang, X. D.; Chen, M. L.; Joiner, M. A.; Sun, G.; Brot, N.; Weissbach, H.; Heinemann, S. H.; Iverson, L.; Wu, C. F.; Hoshi, T. "High-quality life extension by the enzyme peptide methionine sulfoxide reductase." *Proceedings of the National Academy of Sciences of the United States of America* **2002**, *99*, 2748-2753.

(42) Gabbita, S. P.; Aksenov, M. Y.; Lovell, M. A.; Markesbery, W. R. "Decrease in peptide methionine sulfoxide reductase in alzheimer's disease brain." *Journal of Neurochemistry* **1999**, *73*, 1660-1666.

(43) Pryor, W. A.; Dooley, M. M.; Church, D. F. "Inactivation of human alpha-1-proteinase inhibitor by gas-phase cigarette-smoke." *Biochemical and Biophysical Research Communications* **1984**, *122*, 676-681.

(44) Krishnan, S.; Chi, E. Y.; Wood, S. J.; Kendrick, B. S.; Li, C.; Garzon-Rodriguez, W.; Wypych, J.; Randolph, T. W.; Narhi, L. O.; Biere, A. L.; Citron, M.; Carpenter, J. F. "Oxidative dimer formation is the critical rate-limiting step for parkinson's disease alpha-synuclein fibrillogenesis." *Biochemistry* **2003**, *42*, 829-837.

(45) Hokenson, M. J.; Uversky, V. N.; Goers, J.; Yamin, G.; Munishkina, L. A.; Fink, A. L. "Role of individual methionines in the fibrillation of methionine-oxidized alpha-synuclein." *Biochemistry* **2004**, *43*, 4621-4633.

(46) Anbar, M.; Dostrovsky, I. "Ultra-violet absorption spectra of some organic hypohalites." *Journal of the Chemical Society* **1954**, 1105-1108.

(47) Kettle, A. J.; Winterbourn, C. C. "The mechanism of myeloperoxidase-dependent chlorination of monochlorodimedon." *Biochimica et Biophysica Acta* **1988**, *957*, 185-91.

(48) Levy, A. L.; Chung, D. "A simplified procedure for the synthesis of 2,4-dinitrophenyl(dnp)-amino acids." *Journal of the American Chemical Society* **1955**, *77*, 2899-2900.

(49) Fogelman, K. D.; Walker, D. M.; Margerum, D. W. "Nonmetal redox kinetics: Hypochlorite and hypochlorous acid reactions with sulfite." *Inorganic Chemistry* **1989**, *28*, 986-93.

(50) Nagy, P.; Jameson, G. N. L.; Winterbourn, C. C. "Kinetics and mechanisms of the reaction of hypothiocyanous acid with 5-thio-2-nitrobenzoic acid and reduced glutathione." *Chemical Research in Toxicology* **2009**, *22*, 1833-1840.

(51) Peskin, A. V.; Midwinter, R. G.; Harwood, D. T.; Winterbourn, C. C. "Chlorine transfer between glycine, taurine, and histamine: Reaction rates and impact on cellular reactivity." *Free Radical Biology and Medicine* **2004**, *37*, 1622-1630.

(52) Battagli.Cj; Edwards, J. O. "Dissociation constants and kinetics of hydrolysis of peroxymonophosphoric acid." *Inorganic Chemistry* **1965**, *4*, 552-&.

(53) Sanchez, M.; Hadasch, A.; Fell, R. T.; Meunier, B. "Key role of the phosphate buffer in the h2o2 oxidation of aromatic pollutants catalyzed by iron tetrasulfophthalocyanine." *Journal of Catalysis* **2001**, *202*, 177-186.

(54) Pattison, D. I.; Davies, M. J. "Absolute rate constants for the reaction of hypochlorous acid with protein side chains and peptide bonds." *Chemical Research in Toxicology* **2001**, *14*, 1453-1464.

(55) Winterbourn, C. C. "Comparative reactivities of various biological compounds with myeloperoxidase-hydrogen peroxide-chloride, and similarity of the oxidant to hypochlorite." *Biochimica et Biophysica Acta* **1985**, *840*, 204-10.

(56) Ueki, H.; Chapman, G.; Ashby, M. T. "Reactive sulfur species: Kinetics and mechanism of the oxidation of aryl sulfinates with hypochlorous acid." *Journal of Physical Chemistry A* **2010**, *114*, 1670-1676.

Chapter 4: Oxidation of Methionine by Halogens to Produce the Potential Biomarker Dehydromethionine.[1]

4.1 Introduction

4.1.1 Oxidation of proteins

Virtually all biological molecules (e.g. lipids, DNA, RNA, carbohydrates, cholesterol, and proteins) are susceptible to reactive oxidants produced *in vivo*, which include one electron oxidants (e.g. radicals) and two electron oxidants (e.g. hypohalites). Reactions of oxidants with biological molecules can cause a variety of modifications. These modifications cause different degrees of damage, often leading to a loss of function, degradation of the protein, and progression of various diseases. Diseases associated with protein damage include atherosclerosis, chronic inflammation, and some cancers (1). The extent of the damage depends on the rate at which an oxidant reacts with a potential target (i.e. concentration of the target and rate constant for reaction of oxidant with target) as well as the body's ability to regulate the extent of the reaction. Regulation of reaction depends on several factors such as location of target in relation to site of oxidant formation, the availability of oxidant-scavenging reactions (i.e. antioxidants), occurrence of transfer reactions, and ability of the body to repair damage done as a consequence of the reaction. In the biological system (e.g. tissue, cellular fluid, and biological fluid such as plasma), proteins comprise the majority of the dry weight of cells, up to 70% (2-

[1] The work that is described in this chapter has been published: Beal J.L, Foster S.B., Ashby M.T. "Hypochlorous Acid Reacts with the N-Terminal Methionines of Proteins to Give Dehydromethionine, a Potential Biomarker for Neutrophil-Induced Oxidative Stress." *Biochemistry*. **2009**;*48*:11142-8.

3). The large abundance along with their high reactivity with a variety of oxidants makes proteins a major target of oxidants. Different amino acid residues of the protein are more or less susceptible to different oxidants. In general, Trp, Tyr, His, Met, Cys, Phe, and Arg residues are most reactive towards oxidants along with the protein backbone (4).

A large number of rate constants are available in the literature for amino acids with different oxidants under a variety of different experimental condition. This includes a database devoted to solution kinetics (5). Knowledge of the rate constant of an oxidant with the various amino acid residues is helpful in developing computational models that might be used to predict which sites of a protein will undergo oxidation. However, such models must be considered to be approximate, since knowledge of rate constants alone do not allow for inclusion of other determining factors of reactivity (e.g. location, since amino acids buried within the protein will be harder to oxidize then those on the surface). Likewise, kinetic data for the oxidation of the protein with a particular oxidant is limited in its utility. The constants predict the overall rate of reaction but do not give information on selectivity of the oxidant with respect to the different sites of the protein (4).

A variety of techniques have been used to examine the oxidative damage of proteins. A recent review by Hawkins *et al.* (3) points out that most of the methods currently employed are chosen based on the ease of use instead of the importance, and lead to qualitative data, not quantitative, making comparison between different research groups difficult. Oxidized proteins are

typically digested into smaller fragments and then separated and analyzed using GS/MS, LC/MS, or LC/UV-vis (3,6-7). A few of the more commonly used techniques are discussed here.

Analysis of oxidized proteins through its digestive products is the most commonly used method of analysis. Digestion can either be a total, which cleaves all amino acid bonds, or enzymatic, which cleaves only certain amino acid bonds as determined by the type of enzyme used.

Total digestion uses elevated temperatures and either strong acidic or basic conditions, which hydrolyzes the protein into its individual amino acids. Amino acids can then be analyzed directly using Ion Chromatography (8) or derivatized with a chromophore, such as *o*-phthalidialdehyde (OPA), and analyzed by HPLC (3). Advantages of this method include high sensitivity (micro-molar concentration) and experience of being a well understood method. A disadvantage of this method is lack of specificity, so if a protein has two of the same amino acid residue, one cannot be distinguished from the other. Another disadvantage is that problems exist for analyzing certain amino acids. For example Cys and Met are often oxidized during the hydrolysis if care is not taken to rid the system of oxygen. Also, some amino acids are unstable during hydrolysis conditions (e.g. tryptophane) which can lead to misinterpretation of results (3,9).

Digestion is also done using enzymes that cleave the protein at specific peptide bonds. Trypsin, for example, cleaves a peptide bond at the carboxyl side of lysine or arginine (except when either is followed by proline). Unlike total

digestion, products of enzymatic digestion leave peptides, and not individual amino acids. Peptides resulting from the enzyme digestion are typically analyzed using LC/MS (10). Enzymatic digestion has the advantage of using milder conditions (typically 37 ℃ and pH = 7.4; Cys and Met are not likely to be oxidized during the enzymatic digestive process), as well as providing specific information about which residues are modified (peptides not individual amino acids are analyzed) and what modification occurred (based on mass changes). A disadvantage of this method is the possible trouble in separation of peptides. The more complex (i.e. large number of peptides) and less purified the protein, the harder it may be to separate and identify the individual peptides. Also, enzymatic digestion itself may be problematic due to some proteins (e.g. ubiquitin (Ub) (11)) being resistant to digestion as well as possible self digestion of the enzyme resulting in more peptides peaks to separate and possibly complicating analysis (3).

Due to new technological advances, a less common method, yet steadily growing field, for analysis of oxidized protein is analysis of the intact (undigested) protein. Direct analysis of the oxidized protein would have several advantages over digestive methods, including reduced cost in sampling which allows for higher through-put in sample analysis. Also, though methods are developed in the digestive process to avoid unwanted sample modification (e.g. oxidation of Met or Cys), the fewer additional steps during sample preparation the less chance of having unwanted modifications to the protein. Analysis of intact oxidized protein is being done using NMR spectroscopy (both 1D and

2D). A major disadvantage of NMR analysis is the low sensitivity of NMR spectroscopy (compared to MS). Low sensitivity can be overcome by isotopically labeling the protein before analysis; however, labeling leads to higher sample costs. NMR spectroscopy has the advantage of high reproducibility along with non-destructiveness, so the same sample can be run using various NMR sampling techniques without the need to remake samples, as well as allowing for analysis of the same sample through additional methods such as MS (6,12-13). Intact oxidized proteins are sometimes analyzed by other methods such as UV-vis spectroscopy, electron paramagnetic resonance (EPR), electrospray ionization (ESI) mass spectrometry, or matrix-assisted laser desorption/ionization (MALDI) mass spectrometry; however, these methods give information about changes to the protein as a whole, and not to specific sites of the protein (3,6).

Whether proteins are oxidized by radicals or non-radicals, there tends to be specific modification to the protein that researchers look for during analysis. Select amino acids that are highly susceptible to oxidation include Cys, Tyr, Met, and Lys, and are often tested for modification in the protein product. Ptolemy *et al.* (7) and Hawkins *et al.* (3) have written reviews discussing the amino acids that are susceptible to oxidation as well as potential products of oxidation. For example Cys, which exists in proteins as either the Cys (-SH) or cystine (-S-S-), produces the oxidative products sulfinic and sulfonic acid (14). When oxidation of protein occurs by HOCl, Tyr residues are oxidized to monochloro-tyrosine or dichloro-tyrosine.

4.1.2 Biomarkers of oxidation by halogenating agents

Neutrophils, the body's first line of defense against invading pathogens, is a major source of the reactive oxidants and are likely contributors to the oxidative damage associated with inflammatory diseases (15). Neutrophils possess both oxidative and non-oxidative defense mechanisms. Their oxidative defense mechanisms are implicated in the oxidative stress that is associated with many inflammatory diseases, including atherosclerosis (16). Activated neutrophils generate superoxide and H_2O_2 at sites of inflammation via a respiratory burst (1). In addition, MPO is released. MPO is a heme enzyme that utilizes H_2O_2 to oxidize a variety of substrates, namely halides and pseudo-halide ions to generate the ROS HOCl, HOBr, and HOSCN (17-18). MPO is believed to play a central role in many inflammatory diseases (18-21). Methods commonly used to characterize the end products (i.e. targets) of protein oxidation were discussed earlier; however, characterization of the specific oxidants responsible for a given modification of the biomolcules is far more challenging since these reactive oxidants, mainly radicals and ROS, that are associated with biomolecular oxidation are extremely short lived, making direct measurement of them *in vivo* extremely challenging (17,22). As a consequence, considerable research has gone into identifying suitable biomarkers of specific oxidants (15,22). A good biomarker needs to be specific for the reactive species studied as well as both chemically and biologically stable. The target of oxidation needs to have a high enough concentration and reactivity towards the oxidant so that the biomarker can be produced in a large enough quantity to be

detected (17). Identification of biomarkers is important in both determining the extent of oxidative damage as well as possibly identifying the nature of the oxidant that has caused the damage. Biomarkers can provide information that would allow for development of antioxidant therapies to prevent further injury, possibly preventing, or at very least delaying, the onset of inflammatory diseases like atherosclerosis (23).

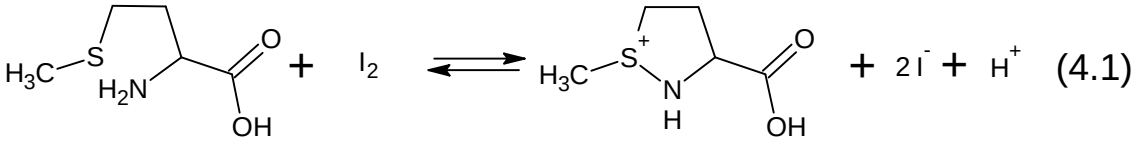
Much effort in the last decade has been put into developing potential biomarkers that uniquely assesses the possible involvement of MPO in the development of inflammatory diseases, in particular the involvement of the ROS HOCl (15,17-18,21,24-26). Neutrophilic MPO is the only naturally occurring mammalian enzyme that is capable of oxidizing Cl^- to HOCl at a significant rate under physiological conditions. HOCl is capable of regulating the inflammatory response by both stimulating and repressing inflammatory mediators. Inflammatory response is critical in the resolution of infection, but overstimulation of neutrophils is a likely contributor to host tissue damage. Therefore, HOCl can be both beneficial and destructive, which accounts for the considerable interest in identifying biomarkers that uniquely assess the involvement of HOCl *in vivo*. A recent review by Winterbourn *et al.* lists the advantages and disadvantages of existing biomarkers for MPO-derived HOCl, which include chlorinated tyrosine (3-TyrCl and 3,5-$TyrCl_2$), lipid chlorohydrins, 5-chlorocytosine, protein carbonyls, and a sulfonamide derivative of glutathione (GSA) (15,27). GSA, characterized and discussed in more detail by Harwood *et al.* (28), is of particular interest as an attractive biomarker for HOCl because

thiols (e.g. glutathione, the precursor to GSA) are among the first chemical targets of HOCl in a biological setting (29). Thioethers are as reactive towards HOCl as thiols. For the thioether Met, it has been suggested that the sulfoxide (MetO) is the final product of oxidation by hypohalous acids (30-37). Studies involving the oxidation of Met by I_3^-, however, show the formation of an intermediate called dehydromethionine (DHM), which is slowly hydrolyzed to the expected MetO product (38-45). We suspected that in addition to oxidation by triiodide, DHM is formed from the oxidation of Met by other halogenating agents such as HOCl and HOBr, which would make it an attractive biomarker for oxidation of Met by halogenating agents.

4.1.3 Dehydromethionine

Prior to 2009, a literature search for DHM results in a little over a dozen papers published, with the latest of which being more then 10 years ago (38-57). DHM was first identified and isolated in 1945 by Lavine (44) from the oxidation of Met with iodine. The product of the reaction was iodine-free and differed from Met by the loss of two hydrogens atoms. In addition, Lavine discovered that the reaction was reversible, regenerating iodine. Lavine found the product (DHM) to be extremely hygroscopic. At pH 7 in aqueous solution, DHM slowly hydrolyzes to MetO. Hydrolysis is accelerated by phosphate and other buffers, as well as acidic and alkaline conditions. Due to the ease of formation of DHM as well as the high stability at neutral pH, Lavine suggested that it may have biological importance (44).

Gensch *et al.* (58) performed a detailed kinetic study of the oxidation of Met by iodine to form DHM (4.1).

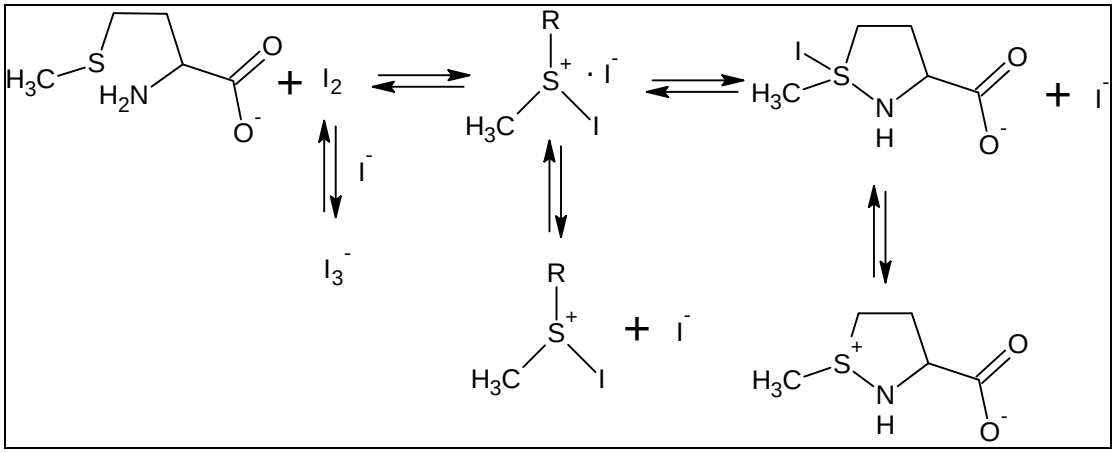


(4.1)

In this study the rate constant for both the forward (formation of DHM) and reverse (reduction of DHM) reactions were determined independently. The rate constant for the forward reaction, oxidation of Met by iodine, was determined to be 6.5×10^5 $M^{-1}s^{-1}$, and the rate constant of the reverse reaction is 27 $M^{-3}s^{-1}$. Reaction rates were found to be dependent on the pH, concentration of iodide, and buffer concentration. The reaction rate for the forward reaction (in a buffered system) was found to increase with an increase in pH (linear between pH 4 and 8), which the authors suggested could be due to the involvement in the mechanism of the free amino group (with pK_a of about 9). In addition, the forward reaction rate is found to be inversely dependent on the concentration of iodide. Iodine, the reactive form of the oxidant, is only slightly soluble in aqueous solutions and instead exists as triiodide (I_3^-). The higher the iodide concentration the more the oxidant exists in the nonreactive form, I_3^-. The rate of the reverse reaction (reduction of DHM), was found to increase with both a decrease in pH (pH 0 to 6) and an increase in iodide concentration [as expected from the equilibrium reaction shown in (4.1)]. Gensch examined two possible mechanisms by which Met oxidation could occur: by iodine attack on either the amine or the alkyl sulfide. A mechanism involving Met oxidation through the amine was supported by experimental data for the forward reaction but not the

reverse reaction. On the other hand, the data supported a mechanism involving oxidation through sulfur for the reverse reaction but not the forward reaction (58). This was further investigated by Young and Hsieh ten years later (56). These authors show that at high buffer concentrations the reaction approaches an inverse-squared dependence on iodide concentration; however, at low concentrations of buffer, the reaction is inversely dependent on concentration of iodide ion. A mechanism that has an inverse-squared dependence on iodide can be explained by a simple scheme that involves Met oxidation by iodine to form iodosulfonium ion that can either be reduced back to Met by addition of iodide or go through ring close (through deprotonated amine) to produce DHM. An inverse dependence is due to the iodine-triiodide equilibrium, while the other inverse dependence is due to reversal of the reaction by attack of iodide on the iodosulfonium ion. Young and Hsieh proposed the mechanism for the formation of DHM (4.1) which takes into account their experimental observations, including dependence on iodide changes with buffer concentration, buffer catalyses the rate of reaction, and the reaction goes to completion rather than equilibrium [contrary to findings by Gensch *et al*. (58)]. Young and Hsieh conclude that at high buffer concentrations, the buffer catalyzed formation of the tetra-coordinated sulfurane is involved as an intermediate and that breakdown of this intermediate to form DHM becomes rate limiting. However, at low buffer concentrations, the dissociation of the iodosulfonium ion-iodide complex must be slow with respect to reduction (to form Met back) and ring closure (leading to DHM formation) (56).

Scheme 4.1: Young's mechanism which supports evidence of base catalysis involvement in production of DHM



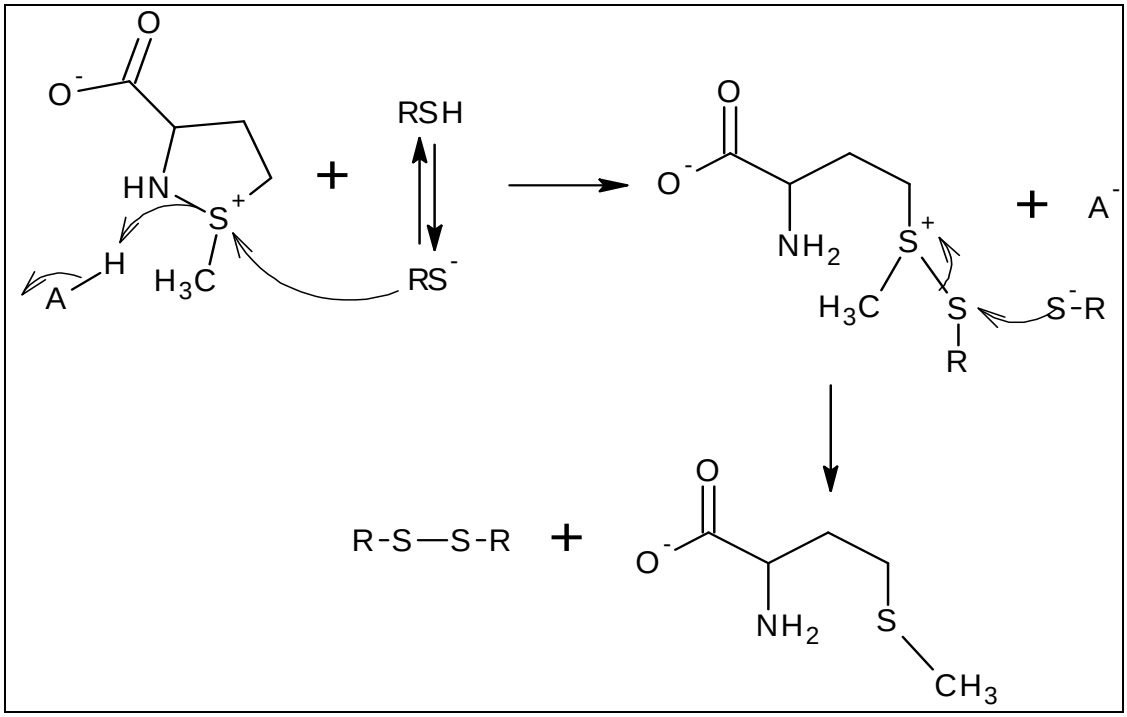
In 1976, a little over 30 years after DHM was first discovered by Lavine (44), Glass and Duchek verified the structure of DHM through X-ray crystallography (42). They concluded that the sulfur atom of DHM was trivalent and that the geometry around the nitrogen is sp^3 hybridized, indicating a single bond between the sulfur and nitrogen. Based on information obtained, Glass and Duchek concluded that the structure originally assigned by Lavine in 1945 (44) was indeed correct (42).

With limited studies appearing in literature, methods previously used to quantify DHM formation are limited. Determination of the presence of DHM has been reported by two methods: 1) indirectly through addition of iodide and acid and subsequently quantifying amount of iodine liberated (58-59) or 2) directly through ^{1}H NMR (39-40). Fortunately DHM has a distinctive $-^+$S-CH_3 NMR chemical shift from that of Met (–S-CH_3) and MetO (–S(O)-CH_3), allowing direct determination of the presence of DHM. In addition to the chemical shift, DHM

shows up as two distinctive peaks, due to the two diastereomers formed (39-40).

Only two papers have been found that discuss reactions of DHM (43,51). In a detailed study by Lambeth (43), DHM has been shown to be reduced by thiols (DTT: dithiothreitol, TNB: thionitrobenzoate, TNP: thionitrophyridine), a reaction that is accelerated many-fold by buffers. Reduction of DHM by the thiol requires a 1:2 ratio; a disulfide is produced from the thiol (scheme 4.2) (43). The rate constant for reduction of DHM by DTT, for example, is 0.3 $M^{-1}s^{-1}$ (0.1 M phosphate, pH = 7). Lambeth concluded that reduction of DHM by biologically relevant thiols, such as Cys and glutathione, may limit the lifetime of DHM and therefore it's biological importance (43). Young and Briedis, just ten years after the study by Lambeth (43), followed up on this statement and investigated the reduction of DHM by glutathione (GSH). The rate constant for the reduction of DHM by GSH was found to be 0.305 $M^{-1}min^{-1}$. Thus in the presence of physiological concentrations of GSH, Young and Briedis estimated the half-life of DHM be from 33-330 mins. The authors conclude by stating "a compound with a half-life ranging between 0.5-5 hours is a prime candidate for *in vivo* functions, suggesting that the possibility that DHM may exist as a natural product should be re-examined (51)."

Scheme 4.2: Lambeth's proposed mechanism for the reduction of DHM by thiols



In literature, DHM formation is most often produced from oxidation of Met by iodine, a two electron process (38-40,42-45). However, DHM has been shown to form in other reactions as well. Chloramine-B oxidation of a small peptide containing a *N*-terminal Met has been shown to form DHM (40). The photo-oxidation of Met by singlet oxygen produces a persulfoxide intermediate that ring closes forming DHM (47,55). Fenton reagents have been found to form DHM, a reaction involving two sequential one-electron steps. These reactions occur when reactive radicals such as hydroxyl and halogen radicals oxidize Met to a sulfide radical cation (40,54), stabilized intramolecularly via a three electron S-N bond (50). Without a reaction partner, this intermediate decomposes

rapidly on the microsecond timescale. In order for DHM to be produced from the sulfide radical cation, the one-electron oxidized intermediate must be trapped before it can decompose. The most efficient trapping agents are radicals, such as superoxide. Reaction of superoxide with the sulfide radical cation forms sulfoxide, not DHM. However, triplet oxygen ($^3O_2$) can react with the intermediate to form DHM. Despite this information, it is not known if these two sequential one-electron steps to produce DHM are kinetically competent with the two electron oxidants (27). That being said, there are no reports of DHM production in proteins upon reaction with either one or two electron oxidants.

4.2 Experimental methods

4.2.1 Materials

All chemicals were A.C.S certified grade or better and were used without further purification. 18.2 MΩ•cm water, obtained from a Millipore Milli-Q A10 ultrapure water purification system, was used for all experiments. Unless otherwise noted, all solutions contained 0.1 M phosphate buffer at pH 7.4, which was prepared from $NaH_2PO_4•H_2O$ and Na_2HPO_4 (used as received from Mallinckrodt). Deuterium oxide (99.9%) and Acetonitrile-d_3 were obtained from Cambridge Isotope Laboratories. Ub from bovine erythrocyte (≥98% by SDS-PAGE, essentially salt-free, lyophilized powder), chloramine-T hydrate (98%), DL-methionine (>99%), taurine (99%), anti-inflammatory peptide 1 (antiflammin-1), H_2O_2 (30 wt %), urea, calcium chloride (powder >97%), and bromine were all obtained from Sigma-Aldrich. *N*-acetyl-L-methionine (>99%) was obtained from

Fluka. Sodium iodide, sodium bromide, and sodium nitrite were obtained from EMD Chemicals. Iodine was obtained from Fisher Scientific. DSS (sodium 2,2-dimethyl-2-silapentane-5-sulfonate) was obtained from TCI chemicals. Sequencing grade trypsin (SA>18,900 units/mg) was obtained from Promega. The *N*-terminal hexapeptide NH_2-Met-Gln-Ile-Phe-Val-Lys-COOH (Ub1-6), purity >95%, was synthesized by the Molecular Biology Proteomic Facility at the University of Oklahoma Health Science Center. pH/pD was adjusted with NaOH, NaOD, HCl, or DCl as required.

4.2.2 Sample preparation

4.2.2.1 Preparation of oxidant stock solutions

The concentration of H_2O_2 in stock solutions was determined spectrophotometrically at 240 nm (ε_{240} = 43.6 $M^{-1}cm^{-1}$) (60). Stock solutions of NaOCl were prepared by sparging Cl_2 into a 2.1 M solution of NaOH. The sparging was stopped when the [OCl^-] achieved ca. 0.99 M (pH > 12), as determined spectrophotometrically at 292 nm (ε_{292} = 350 $M^{-1}cm^{-1}$) (61). Stock solutions of NaOBr were prepared by two methods. In both cases, the solutions of OBr- were standardized spectrophotometrically at 329 nm (ε_{329}= 332 $M^{-1}cm^{-1}$) (61). The first method consisted of adding a 5-fold excess of NaBr to a solution of NaOCl. This reaction mixture was stored in the dark for 5 min before determining its concentration spectrophotometrically. The second method consisted of adding Br_2 to an ice-cold solution of NaOH. All solutions of OBr- were kept at 0 ℃ and used within two hours of their preparations to minimize

errors due to decomposition (62). Stock solutions of $ONOO^-$ were prepared by a method adapted from Koppenol *et al.* (63) Briefly, ice-cold solutions of $NaNO_2$ in water and H_2O_2 in 1 M HCl were rapidly combined with a hand-mixer (comprised of two Hamilton syringes and a T-mixer). The effluent of the hand-mixer was added directly into a stirring solution of 1.1 M NaOH. The concentration of $ONOO^-$ was determined spectrophotometrically (ε_{302} = 1670 $M^{-1}cm^{-1}$) (64). Aqueous I_3^- stock solutions were prepared by addition of I_2 to a stirring solution of 10-fold excess NaI. After all the I_2 dissolved, the concentration of I_3^- was determined spectrophotometrically (ε_{353} = 26,400 $M^{-1}cm^{-1}$) (65). Taurine monohaloamine (TauX, X = Cl or Br) and dihaloamine ($TauX_2$, X = Cl or Br) stock solutions were prepared by methods similar to Thomas *et al.* (66). Briefly, TauX (X = Cl or Br) was prepared by drop-wise addition of the hypohalite solution (OBr^- was prepared by the Br_2/NaOH method as described previously) into an equimolar amount of vortexed taurine in 0.1 M NaOH. $TauX_2$ (X = Cl or Br) was prepared by drop-wise addition of the hypohalite solution to a vortexed taurine (half molar equivalent) in water. Immediately after mixing, the pH was lowered to pH < 5 by addition of HCl, in order to encourage the disproportionation of TauX to $TauX_2$. After 30 min in the dark, the concentrations of the haloamines were determined spectrophotometrically: $\varepsilon(TauCl)_{252}$ = 429 $M^{-1}cm^{-1}$ (66), $\varepsilon(TauCl_2)_{300}$ = 370 $M^{-1}cm^{-1}$ (66), $\varepsilon(TauBr)_{288}$ = 430 $M^{-1}cm^{-1}$ (67), and $\varepsilon(TauBr_2)_{336}$ = 371 $M^{-1}cm^{-1}$ (67). $OSCN^-$ was generated by the LPO-catalyzed oxidation of SCN^- by H_2O_2 at pH 7.4 (68). The SCN^- and LPO were incubated in a 0.1 M

phosphate buffer at 20 ℃, and the reaction was initiated by the addition of H_2O_2. The concentration of $OSCN^-$ was determined spectrophotometrically at 376 nm (ε_{376} = 26.5 $M^{-1}cm^{-1}$) (68).

4.2.2.2 Reaction of free methionine with oxidants

A 75 mM stock solution of Met was prepared in 0.5 M phosphate buffer, pH = 7.4. While vortexing, 400 µL of the oxidant (diluted to the desired concentration with water prior to the reaction) was added drop-wise to 400 µL of the Met solution. After a period of time (< 10 min for halogenating reagents and ca. 3 h for $ONOO^-$, $OSCN^-$, and H_2O_2), 200 µL of D_2O (20% deuterium to lock and shim) containing DSS (the NMR internal standard) was added. The final pH of the solutions was between 7.4-7.6.

4.2.2.3 Reaction of antiflammin-1 and Ub1-6 with oxidants

Stock solutions of the peptides were prepared by dissolving the lyophilized peptide in a 50/50 mixture of water and deuterated acetonitrile-d_3. The peptides were further diluted (to achieve a peptide concentration ca. 100 µM) by addition of a 0.1 M deuterated phosphate buffer (pH 7.4), made by adding DCl to D_2O solutions of anhydrous Na_2HPO_4. The formation of the sulfoxide derivative of the peptide was achieved by addition of excess H_2O_2 (69). The DHM peptide derivative was obtained by reaction of ca. 10% molar excess of I_3^- over the peptide.

4.2.2.4 Reactions and digestion of ubiquitin

Ubiquitin (Ub, 1.9 mg) was dissolved in 0.1 M phosphate buffer (pH 7.4, 100 µL). This solution was subsequently divided into three parts, and equal volumes of water (a control), excess H_2O_2 in water, and 10 molar equivalents of HOCl in water (prepared by diluting a stock solution of NaOCl in 0.1 M NaOH) were added to each part, respectively. The resulting three solutions were placed in the dark for approximately 20 min before initiating the tryptic digestion. The method used for digestion of the modified Ub samples was adapted from Cox *et al.* (11). Briefly, a trypsin solution (7 µg enzyme in 310 µL of digestive buffer consisting of 50 mM Tris-Cl at pH = 7.9, 6.5 M urea, and 10 mM $CaCl_2$) was added to each of the Ub samples (650 µg Ub in 33 µL 0.1 M PBS at pH 7.4). After this first addition of the trypsin, the samples were incubated in a water-shaking bath at 37 ℃ for 2-4 h; then a second trypsin solution (7 µg enzyme in 110 µL of digestive buffer) was added to each Ub sample. After the second aliquot of trypsin was added, the digestion was allowed to continue for 4 h in a shaking water bath at 37 ℃. The digested samples were divided into 50 µL aliquots and stored at -20 ℃ until used. The LC chromatograms of digested samples that were stored at -20 ℃ for up to one month showed no changes.

4.2.3 pH measurements

The $[H^+]$ of the buffered solutions were determined with an Orion Ion Analyzer EA920 using an Ag/AgCl combination pH electrode. pD measurements in D_2O were made using the same pH electrode by adding 0.4 units to the measurement (70).

4.2.4 UV-vis spectroscopy

Electronic spectra were measured using a HP 8452A diode array spectrophotometer with quartz cells calibrated for 1 mm, 2 mm, 1 cm, and 10 cm path lengths at 20 ℃. The 10 cm cell was used to measure the concentration of $OSCN^-$ in stock solutions (vide infra).

4.2.5 ^1H NMR measurements.

For the studies involving the oxidation of free Met by various oxidants, spectra were recorded with a Varian Mercury VX-300 spectrometer at 20 ^oC. For the studies involving the oxidation of antiflammin-1 and Ub1-6, spectra were recorded with a Varian VNMRS-400 NMR spectrometer at 20 ^oC. The chemical shifts (ppm) were referenced to sodium 2,2-dimethyl-2-silapentane-5-sulfonate (DSS, δ = 0.015 ppm). The $–S\text{-}CH_3$ groups of Met, MetO, and DHM have characteristic chemical shifts (40,49). Integration of the peaks corresponding to the $\text{-}S\text{-}CH_3$ groups were used to determine the ratio of Met : MetO : DHM.

4.2.6 HSQC NMR measurements

^{1}H-^{13}C heteronuclear HSQC experiments were performed on a Varian VNMRS 500 spectrometer at 20 ℃. Ub samples were ra n for approximately 15 h, nt = 160, ni = 256. Ub (3.5-4.0 mg) was dissolved in 500 µL of 0.1 M deuterated phosphate buffer (pH 7.0), made by adding DCl to D_2O solutions of anhydrous Na_2HPO_4. While vortexing, 250 µL of oxidant solution was added, giving a final volume of 750 µL and protein concentration around 550-600 µM. Oxidants used were H_2O_2 (6 mM), chloramine-T (3.3 mM) in the presence of iodide (2.5 mM) (iodide was added to protein solution before addition of chloramine-T), and HOCl (5 mM) were all prepared by dilution of stock solutions with D_2O to achieve desired concentration. Other samples were prepared but did not result in usable NMR data. These samples include chloramine-T and iodide at higher concentrations (20 mM and 2.5 mM respectively), modeled after a study done by Cox *et al.* (11), however the excess of chloramine-T produced a dominant peak around 2.4 ppm which left peaks due to Ub undetectable. Several attempts to decrease intensity of chloramine-T peak proved unsuccessful and include using ultra-filtration to separate the protein from remaining oxidant as well as reacting excess oxidant with either SCN^- or TNB, however both methods did not diminish the dominating peak at 2.4 ppm. To overcome this problem, lower concentrations of chloramine-T was chosen (3.3 mM) as mentioned previously. Another unsuccessful reaction was reacting Ub with either two or ten equivalents of I_3^-. The resulting products gave successful NMR spectra, however this did not lead to oxidation of Met due to

triiodide being a weak oxidant (11). When reacting Ub with only two equivalents of HOCl, modification to the protein was observed (but not characterized), however no modification of the Met residue was observed (as indicated by no chemical shift in the $–SCH_3$ peak).

4.2.7 LC-MS of tryptic digested ubiquitin

LC separation of the tryptic digests of native and oxidized Ub was performed using a BAS (Bioanalytical Systems Incorporated, West Lafeyette, IN) 200B HPLC equipped with a BAS Unijet reversed phase microbore column (ODS-18, 100 mm x 1 mm, 3 µm particle size) and a Unijet guard column (ODS-18, 10 mm x 1 mm, 3 µm particle size). Mobile phase A consisted of 0.05% TFA and 0.05% TEA in deionized water. Mobile phase B consisted of 0.05% TFA and 0.05% TEA in 40% acetonitrile. These mobile phase solutions were filtered and vacuum-degassed prior to use. A binary gradient was applied as follows: 0-2 min, 90% solvent A and 10% solvent B; 2-28 min, linear gradient to 30% solvent A and 70% solvent B; 28-35 min, linear gradient to 100% solvent B; 35-65 min, 100% solvent B; 65-75 min, linear gradient to return the mobile phase to 90% solvent A and 10% solvent B, which was maintained for an additional 32 min before injecting the next sample. The microbore column eluent was split (zero dead volume T) to a BAS UV-116A UV-visible detector set at 205 nm (6 µL/min final flow rate) and to a Micromass/Waters (Bedford, MA) Q-Tof-1 Mass Spectrometer operating in ESI (+) mode (13 µL/min final flow rate). The MS operating conditions were as follows: capillary voltage, 3.0 kV;

cone voltage ramp, 10-85 V; source block temperature, 120 ℃; desolvation temperature, 150 ℃; and desolvation gas flow rate, 200 L/hr.

4.3 Results and discussion

4.3.1 Oxidation of free methionine

As mentioned previously, the –S-CH_3 group has a distinctive ^{1}H-NMR for Met (Figure 4.1, A), MetO (Figure 4.1, B), and the two optical isomers of DHM (Figure 4.1, C) (40,49). A representative ^{1}H NMR spectrum is given in Figure 4.1. As shown in Figure 4.1, the –S-CH_3 group of Met has a chemical shift ~2.14 ppm, MetO ~2.76 ppm, and DHM at 2.84 and 2.85 ppm.

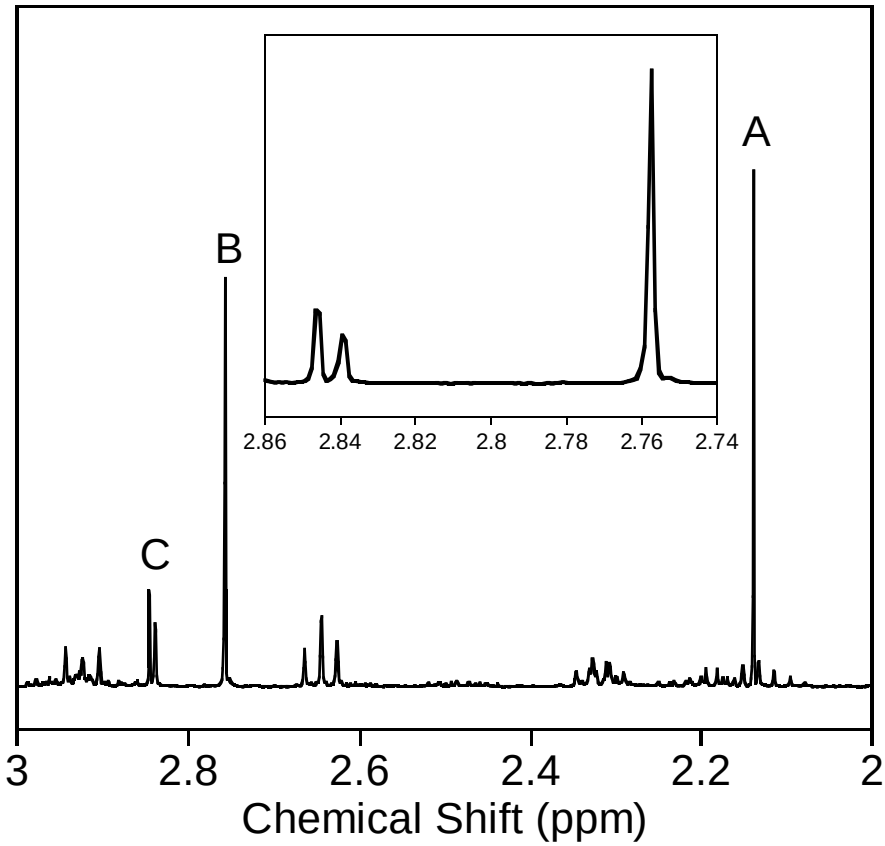


Figure 4.1: Representative ^{1}H NMR spectrum of the –S-CH_3 region of free Met derivatives obtained from the reaction of 30 mM Met with 25 mM halogenating agent in 0.2 M phosphate buffer, pH = 7.4-7.6. This spectrum was obtained from the oxidation of Met with HOCl at pH = 7.5, 20 ℃. The labeled resonances are S-CH_3 of Met (A), MetO (B), and DHM (C). Inset: expansion of chemical shift range from 2.74 to 2.86 ppm, showing the two peaks of the isomers of DHM.

Table 4.1: Product distribution (%) for the reaction of various oxidants with Met to give MetO and DHM[a]. Conditions: 25 mM oxidant and 30 mM Met at pH = 7.4 (0.2 M PBS) and 20 ℃. [a]The oxidant was added to Met dropwise while vortexing. [b]Prior to its addition to Met, HOBr was generated *in situ* by addition of HOCl to Br^- or by addition of Br_2 to base, followed by neutralization. [c]I^- was added to Met prior to the addition of chloramine-T.

Oxidant[a]	MetO	DHM
H_2O_2	100	0
$ONOO^-$	100	0
$OSCN^-$	0	0
Average (Non-X^+)	100	0
HOCl	56	44
TauCl	56	44
$TauCl_2$	57	43
Chloramine-T	58	42
Average (Cl^+)	57	43
HOBr (HOCl/Br^-)[b]	26	74
HOBr (Br_2/NaOH)[b]	22	78
TauBr	23	77
$TauBr_2$	24	76
Average (Br^+)	24	76
I_3^-	3	97
I^- + chloramine-T (5:1)[c]	10	90
Average (I^+)	6	94

Using the distinctive chemical shifts and proton integration (of peaks described in figure 4.1), the ratio of MetO:DHM was determined for the oxidation of Met with various 2 electron oxidants (table 4.1). Examination of data (table 4.1) shows that the percentage of MetO to DHM formed is dependent on the type of oxidation that is occurring rather than the rate at which the reaction is occurring. To better explain this, rate constants for a few of the reactions are listed in table 4.2.

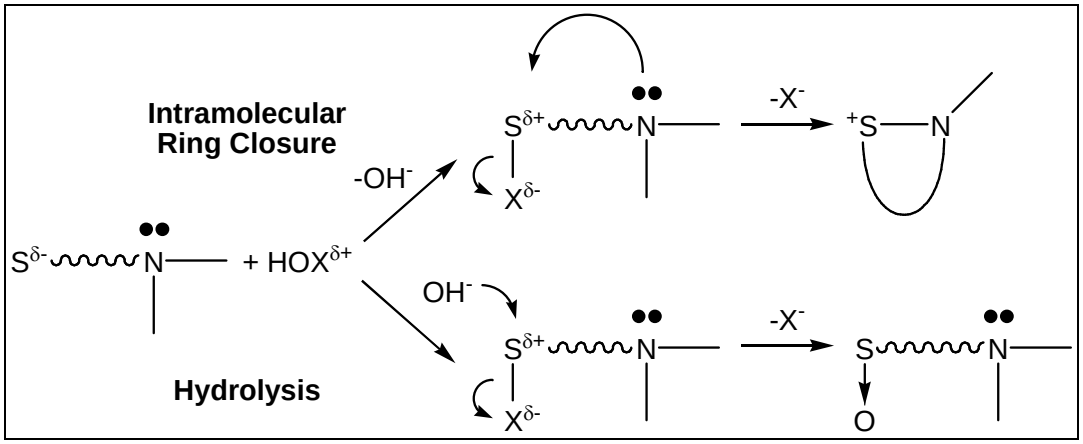
Table 4.2: Comparison of ratio MetO:DHM and rate constants for oxidation of Met by various oxidants (pH = 7, 20 ℃) (29, 48, 58 , 78-81)

Oxidant	Percent MetO:DHM	k ($M^{-1}s^{-1}$) Met + Oxidant
H_2O_2	100:0	$1.0x10^{-2}$
$ONOO^-$	100:0	$1.81x10^{1}$
HOCl	56:44	$3.8x10^{7}$
TauCl	56:44	$3.9x10^{1}$
HOBr ($HOCl/Br^-$)	26:74	$3.5x10^{6}$
TauBr	23:77	$\sim10^{2}$-10^{3}
I_3^-	3:97	$6.5x10^{5}$

Further examination of table 4.2 shows that there is not an apparent correlation between ratios of MetO:DHM formed and rate constant, rather a trend is observed for ratio of MetO:DHM and type of oxidant, [i.e. oxidation through an O-atom transfer (e.g. H_2O_2 and $ONOO^-$) or Cl^+ transfer (e.g. HOCl or TauCl)]. If the oxidants are grouped together by type of halogen, there seems to be a trend in how much DHM is produced. All of the chlorinating agents gave approximately equimolar amounts of MetO and DHM (42-44% DHM); the brominating agents produced higher yields of DHM (74-78% DHM); the iodinating agents gave nearly stoichiometric yields of DHM (90-97% DHM) (table 4.1). Formation of MetO versus DHM is a competition between intramolecular nucleophilic attack of the amine on a sulfonium intermediate to give DHM, or alternatively hydrolysis of the sulfonium intermediate to give MetO (scheme 4.3) (27). The percentage of DHM formed is related to the type of halosulfonium that is formed, whether it is a chlorosulfonium, bromosulfonium, or iodosulfonium species. Comparing analogous halosulfonium species, the

stability towards hydrolysis is I > Br > Cl (71-77), which reflects the trend observed in the yields of DHM. The more stable the halosulfonium intermediate is to hydrolysis, the greater the chance there is for intramolecular ring closure and formation of DHM, versus the hydrolysis to form MetO.

Scheme 4.3: Schematic Branching Mechanisms via a Common Sulfenyl Halide Intermediate that Yield S-N and S-O Derivatives



4.3.2 Oxidation of methionine containing peptides

Formation of DHM, as mentioned previously, is only possible when the amine is available, and as a consequence only *N*-terminal Met of peptides and proteins can form DHM. For comparison with the free amino acid, two small peptides were oxidized to test for DHM formation at the *N*-terminal Met. The two chosen peptides are antiflammin-1 (anti-inflammatory peptide 1), with the sequence Met-Gln-Met-Lys-Lys-Val-Leu-Asp-Ser, and Ub1-6 with the sequence of Met-Gln-Ile-Phe-Val-Lys. Antiflammin-1 was picked due to the presence of both a terminal Met and internal Met. Both peptides were oxidized with H_2O_2, to

form the sulfoxide derivative of the peptide. In addition, peptides were oxidized with I_3^-, forming the DHM derivative of the peptide. DHM and MetO were quantified by examining the NMR spectra of the peptides. Figure 4.2 shows the results of the oxidation of antiiflammin-1.

As observed previously with free Met, the –S-CH_3 groups of the Met residue in the peptide (figure 4.2) has a characteristic chemical shift, with the sulfide ~2.1 ppm, sulfoxide ~2.7 ppm, and DHM moiety at 2.84 and 2.85 ppm. From this information, we are able to identify the modifications of antiflammin-1 when it is oxidized. Unmodified peptide, Met-Gln-Met-Lys-Lys-Val-Leu-Asp-Ser, contains two Mets that have chemical shifts of 2.12 and 2.13 ppm (figure 4.2, bottom). Oxidation of antiflammin-1 with a small excess of H_2O_2 forms the corresponding sulfoxides, MetO-Gln-MetO-Lys-Lys-Val-Leu-Asp-Ser, as indicated by the shifts of the two new sets of –S-CH_3's (figure 4.2, middle). Oxidation of the peptide with an excess of I_3^- formed DHM-Gln-MetO-Lys-Lys-Val-Leu-Asp-Ser (figure 4.2, top), as evidenced by the two new peaks which have chemical shifts corresponding the *N*-terminal Met being converted to a DHM derivative and the internal Met being oxidized to a sulfoxide.

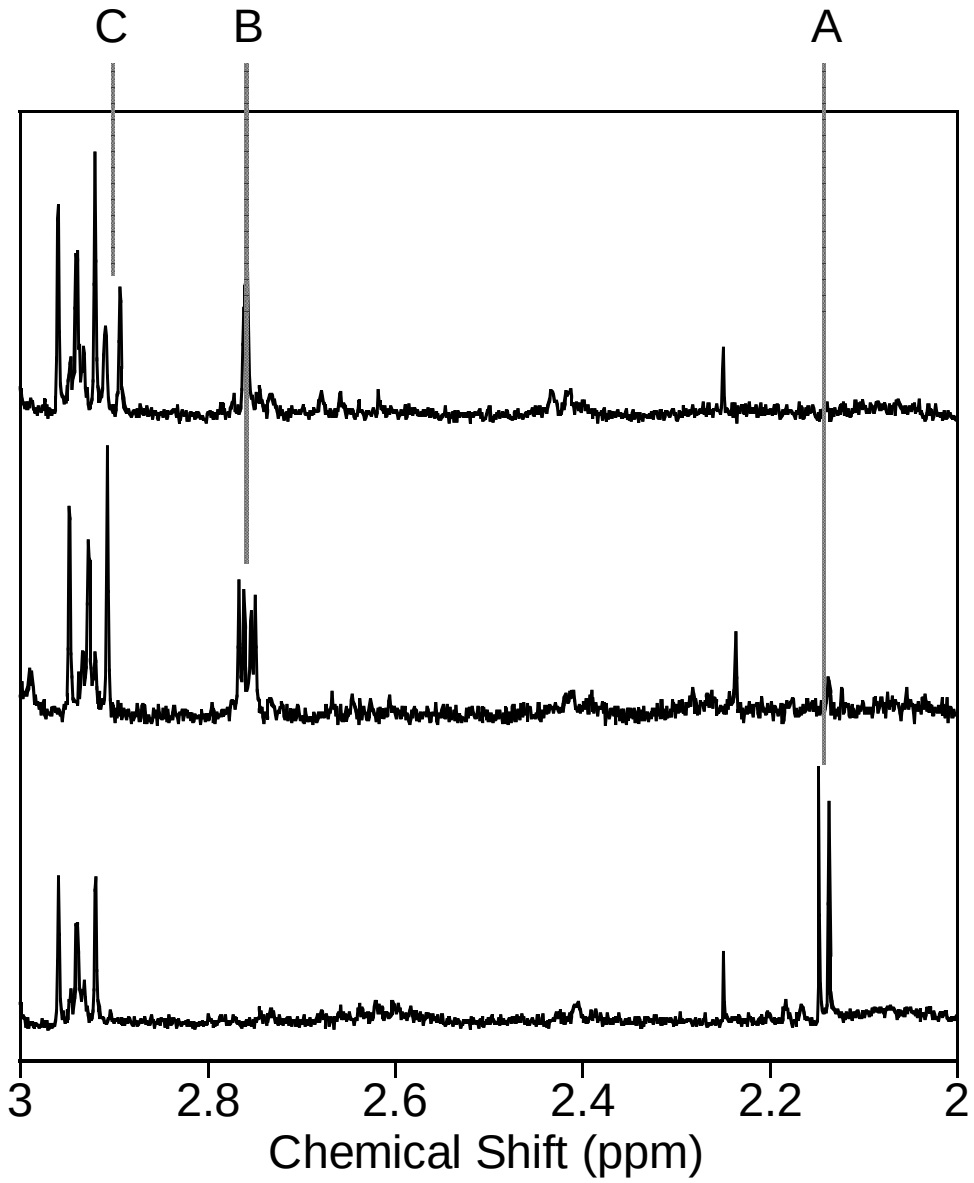


Figure 4.2: ^{1}H NMR spectra of antiflammin-1 (30 µM) in 0.1 M pD PBS (pH = 7.4): native (bottom), oxidized with 10% molar excess of H_2O_2 (middle), and oxidized with 10% molar excess I_3^- (top). Note that the triplet at 2.9 ppm is due to internal standard DSS. The labeled resonances are S-CH_3 of Met (A), MetO (B), and DHM (C).

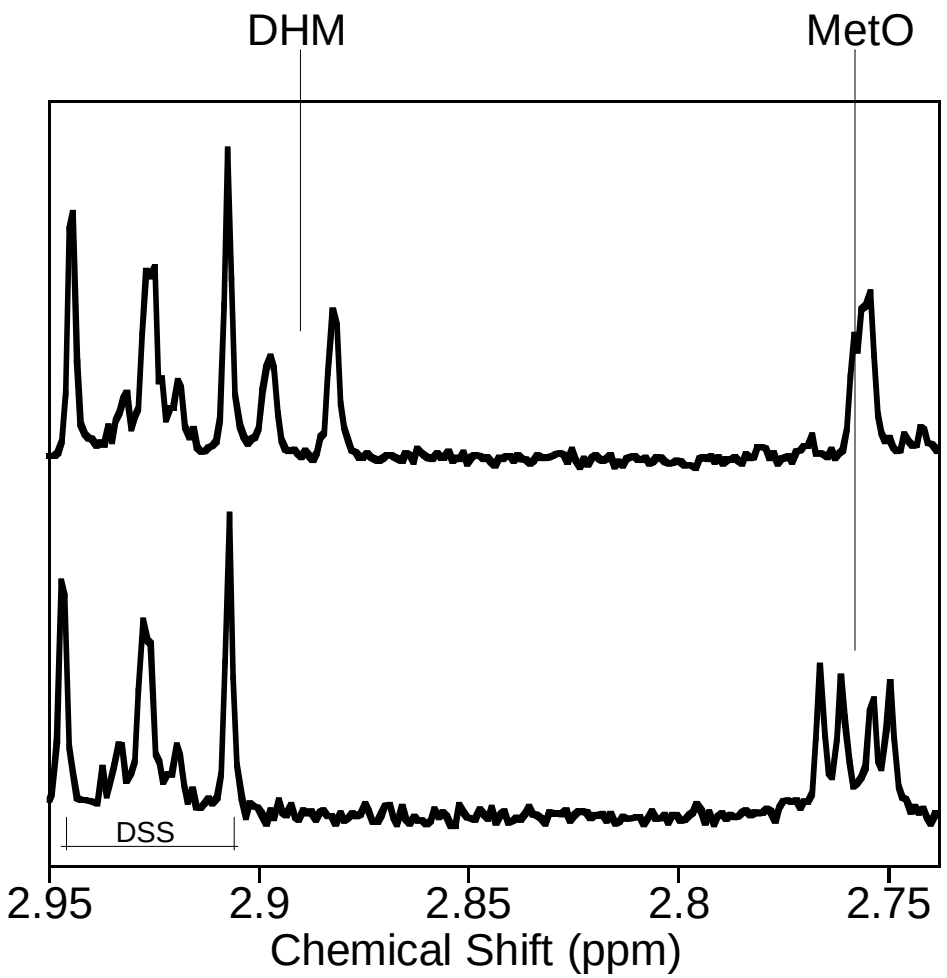


Figure 4.3: (Expansion of Figure 4.2) ^{1}H NMR spectra of antiflammin-1 (30 µM) in 0.1 M pD PBS (pH = 7.4): peptide oxidized with 10% molar excess of H_2O_2 (bottom), and oxidized with 10% molar excess I_3^- (top). Note that the triplet above 2.9 ppm is due to internal standard DSS, used for normalization of chemical shifts.

Figure 4.3 shows an expansion of figure 4.2, focusing on the multiple peaks due to the diastereomers that are formed from oxidization of Met to DHM, which is diasterotopic at the sulfur.

Similar results were seen for Ub1-6, however, this small peptide, with the sequence of Met-Gln-Ile-Phe-Val-Lys, only contains one Met, which is at the *N*-terminus. The NMR spectrum of the Ub1-6 oxidation product is shown in figure 4.4. Oxidation of Ub1-6 with H_2O_2 shows the formation of the sulfoxide (MetO-Gln-Ile-Phe-Val-Lys), while oxidation by I_3^- shows the formation of DHM (DHM-Gln-Ile-Phe-Val-Lys), both evidenced by the characteristic chemical shifts. Similar to the free amino acid Met, *N*-terminal Met (having the amine available for intramolecular ring closure) is oxidized by I_3^- to form the DHM derivative.

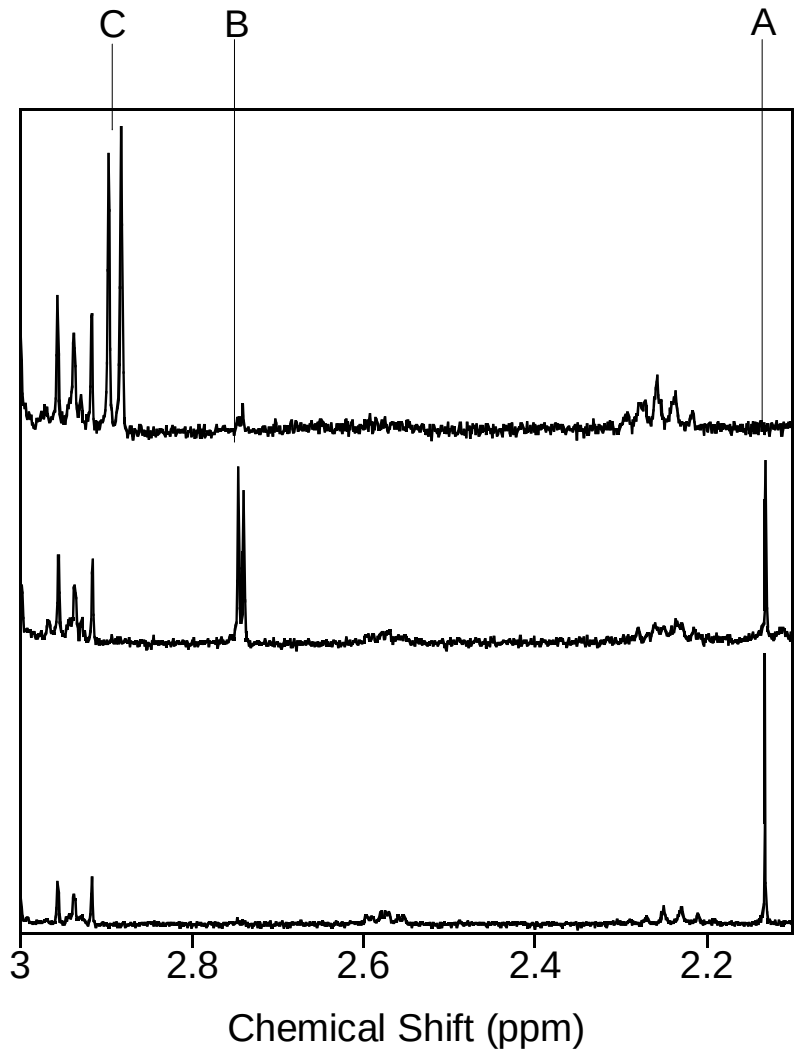


Figure 4.4: ^{1}H NMR spectra of hexapeptide Ub1-6 (40 µM) in 0.1 M in PBS (pD 7.4): native peptide (bottom), oxidized with 10% molar excess of H_2O_2 (middle), and oxidized with 10% molar excess I_3^- (top). The labeled resonances are S-CH_3 of Met (A), MetO (B), and DHM (C). (Note that the triplet above 2.9 ppm is due to internal standard DSS, and that the middle spectrum, still shows the presence of unoxidized Met. This is attributed to the slow oxidation of Met by H_2O_2 and not allowing the sample react long enough before collecting data.)

4.3.3 Oxidation of Met-1 in ubiquitin

Ub, a highly conserved 8.5 kDa eukaryotic regulatory protein, containing 76 amino acids (82), was selected for investigation of whether DHM is formed in proteins because it contains only one Met (at the *N*-terminus) and no Cys residues (a competitive target of hypohalites) (83).

4.3.3.1 HSQC of oxidized ubiquitin

As previously shown, different oxidants produce a different amount of DHM. In order to show that DHM is formed in proteins, I_3^- was chosen for the oxidation of Ub (to optimize chances for formation of DHM; oxidation of free Met by I_3^- formed nearly stoichiometric amounts of DHM). To avoid the possible conversion of DHM to MetO, which could happen during the process of preparing the oxidized protein for analysis (e.g. by digestion and amino acid analysis), NMR was chosen to analyze the intact oxidized protein. Ub has been previously studied by NMR (83-84). To avoid the need for large (mM) concentrations of protein, labeled protein is typically used (^{1}H, ^{13}C, and ^{15}N). Due to the high cost of labeled proteins, this was not appropriate for our experiments. ^{1}H (1D) experiments proved unsuccessful, the spectra of Ub and Ub oxidized with H_2O_2 showed no noticeable differences even after 556 repetitive scans. Fortunately, HSQC (2D) experiments did prove successful. Figure 4.5 shows HSQC for Ub.

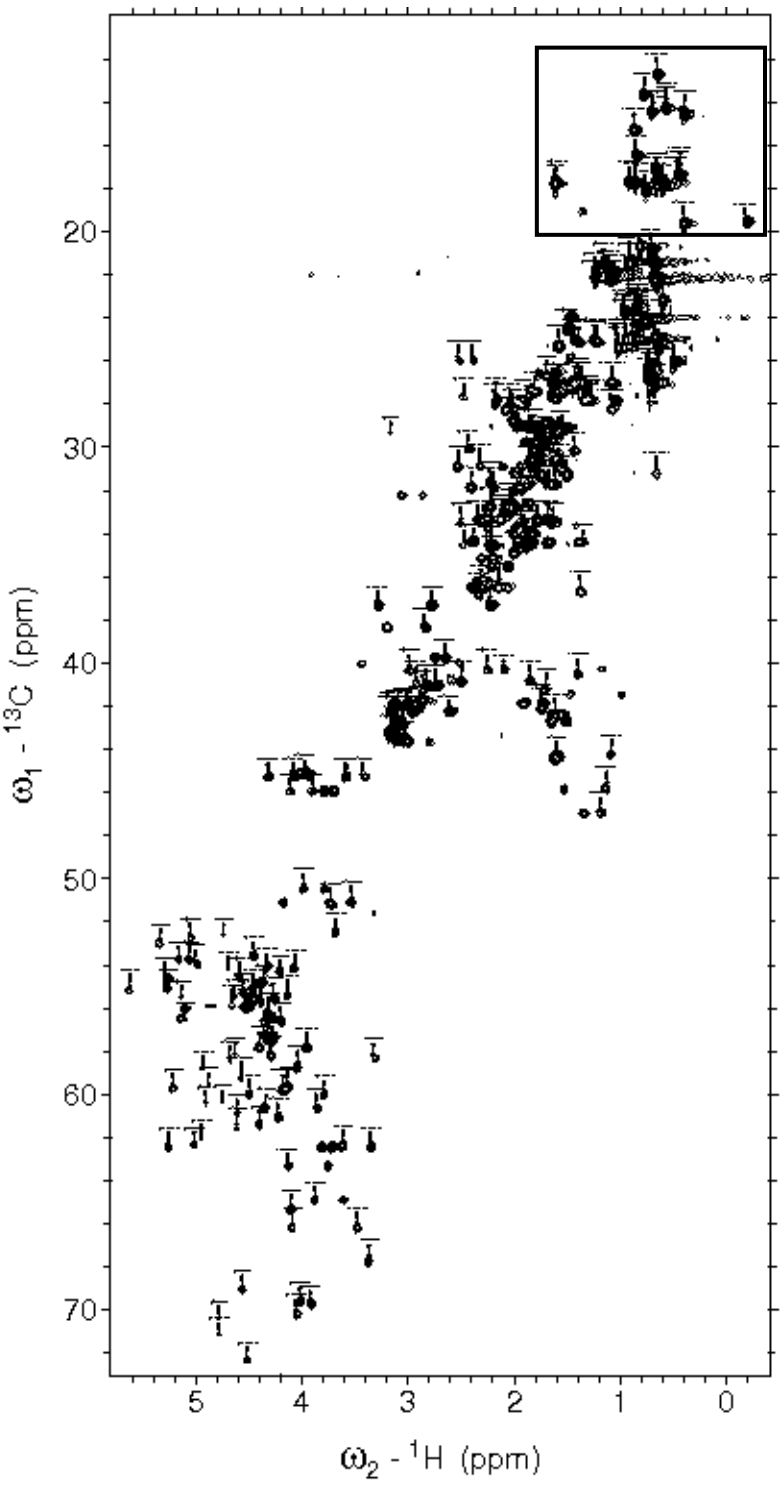


Figure 4.5: HSQC of 1 mM Ub in 0.1 M H_2PO_4 (pH = 7). (Box around approximate zoomed in region discussed further in figures 4.6-4.9.)

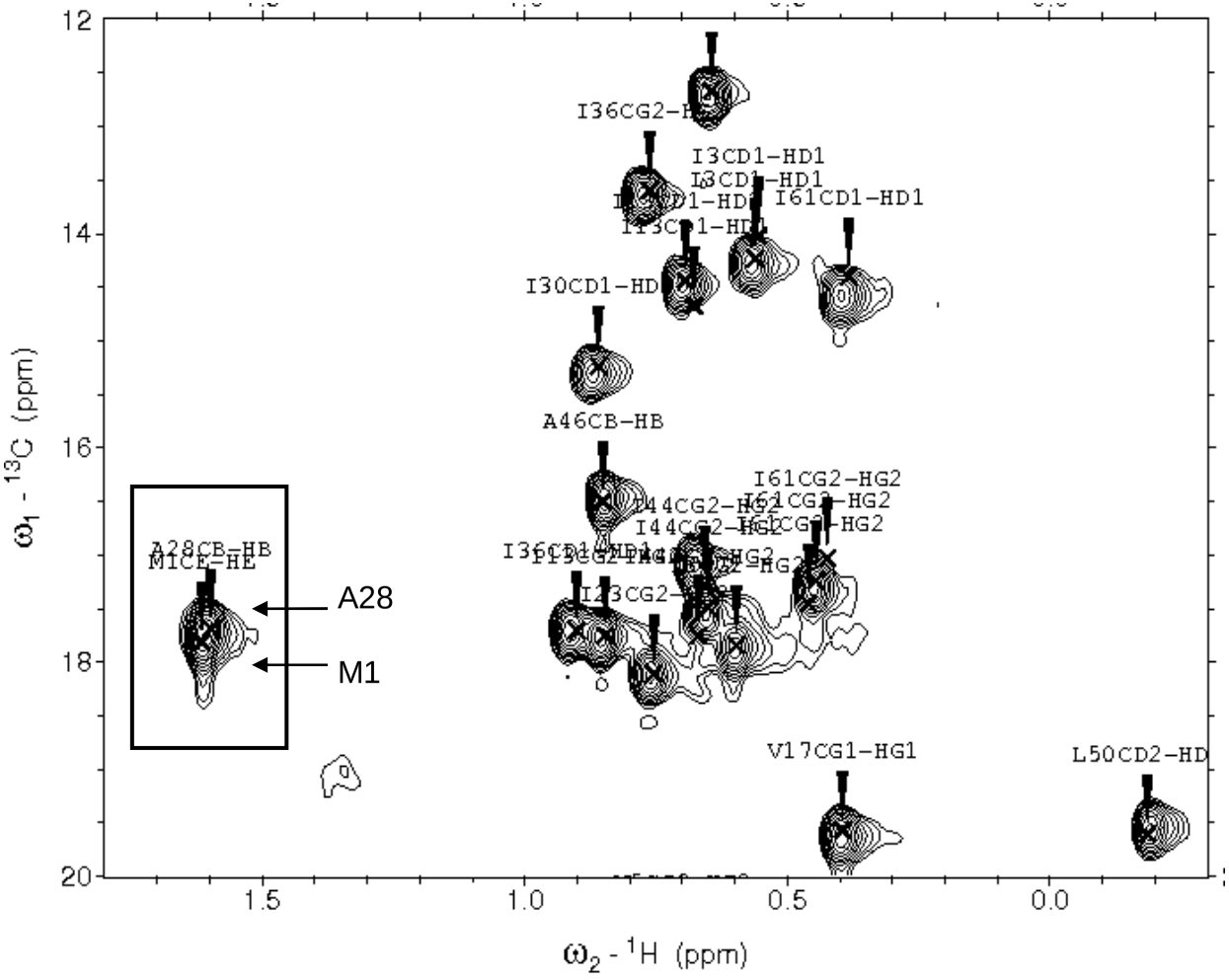


Figure 4.6: HSQC of Ub zoomed in on methyl region. Box around peak that integrates to 6 protons, which is assigned to A28 and M1 (3 protons each)

Though Ub is a small protein, the 2D NMR is still complicated, partially due to the protein being unlabeled. To try and simplify the analysis without doing extensive NMR experiments (such as other 2D experiments), the least complicated region, the methyl region, was focused on for the initial determination of Met modification (figure 4.6). Figure 4.6 shows that the CH_3 of Met overlaps that of Ala28 (amino acids assigned with help from Marquardt *et al.* (85), who determined the chemical shift for all amino acid residues of Ub at pH = 6.6). For Ub, this peak integrates to 6 protons, as would be expected for the three protons of Ala28 and the three for Met1. When Ub is oxidized with H_2O_2, known to selectively oxidize Met to MetO (69), the following spectra (overlapped with figure 4.6) are observed (figure 4.7).

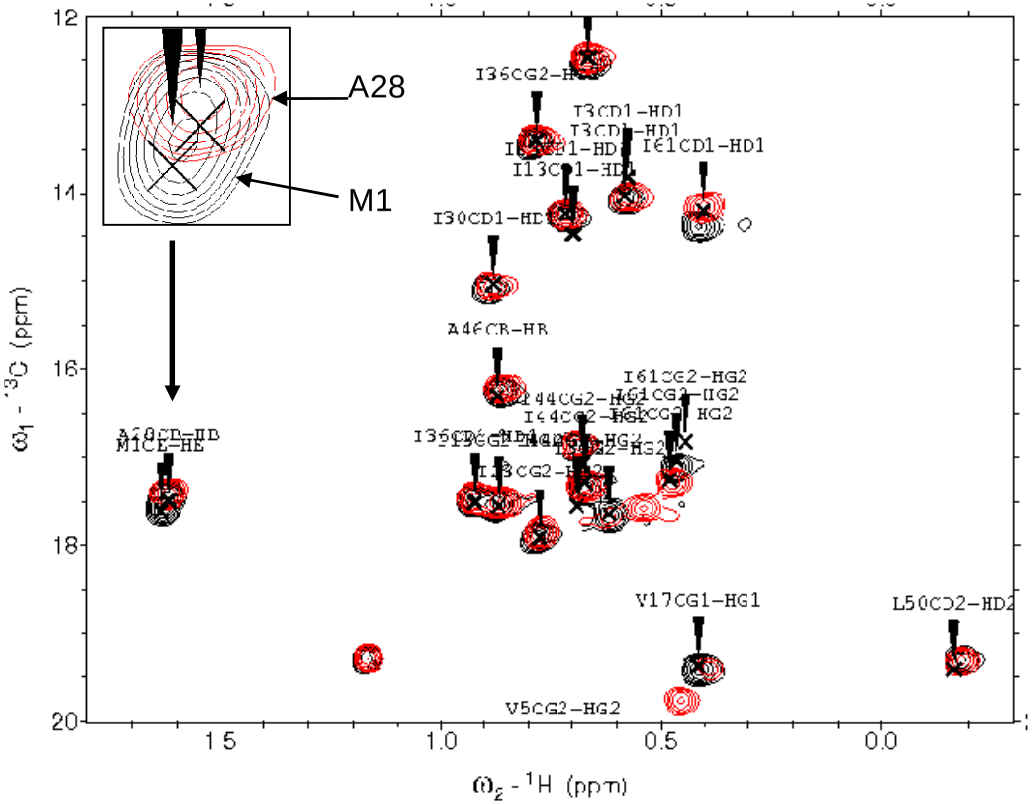


Figure 4.7: HSQC overlay of Ub (black) and Ub + excess H_2O_2 (red); inset shows Met1 modification when Ub is oxidized with excess H_2O_2; Ub (black) integrates to 6 protons (assigned to A28 and M1) while Ub + excess H_2O_2 (red) integrates to 3 protons (assigned to A28)

As can seen from the overlap of Ub and Ub oxidized with H_2O_2 (figure 4.7), a few peaks have small shifts, but the noticeable difference is in the absence of the Met1 peak (inset, figure 4.7) in the oxidized Ub, and the presence of a new peak just below that labeled Val17 (presumed to be MetO). To test for formation of DHM, Ub was oxidized by triiodide. Ub oxidation by the iodine/triiodide system has been previously published (11,86-87). Cox *et al.* (86) report that oxidation of Ub with molecular iodine results in only the oxidation of Tyr59. Cox *et al.* (11) show that the oxidation of Ub with chloramine-T in the presence of iodide oxidizes three residues of Ub, Met-1, Tyr-59, and His-68. Cox *et al.* (11) oxidized Ub, enzymatically digested with trypsin, and initially analyzed using liquid chromatography (LC). After collecting the eluting peptide peaks, they digested the small fragments (using 6 M HCl, 110 ℃, for 24 hrs), and used standard amino acid analysis to determine the modifications that occurred to Ub. Depending on the amount of iodide chosen, Tyr and His were either single or doubly iodinated, and Met was oxidized. The Met containing peptide, when oxidized, showed two distinctive peaks during LC, which authors assign to MetO and $MetO_2$ (11). From experiments we performed with free Met, we know that strong oxidants, such as HOCl and performic acid (88), are needed to oxidize Met up to the sulfone, while weaker oxidants such as H_2O_2 and triiodide only oxidize Met to the sulfoxide. Knowing this, we suspected that the two peaks observed by Cox *et al.* (11) were due to MetO and DHM, not the $MetO_2$. Using the same conditions employed by Cox, we oxidized Ub and analyzed using HSQC. Unfortunately, the chloramine-T peak dominated the

spectrum and no protein peaks were identifiable. Using ultra-filtration, the oxidized protein was filtered to try and separate the protein from the chloramine-T peak, but was unsuccessful. With a lower concentration of chloramine-T, the chloramine-T was not dominating (figure 4.8). Figure 4.8 shows the Met peak is indeed missing in the oxidized Ub, however, various other peaks have also shifted, making it difficult to determine which is the new Met peak without further experiments (note that in figure 4.8 the absence of the peak just below Val-17 which we believed was the MetO (figure 4.7).

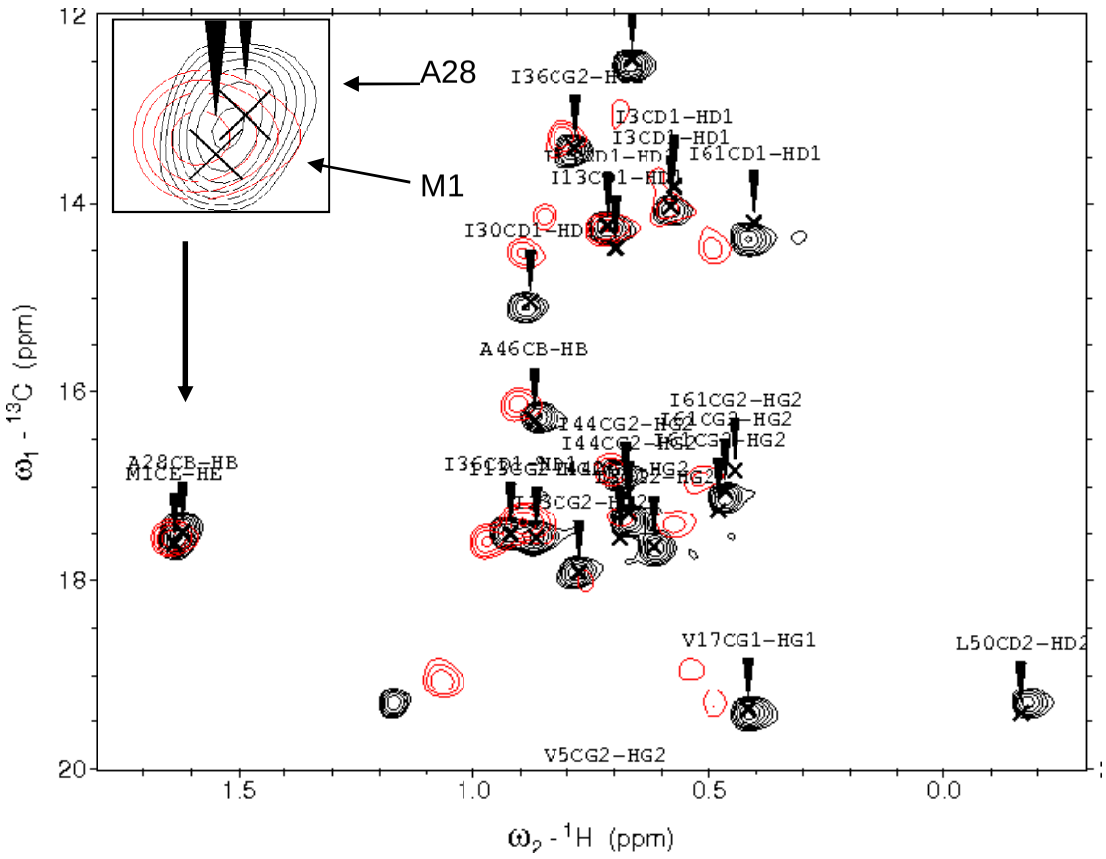


Figure 4.8: HSQC overlay of Ub (black) and Ub + Chloramine-T/I^- (red); inset shows that Met1 remained unmodified; both Ub (black) and Ub + Chloramine-T/I^- (red) integrate to 6 protons (assigned to A28 and M1)

Table 4.3: Rate constants for reaction of HOCl with amino acid residues in Ub

Residue	# residues in Ub	[a] k ($M^{-1}s^{-1}$)
His	1	$1.0x10^5$
Lys	7	$5.0x10^3$
Arg	4	26
Asn	2	0.03
Gln	6	0.03
Cys	0	$3.0x10^7$
Met	1	$3.8x10^7$
Cystine	0	$1.6x10^5$
Tyr	1	44
Trp	0	$1.1x10^4$
Terminal amine	1	$1.0x10^5$
backbone	74	10

[a] Modeled after table 4, reference 29 (note other amino acid residues contained in Ub have side chains which are no reactive with HOCl)

Since the main goal of these experiments was to see qualitatively if DHM is formed in proteins, a different oxidant was tested. HOCl was chosen based on knowledge of the rate constants with the various residues of Ub (table 4.3). Table 4.3, modeled after a similar table by Pattison *et al.* (29) lists the residues of Ub that are reactive to HOCl as well as their predicted rate constants. Using this information, Met would be predicted to be amongst the first amino acid residue in Ub to react with HOCl. Experiments were performed to determine how many HOCl equivalents are needed to add to Ub in order for Met to be oxidized to MetO/DHM, without adding an unnecessary excess (HOCl is a more powerful oxidant than iodide/chloramine-T, which leaves more amino acid residues susceptible to oxidation). A large excess of HOCl would not be desired because the more HOCl added, the more amino acid residues would be modified as well as possibly over-oxidizing Met forming $MetO_2$, making

interpretation of results more difficult. Though unexpected (from known rate constants), addition of 1, 2, or 5 molar equivalents of HOCl caused no modification to the Met residue. The addition of 10 molar equivalents of HOCl did result in Met oxidation (figure 4.9). The HSQC (figure 4.9), is quite complicated, but the Met peak has clearly disappeared. As seen previously with the chloramine-T/iodide system, oxidation of Ub with HOCl did not show a new peak near Val-17, as was seen in Ub oxidized with H_2O_2. Though these HSQC experiments did not conclusively show that DHM formed in the oxidation of Ub, it does show that the halide oxidized products of Ub are quite different from that of Ub oxidized with H_2O_2.

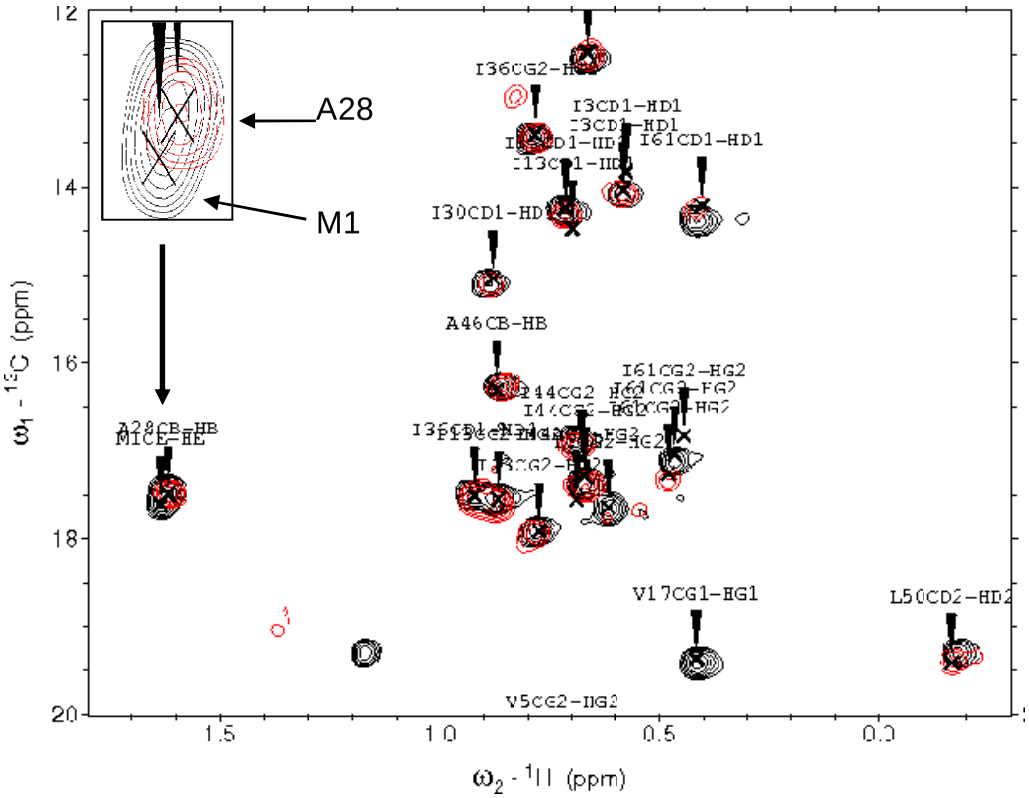


Figure 4.9: HSQC overlay of Ub (black) and Ub + 10 equivalents HOCl (red); inset shows Met1 modification when Ub is oxidized with excess HOCl; Ub (black) integrates to 6 protons (assigned to A28 and M1) while Ub + HOCl (red) integrates to 3 protons (assigned to A28)

4.3.3.2 LC-UV and LC-MS of tryptic digested ubiquitin

Using a procedure similar to Cox *et al.* (11), we oxidized Ub, carried out a tryptic digestion, and analyzed the peptides. Cox *et al.* (11) have shown that conditions needed to cleave the peptide bonds through digestion can cause modification of amino acids. We first needed to determine if DHM is stable enough to survive these conditions. We chose to analyze the peptides by LC-MS. By knowing the mass of the peptides, we would be able to identify which peptides were modified and what products are formed. The enzyme trypsin cleaves peptide bonds at the carboxyl side of lysine or arginine, except when followed by proline. Complete tryptic digestion of Ub leaves the peptides listed in table 4.4.

Table 4.4: Peptides of Ub after tryptic digestion

Peptide	Ub residues
Met-Gln-Ile-Phe-Val-Lys	1-6
Thr-Leu-Thr-Gly-Lys	7-11
Thr-Ile-Thr-Leu-Glu-Val-Glu-Pro-Ser-Asp-Thr-Ile-Glu-Asn-Val-Lys	12-27
Ala-Lys	28-29
Ile-Gln-Asp-Lys	30-33
Glu-Gly-Ile-Pro-Pro-Asp-Gln-Gln-Arg	34-42
Leu-Ile-Phe-Ala-Gly-Lys	43-48
Gln-Leu-Glu-Asp-Gly-Arg	49-54
Thr-Leu-Ser-Asp-Tyr-Asn-Ile-Gln-Lys	55-63
Glu-Ser-Thr-Leu-His-Leu-Val-Leu-Arg	64-72
Leu-Arg-Gly-Gly	73-76

After developing the LC instrumental conditions needed to separate the various peptides, the LC was coupled to the MS, allowing for simultaneous detection of eluting peptides by both LC-UV (at 205 nm) and LC-MS. Figure 4.10 shows representative chromatograms from both detection methods.

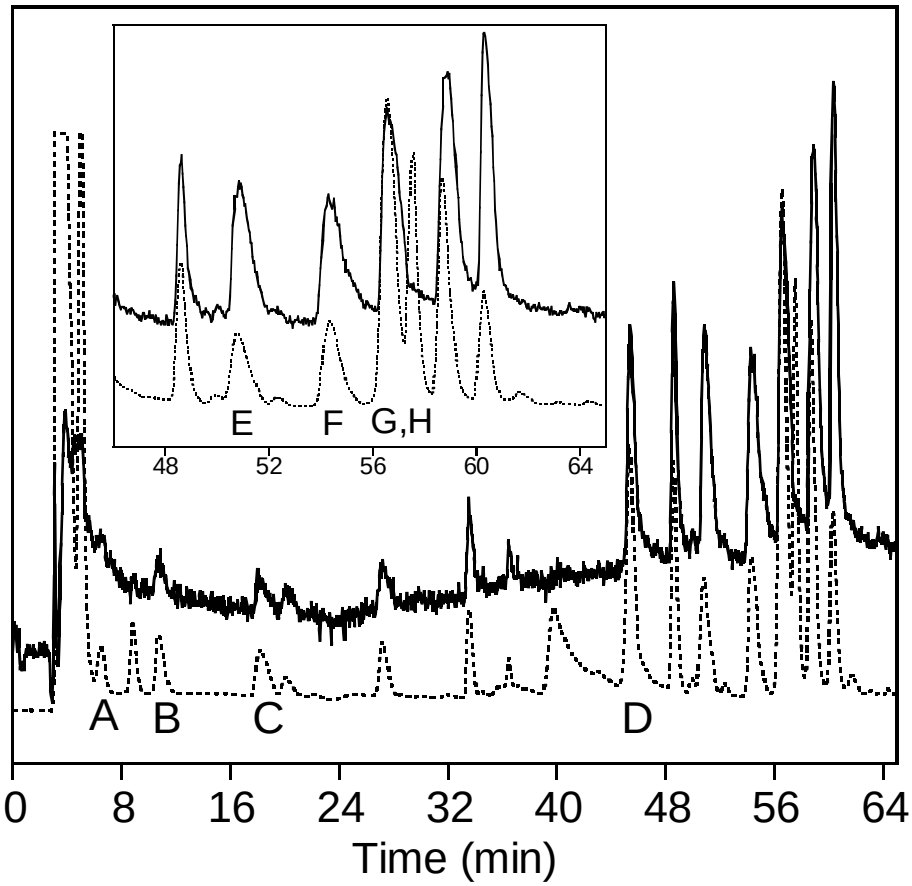


Figure 4.10: Representative MS (solid) and UV (dotted) chromatograms of digested Ub. The scale of the MS chromatogram is shifted by 1.8 min to normalize the two chromatograms. The following peptides from the digested Ub have been assigned (based on observed m/z): A: Leu-Arg-Gly-Gly (73-76); B: Thr-Leu-Thr-Gly-Lys (7-11); C: Gln-Leu-Glu-Asp-Gly-Arg (49-54); D: Thr-Leu-Ser-Asp-Tyr-Asn-Ile-Gln-Lys (55-63); E: Leu-Ile-Phe-Ala-Gly-Lys (43-48); F: Met-Gln-Ile-Phe-Val-Lys (1-6); G: Glu-Ser-Thr-Leu-His-Leu-Val-Leu-Arg (64-72); H: Thr-Ile-Thr-Leu-Glu-Val-Glu-Pro-Ser-Asp-Thr-Ile-Glu-Asn-Val-Lys (12-27). A-G were identified by m/z of $(M+H)^{1+}$ and H was identified as $(M+H)^{2+}$. Unidentified peaks may be due to autodigestion of trypsin. Inset: expansion of the chromatograms between 45 and 65 min.

As can be seen from comparing UV and MS chromatograms (figure 4.10), some peaks are detectable by one method and not the other, as is expected for the two different detection techniques. A UV peak (A, absorbance) is detectable depending on two variables, molar absorptivity (ε), and concentration (c), as determined by Beer's law ($A = \varepsilon * b * c$; b is path-length of observation cell which can sometimes be varied between experiments, but not between analytes in the same sample). Besides illustrating representative chromatograms, figure 4.10 also identifies some of the digested peptides, determined by m/z from MS chromatogram. Knowing which peak is due to the Met-containing peptide allows us to determine what the product is when it is oxidized.

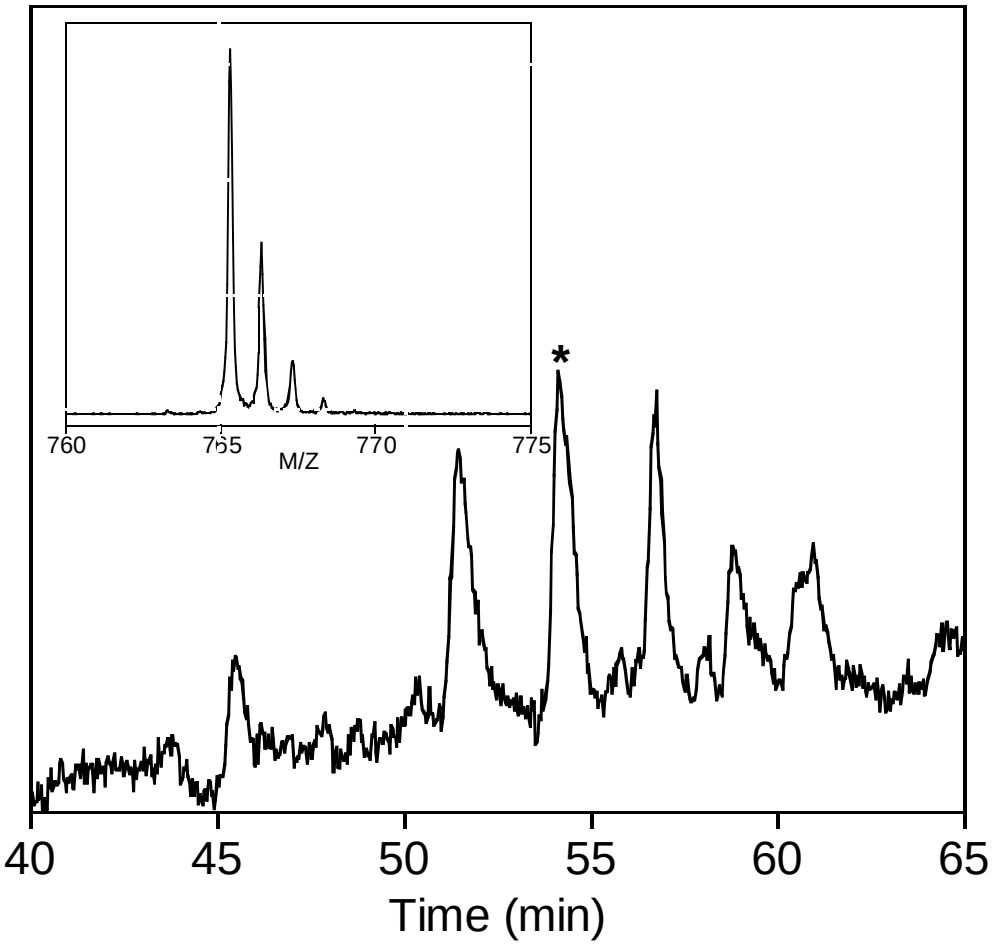


Figure 4.11: LC-MS-ESI$^+$ chromatogram of digested Ub. Inset: MS spectrum of native hexapeptide Ub1-6, eluted at 55 min (*****). The theoretical monoisotopic mass is 764.4. The observed mass is 764.4 + H^+.

Figure 4.11 illustrates the chromatogram and MS spectrum of the unmodified peptide. The peak which has a retention time around 55 mins has a m/z of 765.4 assigned as Met-Gln-Ile-Phe-Val-Lys, which is the mass of the peptide *N*-terminal peptide (764.4) + a hydrogen. Because the MS are taken in positive mode, peaks will be M + H^+. Ub oxidized with H_2O_2 and digested is represented in figure 4.12.

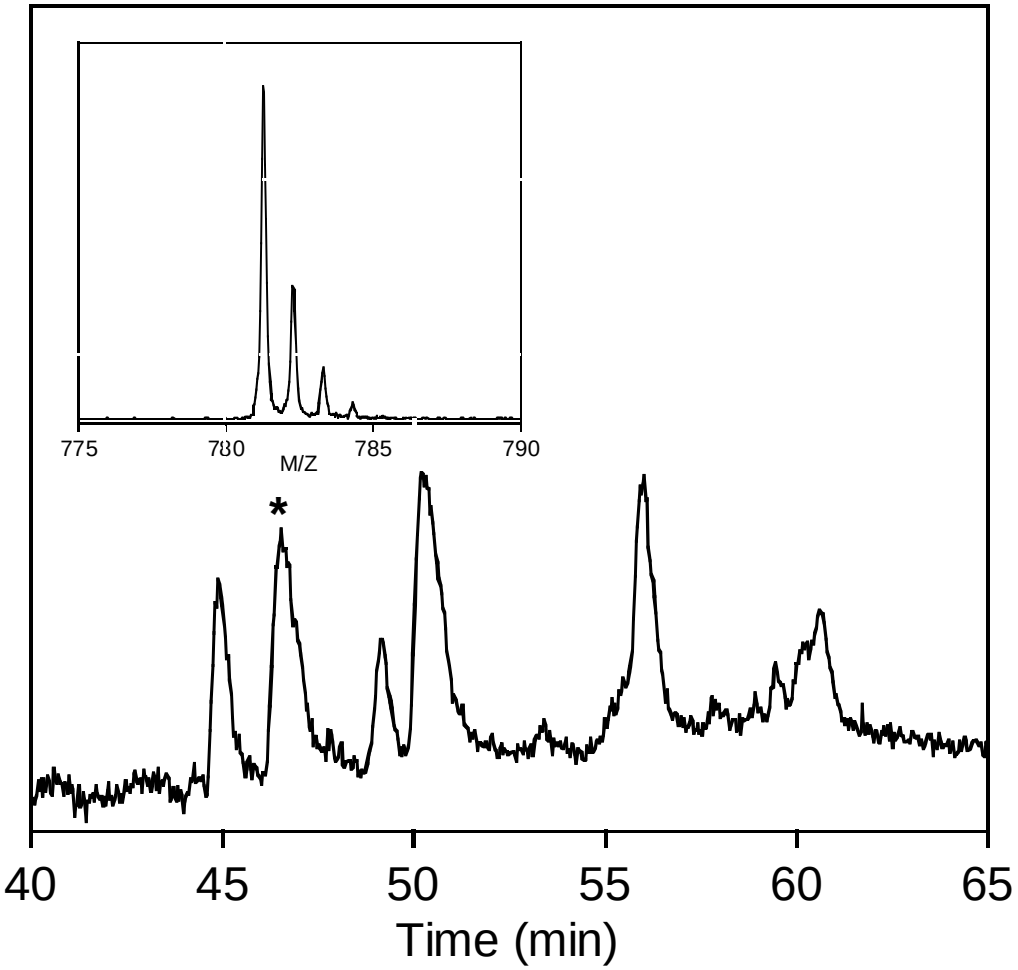


Figure 4.12: LC-MS-ESI$^+$ chromatogram of digested Ub that was oxidized with 10% molar excess of H_2O_2. Inset: MS spectrum of MetO derivative of the hexapeptide Ub1-6, eluted at 47.4 min (*). The theoretical monoisotopic mass is 780.4. The observed mass is 780.3 + H^+.

Comparing figures 4.11 and 4.12, in Ub oxidized with H_2O_2, the Met peak disappears and a new peak with a retention time around 47 mins is observed. The MS spectrum of this peptide gives a m/z of 780.3 + H^+, which is expected for the addition of a oxygen to the Met peptide (764.4+16) + H^+ forming MetO-Gln-Ile-Phe-Val-Lys.

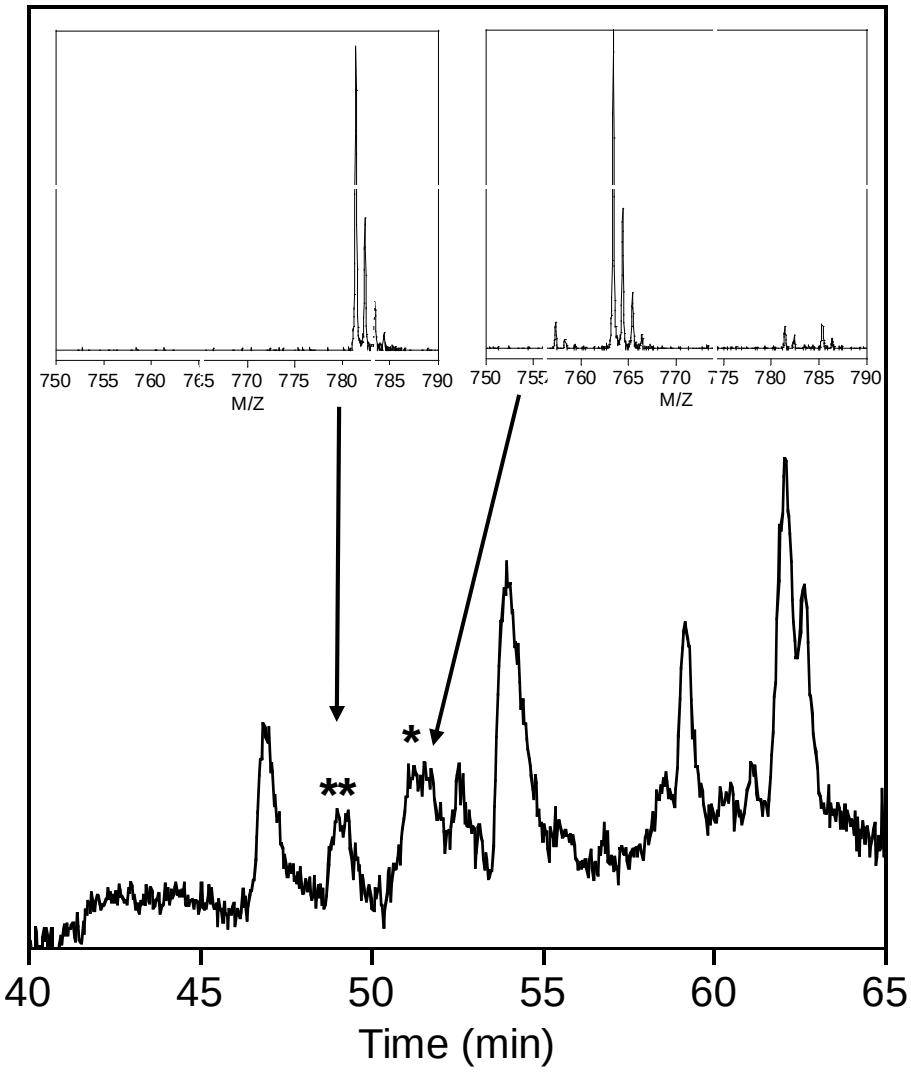


Figure 4.13: LC-MS-ESI$^+$ chromatogram of digested Ub that was oxidized with 10 molar equivalents of HOCl. Inset (left): MS of MetO derivative of the hexapeptide Ub1-6, eluted at 49.0 min (**). The theoretical monoisotopic mass is 780.4. The observed mass is 780.4 + H^+. Inset (right): MS of DHM derivative of the hexapeptide Ub1-6, eluted at 51.5 min (*). The theoretical monoisotopic mass is 762.4. The observed mass is 762.4 + H^+.

Oxidation of Ub with ten molar equivalents of HOCl led to modifications of the Met peptide (figure 4.13). A peak was observed with retention time around 49 min, with m/z of 780.4 + H^+ and another with retention time around 51.5 min, with m/z of 762.4 + H^+ (or the Met peptide, 764.4 - 2 hydrogens, as would be expected for the DHM moiety). One modification of the Met-Gln-Ile-Phe-Val-Lys (observed 764.4 + H^+, figure 4.11) was its conversion to the sulfoxide, MetO-Gln-Ile-Phe-Val-Lys (observed 780.4 + H+, figure 4.13 left inset), evidenced using a sample of Ub that was selectively oxidized by H_2O_2 to MetO (figure 4.12). The other modification was attributed to the DHM derivative DHM-Gln-Ile-Phe-Val-Lys (observed 762.4 + H^+, figure 4.13 right inset). Confirmation of the DHM derivatized peptide was achieved by independent synthesis of the hexapeptide, Met-Gln-Ile-Phe-Val-Lys and oxidation with a small excess of I_3^- followed by ^{1}H NMR of the synthesized DHM-Gln-Ile-Phe-Val-Lys which had the characteristic pattern of the two diastereomeric methyl groups of DHM, figure 4.4, top). The MS spectrum of DHM-Gln-Ile-Phe-Val-Lys was achieved by direct injection of the peptide onto the MS and compared to that of the DHM containing peptide from the tryptic digest of oxidized Ub analyzed by LC-MS (figure 4.14). Comparing the spectra in figure 4.14, there are small differences in the two which we attribute to the different methods of preparation (top spectrum: peptide oxidized with excess I_3^-, which may not be a clean reaction, and injected into MS without any cleanup; bottom spectrum: peptide eluted from LC into the MS).

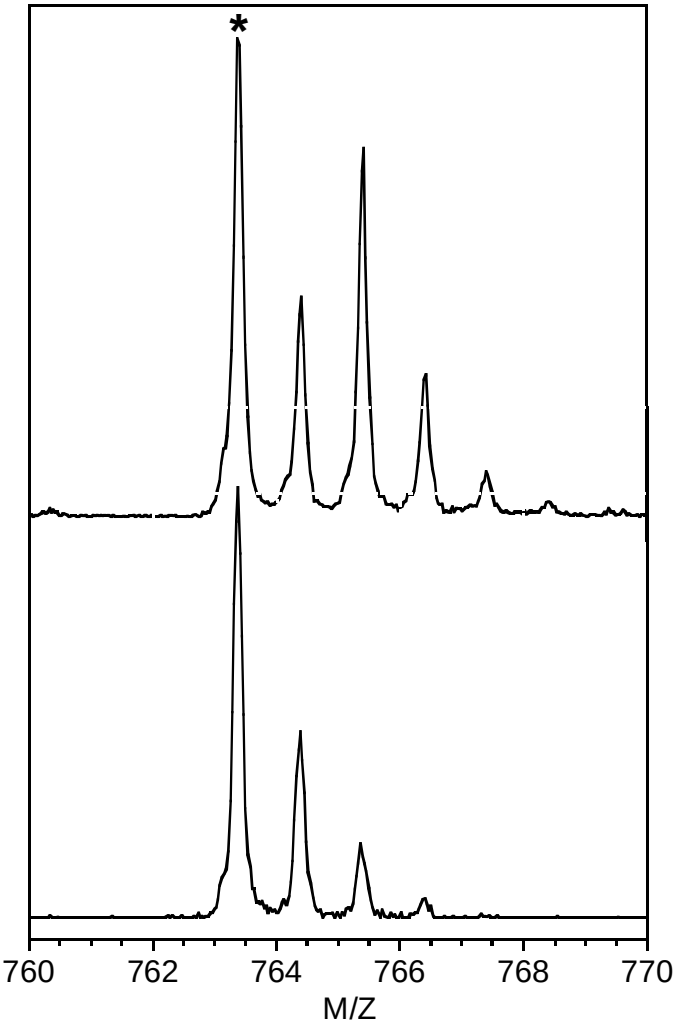


Figure 4.14: Comparison of MS spectra of the DHM derivative of the Ub1-6 hexapeptide, top: prepared from addition of a small excess of I_3^- to Ub1-6 and directly injected into the mass spectrometer, and bottom: LC-MS of peak with retention time of 51.5 min (*figure 4.13) from the tryptic digest of Ub oxidized with 10 molar equivalents of HOCl. The theoretical monoisotopic mass of DHM-Gln-Ile-Phe-Val-Lys is 762.4, observed mass is 762.4 + H^+ (*).

To further confirm that the DHM derivative formed, the tryptic digest of Ub treated with 10 molar equivalents of HOCl (analyzed by LC-UV) was spiked with an authentic sample of DHM-Gln-Ile-Phe-Val-Lys. The spiking of the enzymatically digested oxidized Ub sample was qualitative, not quantitative, so the concentration of the peptides separated using LC-UV was approximately known, and spiked with the DHM hexapeptide sample (synthesized using a 10% excess of I_3^-) that was about two and a half times its concentration. The authentic DHM hexapeptide exhibited the same chromatographic retention time as the corresponding hexapeptide in the tryptic digest of oxidized Ub (figure 4.15). The peak, which has been identified using MS, having a LC-UV retention time around 51.5 mins, increases with addition of DHM-Gln-Ile-Phe-Val-Lys. In addition, other peaks change as well. For example, the peak around 47 mins, assigned to the peptide fragment Thr-Leu-Ser-Asp-Tyr-Asn-Ile-Gln-Lys (figure 4.10), disappears and two peaks, around 59 mins and 65.5 mins appear along with peak around 57 mins increasing slightly. The two new peaks are associated with single and double iodination of the tyrosine containing peptide (peak that increased in intensity at 57 min was not assigned to the digested Ub, but a product of autodigestion of the trypsin).

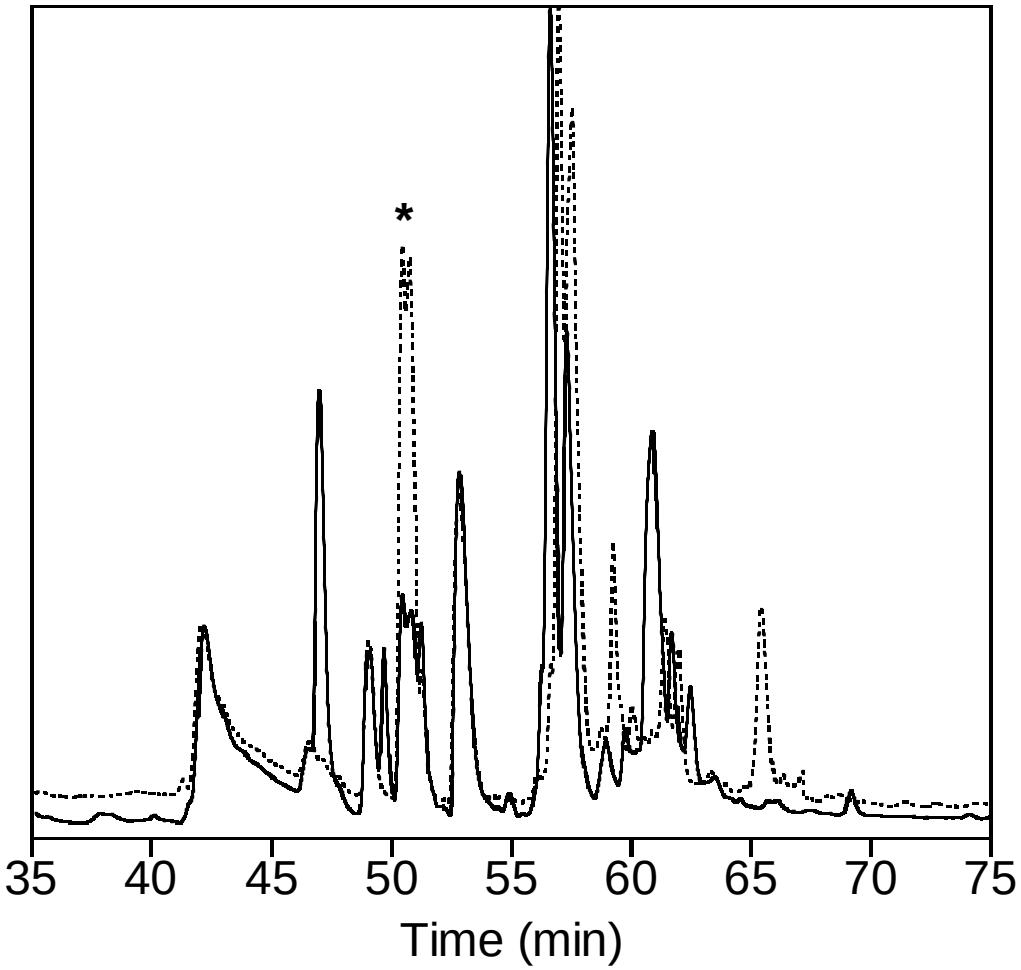


Figure 4.15: LC-UV (205 nm) of Ub oxidized with 10 molar equivalents of HOCl and subsequently digested using trypsin (solid line). Same sample spiked with an authentic sample of the DHM derivative of Ub1-6 (prepared in 0.1 M phosphate buffer by adding a 10% molar excess of I_3^-; the product was characterized by ^{1}H NMR) in order to verify retention time.

4.4 Summary and conclusions

Oxidation of Met, which has a free amine, can form either MetO or DHM. Different oxidants form different percentages of DHM. Two electron oxidants that react through oxygen transfer do not produce DHM, while halogenating species (but not the pseudohypohalous acid HOSCN) which react through a halide cation (X^+, where X = I, Br, or Cl) transfer, produce a significant amount of DHM. The halogenating agents can be grouped by the yields of DHM they produce; chlorinating agents produce around 43% DHM, brominating agents approximately 75%, and iodinating agents close to 100% DHM. Assuming that the oxidation of Met by halogens initially produces a halosulfonium intermediate (either hydrolyzes to give MetO or goes through intramolecular nucleophilic attack of the amine on this sulfonium intermediate to give DHM) the percent yield of DHM is related to the type of intermediate formed. The relative order of stability towards hydrolysis is expected to be I > Br > Cl, which reflects the trends observed in the yields of DHM relative to MetO. The data shown demonstrates that when the amine is available, DHM forms in the free amino acid, small peptides, and the small protein Ub. The experiments in which the small peptide Antiflammin-1 (contains two Met, one at the *N*-terminus having the amine available, and one within the peptide that has the amine tied up in an amide bond) is oxidized confirms what has been previously mentioned in literature, that an amine has to be within close proximity to the sulfonium intermediate to form DHM; amide nitrogen atoms are apparently not sufficiently nucleophilic to form isothiazolidinium rings due to the electronic conjugation

with an adjacent carbonyl (89). Because the start codon for eukaryotic protein synthesis encodes Met (90), mammalian proteins are produced *in vivo* with Met at the *N*-terminus. As a consequence of post-translational modifications, roughly 40% of the *N*-terminal Met residues are cleaved, but the majority remains after protein processing (91). Ub was chosen to investigate whether DHM can be formed in proteins because it contains only one Met (at the *N*-terminus) and no Cys residues (a competitive target of HOCl) (83). The results from the Ub studies suggest the *N*-terminal Met residues of protein yield DHM derivatives when reacted with electrophilic halogenating agents, while producing just the corresponding sulfoxide when reacting with non-halogenating oxidants such as H_2O_2 and peroxynitrite. This along with the high kinetic stability of DHM at neutral pH, which in the absence of catalysts has a half life of over 600 days (58), shows the high potential for DHM as a biomarker of protein oxidation by halogenating agents.

4.5 Future experiments

- Test other oxidants for ability to form DHM
    - Test both one electron and two electron oxidants (*e.g.* radicals) to expand the library of oxidants for %DHM vs. %MetO formed
- Stability tests of DHM-proteins
    - pH and temperature profile to determine what conditions a DHM-protein can survive (e.g. digestion conditions)
- Develop method to quantify the amount of DHM formed in proteins
    - Isotopically label protein so can use 2D-NMR more efficiently
    - Develop antibody which recognizes the DHM moiety
- Test other proteins which contain *N*-terminal Met to determine if DHM forms
- Look for DHM-proteins *in vivo*

4.6 References

(1) Hawkins, C. L.; Pattison, D. I.; Davies, M. J. "Hypochlorite-induced oxidation of amino acids, peptides and proteins." *Amino Acids* **2003**, *25*, 259-274.

(2) Dean, R. T.; Fu, S. L.; Stocker, R.; Davies, M. J. "Biochemistry and pathology of radical-mediated protein oxidation." *Biochemical Journal* **1997**, *324*, 1-18.

(3) Hawkins, C. L.; Morgan, P. E.; Davies, M. J. "Quantification of protein modification by oxidants." *Free Radical Biology and Medicine* **2009**, *46*, 965-988.

(4) Davies, M. J. "The oxidative environment and protein damage." *Biochimica Et Biophysica Acta-Proteins and Proteomics* **2005**, *1703*, 93-109.

(5) In *NDRL/NIST Solution Kinetics Database on the Web*; Notre Dame University: Notre Dame, Indiana; Vol. 2009.

(6) Issaq, H. J.; Van, Q. N.; Waybright, T. J.; Muschik, G. M.; Veenstra, T. D. "Analytical and statistical approaches to metabolomics research." *Journal of Separation Science* **2009**, *32*, 2183-2199.

(7) Ptolemy, A. S.; Lee, R.; Britz-Mckibbin, P. "Strategies for comprehensive analysis of amino acid biomarkers of oxidative stress." *Amino Acids* **2007**, *33*, 3-18.

(8) Clarke, A. P.; Jandik, P.; Rocklin, R. D.; Liu, Y.; Avdalovic, N. "An integrated amperometry waveform for the direct, sensitive detection of amino acids and amino sugars following anion-exchange chromatography." *Analytical Chemistry* **1999**, *71*, 2774-2781.

(9) Chiou, S. H.; Wang, K. T. "Simplified protein hydrolysis with methanesulphonic acid at elevated-temperature for the complete amino-acid analysis of proteins." *Journal of Chromatography* **1988**, *448*, 404-410.

(10) Schoneich, C.; Sharov, V. S. "Mass spectrometry of protein modifications by reactive oxygen and nitrogen species." *Free Radical Biology and Medicine* **2006**, *41*, 1507-1520.

(11) Cox, M. J.; Shapira, R.; Wilkinson, K. D. "Tryptic peptide mapping of ubiquitin and derivatives using reverse-phase high performance liquid chromatography." *Analytical Biochemistry* **1986**, *154*, 345-52.

(12) Baldwin, A. J.; Kay, L. E. "Nmr spectroscopy brings invisible protein states into focus." *Nature Chemical Biology* **2009**, *5*, 808-814.

(13) Saeed, S.; Gillies, D.; Wagner, G.; Howell, N. K. "Esr and nmr spectroscopy studies on protein oxidation and formation of dityrosine in emulsions containing oxidised methyl linoleate." *Food and Chemical Toxicology* **2006**, *44*, 1385-1392.

(14) Gianazza, E.; Crawford, J.; Miller, I. "Detecting oxidative post-translational modifications in proteins." *Amino Acids* **2007**, *33*, 51-56.

(15) Winterbourn, C. C.; Kettle, A. J. "Biomarkers of myeloperoxidase-derived hypochlorous acid." *Free Radical Biology and Medicine* **2000**, *29*, 403-409.

(16) Fialkow, L.; Wang, Y.; Downey, G. P. "Reactive oxygen and nitrogen species as signaling molecules regulating neutrophil function." *Free Radical Biology and Medicine* **2007**, *42*, 153-164.

(17) Winterbourn, C. C. "Biological reactivity and biomarkers of the neutrophil oxidant, hypochlorous acid." *Toxicology* **2002**, *181-182*, 223-227.

(18) Pattison, D. I.; Davies, M. J. "Reactions of myeloperoxidase-derived oxidants with biological substrates: Gaining chemical insight into human inflammatory diseases." *Current Medicinal Chemistry* **2006**, *13*, 3271-3290.

(19) Lau, D.; Baldus, S. "Myeloperoxidase and its contributory role in inflammatory vascular disease." *Pharmacology & Therapeutics* **2006**, *111*, 16-26.

(20) Davies, M. J.; Hawkins, C. L.; Pattison, D. I.; Rees, M. D. "Mammalian heme peroxidases: From molecular mechanisms to health implications." *Antioxidants & Redox Signaling* **2008**, *10*, 1199-1234.

(21) Nicholls, S. J.; Hazen, S. L. "Myeloperoxidase and cardiovascular disease." *Arteriosclerosis Thrombosis and Vascular Biology* **2005**, *25*, 1102-1111.

(22) Ogino, K.; Wang, D. H. "Biomarkers of oxidative/nitrosative stress: An approach to disease prevention." *Acta Medica Okayama* **2007**, *61*, 181-189.

(23) Tsukahara, H. "Biomarkers for oxidative stress: Clinical application in pediatric medicine." *Current Medicinal Chemistry* **2007**, *14*, 339-351.

(24) Wu, A. H. B. "Novel biomarkers of cardiovascular disease: Myeloperoxidase for acute and/or chronic heart failure?" *Clinical Chemistry* **2009**, *55*, 12-14.

(25) Loria, V.; Dato, I.; Graziani, F.; Biasucci, L. M. "Myeloperoxidase: A new biomarker of inflammation in ischemic heart disease and acute coronary syndromes." *Mediators of Inflammation* **2008**.

(26) Malle, E.; Furtmuller, P. G.; Sattler, W.; Obinger, C. "Myeloperoxidase: A target for new drug development?" *British Journal of Pharmacology* **2007**, *152*, 838-854.

(27) Beal Jennifer, L.; Foster Steven, B.; Ashby Michael, T. "Hypochlorous acid reacts with the n-terminal methionines of proteins to give dehydromethionine, a potential biomarker for neutrophil-induced oxidative stress." *Biochemistry* **2009**, *48*, 11142-8.

(28) Harwood, D. T.; Nimmo, S. L.; Kettle, A. J.; Winterbourn, C. C.; Ashby, M. T. "Molecular structure and dynamic properties of a sulfonamide derivative of glutathione that is produced under conditions of oxidative stress by hypochlorous acid." *Chemical Research in Toxicology* **2008**, *21*, 1011-1016.

(29) Pattison, D. I.; Davies, M. J. "Absolute rate constants for the reaction of hypochlorous acid with protein side chains and peptide bonds." *Chemical Research in Toxicology* **2001**, *14*, 1453-1464.

(30) Cuq, J. L.; Aymard, C.; Cheftel, C. "Effects of hypochlorite treatments on a methionyl peptide." *Food Chemistry* **1977**, *2*, 309-14.

(31) Drozdz, R.; Naskalski, J. W.; Sznajd, J. "Oxidation of amino acids and peptides in reaction with myeloperoxidase, chloride and hydrogen peroxide." *Biochimica et Biophysica Acta, Protein Structure and Molecular Enzymology* **1988**, *957*, 47-52.

(32) Maier, K. L.; Matejkova, E.; Hinze, H.; Leuschel, L.; Weber, H.; Beck-Speier, I. "Different selectivities of oxidants during oxidation of methionine residues in the alpha -1-proteinase inhibitor." *FEBS Letters* **1989**, *250*, 221-6.

(33) Sharov, V. S.; Schoneich, C. "Diastereoselective protein methionine oxidation by reactive oxygen species and diastereoselective repair by methionine sulfoxide reductase." *Free Radical Biology & Medicine* **2000**, *29*, 986-994.

(34) Khor, H. K.; Fisher, M. T.; Schoeneich, C. "Potential role of methionine sulfoxide in the inactivation of the chaperone groel by hypochlorous acid (hocl) and peroxynitrite (onoo-)." *Journal of Biological Chemistry* **2004**, *279*, 19486-19493.

(35) Shao, B.; Belaaouaj, A.; Verlinde, C. L. M. J.; Fu, X.; Heinecke, J. W. "Methionine sulfoxide and proteolytic cleavage contribute to the inactivation of cathepsin g by hypochlorous acid: An oxidative mechanism for regulation of

serine proteinases by myeloperoxidase." *Journal of Biological Chemistry* **2005**, *280*, 29311-29321.

(36) Pattison, D. I.; Hawkins, C. L.; Davies, M. J. "Hypochlorous acid-mediated protein oxidation: How important are chloramine transfer reactions and protein tertiary structure?" *Biochemistry* **2007**, *46*, 9853-9864.

(37) Pattison, D. I.; Hawkins, C. L.; Davies, M. J. "What are the plasma targets of the oxidant hypochlorous acid? A kinetic modeling approach." *Chemical Research in Toxicology* **2009**, *22*, 807-817.

(38) Billington, D. C.; Golding, B. T. "Proton exchange in dehydromethionine; synthesis of l-methionine-methyl-2h3." *Tetrahedron Letters* **1979**, 2937-8.

(39) Billington, D. C.; Golding, B. T. "Aspects of the chemistry of dehydromethionine." *Journal of the Chemical Society, Perkin Transactions 1 Organic and Bio-Organic Chemistry (1972-1999)* **1982**, 1283-90.

(40) Fruttero, R.; Amiconi, G.; Ascoli, F.; Bolegnesi, M.; Ascenzi, P. "Identification of l-methionine oxidation products in tripeptides, in met-enkephalin and in the bovine basic pancreatic trypsin inhibitor: 1h and 13c nmr study." *Biochemistry and Molecular Biology International* **1995**, *35*, 861-74.

(41) Gensch, K. H.; Higuchi, T. "Kinetic investigation of the reversible reaction between methionine and iodine. Improved iodometric determination of methionine." *Journal of Pharmaceutical Sciences* **1967**, *56*, 177-84.

(42) Glass, R. S.; Duchek, J. R. "The structure of dehydromethionine. An azasulfonium salt." *Journal of the American Chemical Society* **1976**, *98*, 965-9.

(43) Lambeth, D. O. "Reduction of dehydromethionine by thiols. Kinetics and mechanism." *Journal of the American Chemical Society* **1978**, *100*, 4808-13.

(44) Lavine, T. F. "Dehydromethionine, a new methionine derivative." *Federation Proceedings* **1945**, *4*, 96-96.

(45) Swank, D. W.; Lambeth, D. O. "Formation and properties of the azasulfonium functionality in dehydromethionine and other isothiazolidinium salts." *Federation Proceedings* **1981**, *40*, 1683-1683.

(46) Lavine, T. F.; (Lankenau Hospital). US, 1949.

(47) Weil, L.; Gordon, W. G.; Buchert, A. R. "Photooxidation of amino acids in the presence of methylene blue." *Archives of Biochemistry and Biophysics* **1951**, *33*, 90-109.

(48) Sysak, P. K.; Foote, C. S.; Ching, T.-Y. "Chemistry of singlet oxygen. Xxv. Photooxygenation of methionine." *Photochemistry and Photobiology* **1977**, *26*, 19-27.

(49) Lambeth, D. O.; Swank, D. W. "Oxidative cyclization of 3-(amino)thioethers to form s-substituted isothiazolidinium salts." *Journal of Organic Chemistry* **1979**, *44*, 2632-6.

(50) Asmus, K. D.; Goebl, M.; Hiller, K. O.; Mahling, S.; Moenig, J. "Sulfur-nitrogen and sulfur-oxygen three-electron-bonded radicals and radical cations in aqueous solutions." *Journal of the Chemical Society, Perkin Transactions 2: Physical Organic Chemistry (1972-1999)* **1985**, 641-6.

(51) Young, P. R.; Briedis, A. V. "Kinetics and mechanism of the glutathione-dependent reduction of dehydromethionine." *Biochimica et Biophysica Acta, General Subjects* **1988**, *967*, 318-21.

(52) Alks, V.; Keith, D. D.; Sufrin, J. R. "Synthesis of the constrained l-methionine analog, (z)-l-2-amino-4-(methylthio)-3-butenoic acid." *Synthesis* **1992**, 623-5.

(53) Schoneich, C. "Diastereoselectivity and neighboring group effects in the oxidation of methionine-containing peptides." *Book of Abstracts, 211th ACS National Meeting, New Orleans, LA, March 24-28* **1996**, BTEC-013.

(54) Hong, J. Y.; Schoneich, C. "The metal-catalyzed oxidation of methionine in peptides by fenton systems involves two consecutive one-electron oxidation processes." *Free Radical Biology and Medicine* **2001**, *31*, 1432-1441.

(55) Miller, B. L.; Kuczera, K.; Schoneich, C. "One-electron photooxidation of n-methionyl peptides. Mechanism of sulfoxide and azasulfonium diastereomer formation through reaction of sulfide radical cation complexes with oxygen or superoxide." *Journal of the American Chemical Society* **1998**, *120*, 3345-3356.

(56) Young, P. R.; Hsieh, L. S. "General base catalysis and evidence for a sulfurane intermediate in iodine oxidation of methionine." *Journal of the American Chemical Society* **1978**, *100*, 7121-7122.

(57) Lavine, T. F. "An iodometric determination of methionine." *Journal of Biological Chemistry* **1943**, *151*, 281-297.

(58) Gensch, K. H.; Higuchi, T. "Kinetic investigation of reversible reaction between methionine and iodine - improved iodometric determination of methionine." *Journal of Pharmaceutical Sciences* **1967**, *56*, 177-&.

(59) Peskin, A. V.; Turner, R.; Maghzal, G. J.; Winterbourn, C. C.; Kettle, A. J. "Oxidation of methionine to dehydromethionine by reactive halogen species generated by neutrophils." *Biochemistry* **2009**, *48*, 10175-10182.

(60) Beers, R. F.; Sizer, I. W. "A spectrophotometric method for measuring the breakdown of hydrogen peroxide by catalase." *Journal of Biological Chemistry* **1952**, *195*, 133-140.

(61) Anbar, M.; Dostrovsky, I. "Ultra-violet absorption spectra of some organic hypohalites." *Journal of the Chemical Society* **1954**, 1105-1108.

(62) Nagy, P.; Beal, J. L.; Ashby, M. T. "Thiocyanate is an efficient endogenous scavenger of the phagocytic killing agent hypobromous acid." *Chemical Research in Toxicology* **2006**, *19*, 587-593.

(63) Koppenol, W. H.; Kissner, R.; Beckman, J. S. "Syntheses of peroxynitrite: To go with the flow or on solid grounds?" *Methods in Enzymology* **1996**, *269*, 296-302.

(64) Romero, N.; Radi, R.; Linares, E.; Augusto, O.; Detweiler, C. D.; Mason, R. P.; Denicola, A. "Reaction of human hemoglobin with peroxynitrite isomerization to nitrate and secondary formation of protein radicals." *Journal of Biological Chemistry* **2003**, *278*, 44049-44057.

(65) Awtrey, A. D.; Connick, R. E. "The absorption spectra of i-2,i-3-,i-, io3-,s4o6 and s2o3= heat of the reaction i-3-=i-2+i." *Journal of the American Chemical Society* **1951**, *73*, 1842-1843.

(66) Thomas, E. L.; Grisham, M. B.; Jefferson, M. M. "Preparation and characterization of chloramines." *Methods in Enzymology* **1986**, *132*, 569-85.

(67) Thomas, E. L.; Bozeman, P. M.; Jefferson, M. M.; King, C. C. "Oxidation of bromide by the human leukocyte enzymes myeloperoxidase and eosinophil peroxidase: Formation of bromamines." *Journal of Biological Chemistry* **1995**, *270*, 2906-2913.

(68) Nagy, P.; Alguindigue Susan, S.; Ashby Michael, T. "Lactoperoxidase-catalyzed oxidation of thiocyanate by hydrogen peroxide: A reinvestigation of hypothiocyanite by nuclear magnetic resonance and optical spectroscopy." *Biochemistry* **2006**, *45*, 12610-6.

(69) Simpson, R. J. In *Proteins and proteomics: A laboratory manual*; Cold Spring Harbor: New York, 2002, p 370.

(70) Glasoe, P. K.; Long, F. A. "Use of glass electrodes to measure acidities in deuterium oxide." *Journal of Physical Chemistry* **1960**, *64*, 188-90.

(71) Wilson, G. E., Jr. "Fragmentations of halosulfonium salts and related reactions. Role of sulfenyl intermediates." *Quarterly Reports on Sulfur Chemistry* **1967**, *2*, 313-17.

(72) Wilson, G. E., Jr. "Structure and reactivity of halosulfonium salts." *Tetrahedron* **1982**, *38*, 2597-625.

(73) Wilson, G. E., Jr.; Huang, M. G. "Sulfonium salts. Iv. Cleavage--alpha -substitution competition of dibenzylhalosulfonium salts." *Journal of Organic Chemistry* **1970**, *35*, 3002-7.

(74) Allegra, G.; Wilson, G. E., Jr.; Benedetti, E.; Pedone, C.; Albert, R. "Structure of a halosulfonium salt. The 1:1 adduct of thiophane with bromine." *Journal of the American Chemical Society* **1970**, *92*, 4002-7.

(75) Minkwitz, R.; Gerhard, V.; Preut, H. "Crystal structure of chlorodimethylsulfonium(1+) hexafluoroantimonate(1-) and comparing interionic effects in halosulfonium hexafluorometallates." *Zeitschrift fuer Anorganische und Allgemeine Chemie* **1991**, *596*, 99-105.

(76) Minkwitz, R.; Werner, A. "Chemistry of sulfur halides. 25. Methyl(trifluoromethyl)halosulfonium salts. Halogen = f, cl, br, i." *Zeitschrift fuer Naturforschung, B Chemical Sciences* **1988**, *43*, 403-11.

(77) Armesto, X. L.; Canle L, M.; Fernandez, M. I.; Garcia, M. V.; Santaballa, J. A. "First steps in the oxidation of sulfur-containing amino acids by hypohalogenation: Very fast generation of intermediate sulfenyl halides and halosulfonium cations." *Tetrahedron* **2000**, *56*, 1103-1109.

(78) Pryor, W. A.; Jin, X.; Squadrito, G. L. "One-electron and 2-electron oxidations of methionine by peroxynitrite." *Proceedings of the National Academy of Sciences of the United States of America* **1994**, *91*, 11173-11177.

(79) Peskin, A. V.; Winterbourn, C. C. "Kinetics of the reactions of hypochlorous acid and amino acid chloramines with thiols, methionine, and ascorbate." *Free Radical Biology and Medicine* **2001**, *30*, 572-579.

(80) Pattison, D. I.; Davies, M. J. "Kinetic analysis of the reactions of hypobromous acid with protein components: Implications for cellular damage and use of 3-bromotyrosine as a marker of oxidative stress." *Biochemistry* **2004**, *43*, 4799-4809.

(81) Prutz, W. A.; Kissner, R.; Nauser, T.; Koppenol, W. H. "On the oxidation of cytochrome c by hypohalous acids." *Archives of Biochemistry and Biophysics* **2001**, *389*, 110-122.

(82) Hershko, A.; Ciechanover, A. "The ubiquitin system." *Annual Review of Biochemistry* **1998**, *67*, 425-479.

(83) Vijaykumar, S.; Bugg, C. E.; Cook, W. J. "Structure of ubiquitin refined at 1.8 a resolution." *Journal of Molecular Biology* **1987**, *194*, 531-544.

(84) Bamezai, S.; Banez, M. A.; Breslow, E. "Structural and functional changes associated with modification of the ubiquitin methionine." *Biochemistry* **1990**, *29*, 5389-96.

(85) Cornilescu, G.; Marquardt, J. L.; Ottiger, M.; Bax, A. "Validation of protein structure from anisotropic carbonyl chemical shifts in a dilute liquid crystalline phase." *Journal of the American Chemical Society* **1998**, *120*, 6836-6837.

(86) Cox, M. J.; Haas, A. L.; Wilkinson, K. D. "Role of ubiquitin conformations in the specificity of protein-degradation - iodinated derivatives with altered conformations and activities." *Archives of Biochemistry and Biophysics* **1986**, *250*, 400-409.

(87) Pickart, C. M.; Haldeman, M. T.; Kasperek, E. M.; Chen, Z. J. "Iodination of tyrosine-59 of ubiquitin selectively blocks ubiquitins acceptor activity in diubiquitin synthesis catalyzed by e2(25k)." *Journal of Biological Chemistry* **1992**, *267*, 14418-14423.

(88) Neumann, N. P.; Stein, W. H.; Moore, S. "Modification of methionine residues in ribonuclease." *Biochemistry* **1962**, *1*, 68-&.

(89) Chesnut, D. B. "The electron localization function signature of the amide bond exhibits nitrogen lone pair character." *Journal of Physical Chemistry A* **2000**, *104*, 7635-7638.

(90) Kozak, M. "Initiation of translation in prokaryotes and eukaryotes." *Gene* **1999**, *234*, 187-208.

(91) Bradshaw, R. A.; Hope, C. J.; Yi, E.; Walker, K. W. "Co- and posttranslational processing: The removal of methionine." *Enzymes (3rd Edition)* **2002**, *22*, 387-420, 505-508.

Chapter 5: Concluding Remarks and Future Experiments

5.1 Summary of findings

The rate constant for the oxidation of SCN^- by HOCl at neutral pH was measured. Using competition kinetics, we obtain a rate constant of approximately $2x10^7$ $M^{-1}s^{-1}$, remarkably comparable to that reported in literature which had been extrapolated from alkaline conditions ($2.3x10^7$ $M^{-1}s^{-1}$). The reaction of HSA with HOCl also was studied. Though an appropriate model could not be found to accurately fit the data, a stoichiometry of 7:1 was observed which supports predictions that the one Cys and six Met groups of HSA are the most reactive. These experiments give insight into the importance of fitting the complete data set (not just the 50% inhibition point) as well as consideration of stoichiometry (i.e. rate law) when trying to accurately fit competition reaction data. Though just briefly studied, HSA experiments demonstrate potential problems when homogenous reaction conditions are not obtained, causing reproducibility problems.

The rate constant for the reaction of HOCl with four thioethers (Met, MetO, DNPMet, and TNBMe) was measured at neutral pH. The reactions studied did not show definitive evidence for the formation of a chlorosulfonium ion intermediate. However, the observed product, DHM, formed in the reaction of Met with HOCl, gives insight into the identity of the intermediate. Due to the hypothesized method by which DHM is formed, from intramolecular attack followed by ring closure, a halosulfonium intermediate can account for the formation of the DHM product. In addition, the thioether reactions studied

allowed us to estimate the half life for an intermediate of 100 ms or less (assuming $\varepsilon_{Reactant} \approx \varepsilon_{Intermediate}$ and $k_{formation\ of\ intermediate} < 10 * k_{intermediate\ reacting}$). With a half-life of 100 ms, an intermediate should be long enough lived to be studied using stopped-flow instrumentation.

DHM was found to form when free Met, peptides containing an *N*-terminus Met, and a protein containing an *N*-terminus Met, were oxidized by halogenating agents. For free Met, the oxidants can be grouped by the yields of DHM they produce, where chlorinating agents produce around 43% DHM, brominating agents approximately 75%, and iodinating agents close to 100% DHM. Most importantly, oxidation of Ub by HOCl formed DHM-Ub. Ease of formation of the DHM moiety in proteins along with its high stability at neutral pH shows the high potential for DHM as a biomarker of protein oxidation by halogenating agents.

5.2 Recommended future studies

The IT method for measuring rate constants is a promising technique; however, more studies need to be performed to validate the method to show its usefulness for a variety of reactions, not just fast reactions that we have examined. In addition, a model needs to be developed that is appropriate for the oxidation of HSA. This may need additional studies such as experiments in which certain reactive groups on HSA are blocked (e.g. Cys group) to help make the reaction and subsequent interpretation less complex. Additionally, a

smaller protein could be examined, one which has fewer reactive groups than HSA .

Additional studies need to be performed on the oxidation of thioethers to find definitive evidence for a halosulfonium ion intermediate. Due to the high molar absorptivity and difference in reactant and product absorbance spectra, TNBMe system showed the most promise of the four thioethers studied. pH studies of the reaction of TNBMe and HOCl need to be performed, in particular under acidic conditions in which hydrolysis of an intermediate would be slower, possibly allowing a buildup of an intermediate to be observed. Other thioethers need to be studied, in particular ones which have high molar absorptivities so the kinetics can be monitored directly instead of by competition methods. The reaction of thioethers with HOBr is worth examining since the rate of reaction is slower (relative to HOCl) and the hydrolysis of a bromosulfonium intermediate may also be slower, possibly allowing an intermediate to buildup.

Additional experiments are needed to study the formation of DHM in proteins. The work described in this dissertation is just the beginning of these studies. A method is needed to quantify the amount of DHM formed in proteins. In addition other oxidants need to be tested for their ability to form DHM-proteins. One possibility to allow detection of DHM-derivatized proteins in complex physiologic fluids may be to create an antibody which recognizes the DHM moiety, making it possible to isolate or fluorescently tag any DHM formed.

Appendices

Appendix A: Data for the reaction of HOCl (1 mM) with mixtures of MCD (1 mM) and SCN^- (0-4.6 mM) at pH 7.4, 0.1 M phosphate and 0.1 M NaCl. All samples had a varied amount of SCN^- added to MCD (1 mM). The first data point (listed as 0 mM SCN^-) is the 0% reaction data point (no HOCl added so 100% of the MCD is remaining). The second data point is the 100% reaction data point (no SCN^- added, only a reaction between the MCD and HOCl)

Column Heading	Brief Description
$[SCN^-]$ mM	amount of SCN^- added to the sample
A_{290}	measured absorbance at 290 nm
Dilution factor correction	calculation of absorbance if consider dilution factor (e.g. the sample which contained 4.58 mM SCN^- was diluted by a factor of two before measuring absorbance spectrum (to keep absorbance within instrumental limitations), so the measured absorbance of 0.829 was multiplied by two giving 1.658)
A_{scatt}	absorbance due to scattering (absorbance at 600 nm)
ΔA	change in absorbance (Dilution factor correction - absorbance scattering)
Corrected A	ΔA - correction factor (for this sample set its 0.017) calculated from the absorbance observed from the reaction of MCD and HOCl without any SCN^- present (believed to be due to the buffer present in the sample)
%MCD	% MCD remaining, calculated from Corrected A (for each sample point) divided by Corrected A for 0% reaction (first data point in table), multiplied by 100
Stoichiometry	calculated using the following equation stoichiometry = $([HOCl]_{initial} - ([MCD]_{initial} - [MCD]_{final})) / SCN^-_{initial}$

$[SCN^-]$ mM	A_{290}	Dilution factor correction	A_{scatt}	ΔA	Corrected A	%MCD	Stoichiometry
0.00	0.865	1.730	0.002	1.729	1.712	100.0	
0.00	0.022	0.022	0.004	0.017	0.000	0.0	
0.06	0.187	0.187	0.006	0.181	0.164	9.6	1.7
0.11	0.449	0.449	0.004	0.445	0.427	25.0	2.4
0.23	0.758	0.758	0.004	0.753	0.736	43.0	2.1
0.34	0.505	1.011	0.005	1.006	0.989	57.8	1.9
0.46	0.553	1.105	0.004	1.101	1.084	63.3	1.6
0.57	0.584	1.168	0.005	1.163	1.146	67.0	1.3
0.69	0.634	1.268	0.002	1.266	1.249	73.0	1.2
0.80	0.652	1.303	0.002	1.301	1.283	75.0	1.0
0.92	0.684	1.368	0.002	1.365	1.348	78.7	1.0
1.03	0.699	1.399	0.002	1.397	1.380	80.6	0.9
1.14	0.720	1.440	0.001	1.439	1.421	83.0	0.9
1.43	0.765	1.530	0.007	1.523	1.506	88.0	1.0
1.72	0.766	1.532	0.000	1.532	1.515	88.5	1.0
2.00	0.778	1.555	0.003	1.552	1.535	89.7	1.0
2.29	0.793	1.586	0.000	1.586	1.569	91.6	1.0
2.57	0.801	1.601	0.002	1.599	1.582	92.4	1.0
2.86	0.803	1.606	0.002	1.604	1.587	92.7	1.0
3.15	0.808	1.616	0.001	1.615	1.598	93.3	1.0
3.43	0.815	1.631	0.001	1.629	1.612	94.2	1.0
3.72	0.824	1.648	0.001	1.647	1.630	95.2	1.0
4.00	0.830	1.660	0.003	1.657	1.640	95.8	1.0
4.29	0.826	1.652	0.001	1.651	1.634	95.4	1.0
4.58	0.829	1.658	0.001	1.657	1.640	95.8	1.0

Appendix B: C++ code for computing the constants using experimental data for the reaction of HOCl (1 mM) with mixtures of MCD (1 mM) and SCN^- (0-4.6 mM) at pH 7.4 in 0.1 M phosphate and 0.1 M NaCl.

```
#include  <stdio.h>
#include  <math.h>
#include  <stdlib.h>

FILE *pStream;

main()
{
        int i,xsteps;
        double h, incamt,dampfac, MCD, MCDint, MCDold, X, Xint, Xold,
HOClint, HOCltotal, kMCDeff, kXeff, H, Ka;
        double calMCD[23],kXcalc[23];
        double expMCD[23] = {9.6, 25.0, 43.0, 57.8, 63.3, 67.0, 73.0, 75.0, 78.7,
80.6, 83.0, 88.0, 88.5, 89.7, 91.6, 92.4, 92.7,
            93.3, 94.2, 95.2, 95.8, 95.4, 95.8};
        double expX[23] = {0.06e-3, 0.11e-3, 0.23e-3, 0.34e-3, 0.46e-3, 0.57e-3,
0.69e-3, 0.80e-3, 0.92e-3, 1.03e-3, 1.14e-3,
            1.43e-3, 1.72e-3, 2.00e-3, 2.29e-3, 2.57e-3, 2.86e-3, 3.15e-3, 3.43e-
3, 3.72e-3, 4.00e-3, 4.29e-3, 4.58e-3};
        double stoich[23] = {1.7, 2.4, 2.1 ,1.9 ,1.6 ,1.3 ,1.2 ,1.0 ,1.0 ,0.9 ,0.9 ,1.0
,1.0 ,1.0 ,1.0 ,1.0 ,1.0 ,1.0 , 1.0, 1.0, 1.0, 1.0,
            1.0};

        pStream = fopen("test21.txt", "w+" );
        fprintf(pStream,"i\texpX\texpMCD\tcalMCD\tkXcalc\n");

        xsteps = 23;
        dampfac = 0.1;
        h = 0.00001;
        kMCDeff = 4.0e6;    /* an experimental value; kMCDeff*[HOCl]T =
kMCD*[HOCl] */
        MCDint = 0.001;
        HOClint = 0.001;  /* this is the [HOCl]T = [HOCl] + [OCl-] */
        H = 3.98e-8;    /* pH = 7.4 */
        Ka = 3.98e-8;   /* pKa of HOCl is 7.4 */
```

```
        for (i = 0; i < xsteps; ++i) {
                Xint = expX[i];
                X=Xint;
                kXeff = 5.0e5;  /* a starting estimate */
                calMCD[i] = expMCD[i]*2.0; /* give calMCD something to start with
*/
                while (fabs((calMCD[i] - expMCD[i])/expMCD[i]) > 0.001 && X !=
0.0) { /* until calMCD is within 99.9% expMCD */
                        incamt = dampfac*fabs((expMCD[i] -
calMCD[i])/expMCD[i]); /* dampen the increment as calMCD
                                approached expMCD */
                        if (expMCD[i] > calMCD[i])
                                kXeff = kXeff + kXeff*incamt;
                        else
                                kXeff = kXeff - kXeff*incamt;
//              printf("i = %2d\tincamt = %.2e \n", i, incamt);
                        MCD=MCDint;
                        X=Xint;
                        HOCltotal = HOClint;
                        while (HOCltotal > HOClint/100.0) {   /* until 99.9% HOCl
reacts */
                                MCDold = MCD;
                                MCD = MCD - h*kMCDeff*MCD*HOCltotal;
                                Xold = X;
                                X = X - h*kXeff*X*HOCltotal/stoich[i];
                                if (X < 0.0) X = 0.0;
                                HOCltotal = HOCltotal -
h*kMCDeff*MCDold*HOCltotal - h*kXeff*Xold*HOCltotal;
//                              printf("flag1: MCD = %.2e X = %.2e HOCl = %.2e kX
= %.2e\n", MCD, X, HOCltotal, kXeff);
                        };
//                      kXcalc[i] = stoich[i]*kXeff*(Ka+H)/H; /* convert kXeff to kX
and save in case this is the right one */
                        kXcalc[i] = kXeff*(Ka+H)/H; /* convert kXeff to kX and save
in case this is the right one */
                        calMCD[i] = 100.0*MCD/MCDint; /* save percent MCD in
case this is the right one */
                };
```

```
                fprintf(pStream,"%2d\t%.2e\t%.1f\t%.1f\t%.2e\n", i, expX[i],
expMCD[i], calMCD[i], kXcalc[i]);
        };
        fclose (pStream);
}
```

Appendix C: C++ code used to fit the experimental data (using a defined rate constant for k_{SCN}) for the reaction of HOCl (1 mM) with mixtures of MCD (1 mM) and SCN^- (0-4.6 mM) at pH 7.4 in 0.1 M phosphate and 0.1 M NaCl. First loop calculates %MCD remaining when no stoichiometry of the reaction is taken into account, the second loop calculates %MCD remaining when the stoichiometry of the reaction is considered. The program uses $k_x : k_{XO} : k_{XO2}$= 1.0 : 0.1 : 0.4 and $k_{SCN} = k_X = 1.9 \times 10^7\ M^{-1}s^{-1}$ to fit the data, which was found to give a good fit.

```
#include  <stdio.h>
#include  <math.h>
#include  <stdlib.h>

FILE *pStream;

main()
{
        int i,xsteps;
        double h, MCD, MCDint, MCDold, X, Xint, Xfinal, Xold, XO, XOold, XOO,
XOOold, HOClint, HOCltotal, kMCDeff, kXeff, Ka, H, kOscale,
                kOOscale;
        double calMCD[100];

        pStream = fopen("test23.txt", "w+" );
        fprintf(pStream,"i\tXint\tcalMCD\n");

        xsteps = 100;
        Xfinal = 0.0036;

        h = 0.00001;

        kMCDeff = 4.0e6;
        kXeff = 1.9e7;
        kOscale = 0.1;
        kOOscale = 0.4;

        MCDint = 0.001;
```

```
	HOClint = 0.001;

	for (i = 0; i < xsteps; ++i) {

		Xint = i*Xfinal/100.0;
			;
		MCD=MCDint;
		X=Xint;
		XO=0.0;
		XOO=0.0;
		HOCltotal = HOClint;

		while (HOCltotal > HOClint/100.0) {   /* until 99% HOCl reacts */
				MCDold = MCD;
				MCD = MCD - h*kMCDeff*MCD*HOCltotal;
				Xold = X;
				X = X - h*kXeff*X*HOCltotal;
				if (X < 0.0) {X = 0.0; printf("Error: X underflow for
datapoint %2d\n", i);};
				HOCltotal = HOCltotal -
h*kMCDeff*MCDold*HOCltotal - h*kXeff*Xold*HOCltotal;
		};

		calMCD[i] = 100.0*MCD/MCDint; /* save percent MCD in case this
is the right one */
		fprintf(pStream,"%2d\t%.2e\t%.1f\n", i, Xint, calMCD[i]);
	};
	for (i = 0; i < xsteps; ++i) {

		Xint = i*Xfinal/100.0;
			;
		MCD=MCDint;
		X=Xint;
		XO=0.0;
		XOO=0.0;
		HOCltotal = HOClint;

		while (HOCltotal > HOClint/100.0) {   /* until 99% HOCl reacts */
				MCDold = MCD;
				MCD = MCD - h*kMCDeff*MCD*HOCltotal;
```

```
                                Xold = X;
                                X = X - h*kXeff*X*HOCltotal;
                                if (X < 0.0) {X = 0.0; printf("Error: X underflow for
datapoint %2d\n", i);};
                                XOold = XO;
                                XO = XO + h*kXeff*X*HOCltotal -
h*kXeff*kOscale*XO*HOCltotal;
                                if (XO < 0.0) {XO = 0.0; printf("Error: XO underflow
for datapoint %2d\n", i);};
                                XOOold = XOO;
                                XOO = XOO + h*kXeff*kOscale*XO*HOCltotal -
h*kXeff*kOOscale*XOO*HOCltotal;
                                if (XOO < 0.0) {XOO = 0.0; printf("Error: XOO
underflow for datapoint %2d\n", i);};
                                HOCltotal = HOCltotal -
h*kMCDeff*MCDold*HOCltotal - h*kXeff*Xold*HOCltotal –

h*kXeff*kOscale*XOold*HOCltotal- h*kXeff*kOOscale*XOold*HOCltotal;
                        };

                        calMCD[i] = 100.0*MCD/MCDint; /* save percent MCD in case this
is the right one */
                        fprintf(pStream,"%2d\t%.2e\t%.1f\n", i, Xint, calMCD[i]);
                };
                fclose (pStream);
}
```

Appendix D: Results obtained from the code listed in appendix C. The left column is the result when no stoichiometry is taken into consideration (first “for” loop in code), while right column is the result when stoichiometry is taken into account (second “for” loop in code). Listed is the increment number i (code incremented for 99 points), the concentration of X initial used, and the resulting MCD calculated.

i	X_{int}	MCD_{calc}
0	0.00E+00	1.0
1	3.60E-05	4.6
2	7.20E-05	8.2
3	1.08E-04	11.8
4	1.44E-04	15.4
5	1.80E-04	19.0
6	2.16E-04	22.6
7	2.52E-04	26.2
8	2.88E-04	29.7
9	3.24E-04	33.3
10	3.60E-04	36.7
11	3.96E-04	40.1
12	4.32E-04	43.5
13	4.68E-04	46.7
14	5.04E-04	49.7
15	5.40E-04	52.7
16	5.76E-04	55.4
17	6.12E-04	58.0
18	6.48E-04	60.3
19	6.84E-04	62.5
20	7.20E-04	64.6
21	7.56E-04	66.4
22	7.92E-04	68.2
23	8.28E-04	69.7
24	8.64E-04	71.2
25	9.00E-04	72.5
26	9.36E-04	73.7
27	9.72E-04	74.9
28	1.01E-03	75.9
29	1.04E-03	76.8
30	1.08E-03	77.7
31	1.12E-03	78.6
32	1.15E-03	79.3

i	X_{int}	MCD_{calc}
0	0.00E+00	1.0
1	3.60E-05	13.3
2	7.20E-05	22.0
3	1.08E-04	29.1
4	1.44E-04	35.0
5	1.80E-04	40.1
6	2.16E-04	44.6
7	2.52E-04	48.4
8	2.88E-04	51.9
9	3.24E-04	55.0
10	3.60E-04	57.7
11	3.96E-04	60.2
12	4.32E-04	62.4
13	4.68E-04	64.4
14	5.04E-04	66.3
15	5.40E-04	67.9
16	5.76E-04	69.5
17	6.12E-04	70.9
18	6.48E-04	72.2
19	6.84E-04	73.4
20	7.20E-04	74.5
21	7.56E-04	75.5
22	7.92E-04	76.4
23	8.28E-04	77.3
24	8.64E-04	78.1
25	9.00E-04	78.9
26	9.36E-04	79.6
27	9.72E-04	80.3
28	1.01E-03	80.9
29	1.04E-03	81.5
30	1.08E-03	82.1
31	1.12E-03	82.6
32	1.15E-03	83.1

33	1.19E-03	80.1	33	1.19E-03	83.6
34	1.22E-03	80.8	34	1.22E-03	84.0
35	1.26E-03	81.4	35	1.26E-03	84.4
36	1.30E-03	82.0	36	1.30E-03	84.8
37	1.33E-03	82.6	37	1.33E-03	85.2
38	1.37E-03	83.1	38	1.37E-03	85.6
39	1.40E-03	83.6	39	1.40E-03	85.9
40	1.44E-03	84.0	40	1.44E-03	86.3
41	1.48E-03	84.5	41	1.48E-03	86.6
42	1.51E-03	84.9	42	1.51E-03	86.9
43	1.55E-03	85.3	43	1.55E-03	87.2
44	1.58E-03	85.7	44	1.58E-03	87.5
45	1.62E-03	86.0	45	1.62E-03	87.7
46	1.66E-03	86.4	46	1.66E-03	88.0
47	1.69E-03	86.7	47	1.69E-03	88.2
48	1.73E-03	87.0	48	1.73E-03	88.4
49	1.76E-03	87.3	49	1.76E-03	88.7
50	1.80E-03	87.6	50	1.80E-03	88.9
51	1.84E-03	87.9	51	1.84E-03	89.1
52	1.87E-03	88.1	52	1.87E-03	89.3
53	1.91E-03	88.4	53	1.91E-03	89.5
54	1.94E-03	88.6	54	1.94E-03	89.7
55	1.98E-03	88.9	55	1.98E-03	89.9
56	2.02E-03	89.1	56	2.02E-03	90.1
57	2.05E-03	89.3	57	2.05E-03	90.2
58	2.09E-03	89.5	58	2.09E-03	90.4
59	2.12E-03	89.7	59	2.12E-03	90.6
60	2.16E-03	89.9	60	2.16E-03	90.7
61	2.20E-03	90.1	61	2.20E-03	90.8
62	2.23E-03	90.2	62	2.23E-03	91.0
63	2.27E-03	90.4	63	2.27E-03	91.1
64	2.30E-03	90.6	64	2.30E-03	91.3
65	2.34E-03	90.7	65	2.34E-03	91.4
66	2.38E-03	90.9	66	2.38E-03	91.5
67	2.41E-03	91.0	67	2.41E-03	91.6
68	2.45E-03	91.2	68	2.45E-03	91.8
69	2.48E-03	91.3	69	2.48E-03	91.9
70	2.52E-03	91.5	70	2.52E-03	92.0
71	2.56E-03	91.6	71	2.56E-03	92.1
72	2.59E-03	91.7	72	2.59E-03	92.2
73	2.63E-03	91.9	73	2.63E-03	92.3
74	2.66E-03	92.0	74	2.66E-03	92.4
75	2.70E-03	92.1	75	2.70E-03	92.5
76	2.74E-03	92.2	76	2.74E-03	92.6
77	2.77E-03	92.3	77	2.77E-03	92.7
78	2.81E-03	92.4	78	2.81E-03	92.8
79	2.84E-03	92.5	79	2.84E-03	92.9

80	2.88E-03	92.6
81	2.92E-03	92.7
82	2.95E-03	92.8
83	2.99E-03	92.9
84	3.02E-03	93.0
85	3.06E-03	93.1
86	3.10E-03	93.2
87	3.13E-03	93.3
88	3.17E-03	93.4
89	3.20E-03	93.4
90	3.24E-03	93.5
91	3.28E-03	93.6
92	3.31E-03	93.7
93	3.35E-03	93.8
94	3.38E-03	93.8
95	3.42E-03	93.9
96	3.46E-03	94.0
97	3.49E-03	94.0
98	3.53E-03	94.1
99	3.56E-03	94.1

80	2.88E-03	93.0
81	2.92E-03	93.1
82	2.95E-03	93.1
83	2.99E-03	93.3
84	3.02E-03	93.3
85	3.06E-03	93.4
86	3.10E-03	93.5
87	3.13E-03	93.5
88	3.17E-03	93.6
89	3.20E-03	93.7
90	3.24E-03	93.8
91	3.28E-03	93.8
92	3.31E-03	93.9
93	3.35E-03	94.0
94	3.38E-03	94.0
95	3.42E-03	94.1
96	3.46E-03	94.2
97	3.49E-03	94.2
98	3.53E-03	94.3
99	3.56E-03	94.3

Appendix E: Complete data set for the reaction of HOCl (100 µM) with mixtures of MCD (100 µM) and HSA (0-61 µM) at pH 7.4, 0.1 M phosphate and 0.1 M NaCl. All samples have a varied amount of HSA added to MCD (100 µM). The first data point (listed as 0 µM HSA) is the 0% reaction data point, it's a sample with no HOCl added, so 100% of the MCD is remaining. The second data point is the 100% reaction data point, (no HSA added, only a reaction between the MCD and HOCl).

Column Heading	Brief Description
[HSA] mg/ml	amount of HSA in the sample
[HSA] µM	amount of HSA in sample calculated in µM
A_{290}	measured absorbance at 290 nm
With dilution factor	calculation of absorbance if consider dilution factor
A_{scatt}	absorbance due to scattering (absorbance at 600 nm)
ΔA	change in absorbance (Dilution factor correction - absorbance scattering)
Corrected A	ΔA - correction factor (for this sample set its 0.01449) calculated from the absorbance observed from the reaction of MCD and HOCl without any HSA present (believed to be due to the buffer present in the sample)
%MCD	% MCD remaining, calculated from Corrected A (for each sample point) divided by Corrected A for 0% reaction (first data point in table), multiplied by 100
Stoichiometry	calculated using the following equation stoichiometry = $([HOCl]_{initial} - ([MCD]_{initial} - [MCD]_{final})) / HSA_{initial}$

[HSA] mg/ml	[HSA] µM	A_{290}	With dilution factor	A_{scatt}	ΔA	Corrected A	%MCD	Stoichiometry
0.00	0.00	-0.01317	-0.01317	-0.02766	0.01449	0	0.00	
0.00	0.00	0.68469	2.73876	-0.01334	2.7521	2.73761	100.00	1.0
0.11	1.67	0.29002	0.29002	-0.02853	0.31855	0.30406	11.11	6.7
0.22	3.34	0.54091	0.54091	-0.02525	0.56616	0.55167	20.15	6.0
0.44	6.68	0.45613	0.91226	-0.02568	0.93794	0.92345	33.73	5.1
0.67	10.02	0.55273	1.10546	-0.02621	1.13167	1.11718	40.81	4.1
1.00	15.03	0.70438	1.40876	-0.02629	1.43505	1.42056	51.89	3.5
1.20	18.03	0.38281	1.53124	-0.02609	1.55733	1.54284	56.36	3.1
1.42	21.37	0.41104	1.64416	-0.0235	1.66766	1.65317	60.39	2.8
1.60	24.04	0.43607	1.74428	-0.02516	1.76944	1.75495	64.11	2.7
1.82	27.38	0.4518	1.8072	-0.02644	1.83364	1.81915	66.45	2.4
2.00	30.06	0.47392	1.89568	-0.02545	1.92113	1.90664	69.65	2.3
2.22	33.39	0.50488	2.01952	-0.02467	2.04419	2.0297	74.14	2.2
2.40	36.07	0.52174	2.08696	-0.0174	2.10436	2.08987	76.34	2.1
2.62	39.41	0.53693	2.14772	-0.02174	2.16946	2.15497	78.72	2.0
2.80	42.08	0.561	2.244	-0.01987	2.26387	2.24938	82.17	2.0
3.02	45.42	0.57115	2.2846	-0.02356	2.30816	2.29367	83.78	1.8
2.89	43.41	0.56792	2.27168	-0.023	2.29468	2.28019	83.29	1.9
3.42	51.43	0.62387	2.49548	-0.01431	2.50979	2.4953	91.15	1.8
4.08	61.45	0.67221	2.68884	-0.01588	2.70472	2.69023	98.27	1.6

Appendix F: C++ code for computing the rate constant for the reaction of HOCl (100 µM) with mixtures of MCD (100 µM) and HSA (0-61 µM) at pH 7.4 in 0.1 M phosphate and 0.1 M NaCl.

```
#include  <stdio.h>
#include  <math.h>
#include  <stdlib.h>

FILE *pStream;

int main()
{
        int i,xsteps;
        double h, incamt,dampfac, MCD, MCDint, MCDold, X, Xint, Xold,
HOClint, HOCltotal, kMCDeff, kXeff, H, Ka;
        double calMCD[18],kXcalc[18];
        double expMCD[18] = {11.1, 20.1, 33.7, 40.8, 51.9, 56.4, 60.4, 64.1,
66.4, 69.7, 74.1, 76.3, 78.7, 82.2, 83.8, 83.3, 91.2,
            98.3};
        double expX[18] = {1.67e-6, 3.34e-6, 6.68e-6, 1.00e-5, 1.50e-5, 1.80e-5,
2.14e-5, 2.40e-5, 2.74e-5, 3.01e-5, 3.34e-5,
            3.61e-5, 3.94e-5, 4.21e-5, 4.54e-5, 4.34e-5, 5.14e-5, 6.15e-5};
        double stoich[18] = {6.7, 6.0, 5.1, 4.1, 3.5, 3.1, 2.8, 2.7, 2.4, 2.3, 2.2, 2.1,
2.0, 2.0, 1.8, 1.9, 1.8, 1.6};

        pStream = fopen("testhsa.txt", "w+" );
        fprintf(pStream,"i\texpX\texpMCD\tcalMCD\tkXcalc\n");

        xsteps = 18;
        i=0;
        dampfac = 0.1;
        h = 0.00001;
        kMCDeff = 4.0e6;    /* an experimental value; kMCDeff*[HOCl]T =
kMCD*[HOCl] */
        MCDint = 0.0001;
        HOClint = 0.0001;  /* this is the [HOCl]T = [HOCl] + [OCl-] */
        H = 3.98e-8;    /* pH = 7.4 */
        Ka = 3.98e-8;   /* pKa of HOCl is 7.4 */
```

```
        for (i = 0; i < xsteps; ++i) {
                Xint = expX[i];
                X=Xint;
                kXeff = 5.0e5;  /* a starting estimate */
                calMCD[i] = expMCD[i]*2.0; /* give calMCD something to start with
*/
                while (fabs((calMCD[i] - expMCD[i])/expMCD[i]) > 0.001 && X !=
0.0) { /* until calMCD is within 99.9% expMCD */
                        incamt = dampfac*fabs((expMCD[i] -
calMCD[i])/expMCD[i]); /* dampen the increment as calMCD
                                approached expMCD */
                        if (expMCD[i] > calMCD[i])
                                kXeff = kXeff + kXeff*incamt;
                        else
                                kXeff = kXeff - kXeff*incamt;
//              printf("i = %2d\tincamt = %.2e \n", i, incamt);
                        MCD=MCDint;
                        X=Xint;
                        HOCltotal = HOClint;
                        while (HOCltotal > HOClint/100.0) {   /* until 99.9% HOCl
reacts */
                                MCDold = MCD;
                                MCD = MCD - h*kMCDeff*MCD*HOCltotal;
                                Xold = X;
                                X = X - h*kXeff*X*HOCltotal/stoich[i];
                                if (X < 0.0) X = 0.0;
                                HOCltotal = HOCltotal -
h*kMCDeff*MCDold*HOCltotal - h*kXeff*Xold*HOCltotal;
//                              printf("flag1: MCD = %.2e X = %.2e HOCl = %.2e kX
= %.2e\n", MCD, X, HOCltotal, kXeff);
                        };
//                      kXcalc[i] = stoich[i]*kXeff*(Ka+H)/H; /* convert kXeff to kX
and save in case this is the right one */
                        kXcalc[i] = kXeff*(Ka+H)/H; /* convert kXeff to kX and save
in case this is the right one */
                        calMCD[i] = 100.0*MCD/MCDint; /* save percent MCD in
case this is the right one */
                };
                fprintf(pStream,"%2d\t%.2e\t%.1f\t%.1f\t%.2e\n", i, expX[i],
expMCD[i], calMCD[i], kXcalc[i]);
```

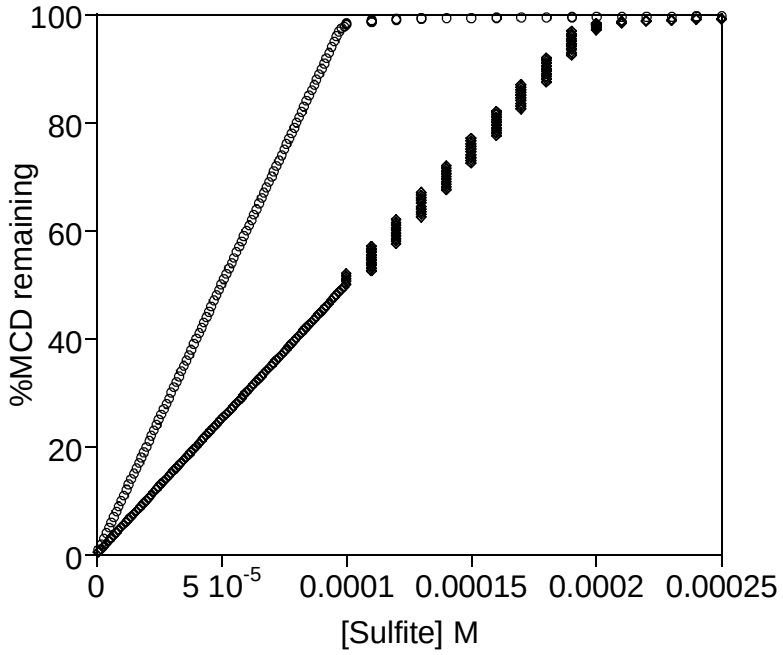
```
        };
        fclose (pStream);
}
```

Appendix G: C++ code used to simulate the data for the reaction of HOCl (1 mM) with mixtures of MCD (1 mM) and Sulfite (0-250 µM)

```
Clear[percentMCD, kMCD,kSO3,h,nsteps,];
xsteps=100; (* should equal nsteps *)
SO30=0.000010; (* start [SO3]=10uM *)
Do[{

Clear[MCD,SO3,HOCl,n,MCDdata,SO3data,HOCldata,MCDPlot,SO3Plot,HOCl
Plot];
    kMCD=3.6*10^6;
    kSO3=7.6*10^8;
    totaltime=0.001000; (* 1000usec *)
    h=0.000010; (* every 10usec *)
    MCD[0]=0.001000; (* 1mM *)
    SO3[0]=SO30*(x+1); (* increase [SO3] by 10uM each time *)
    HOCl[0]=0.001000;(* 1mM *)
    nsteps = Round[totaltime/h]; (* so this does it every 10 *)
    n=1;
    While[HOCl[n-1]>HOCl[0]/10000, (* react until 99.99% initial, since /100
would be 99% *)
        {
          MCD[n] =MCD[n-1] - h*kMCD*MCD[n-1]*HOCl[n-1],
          SO3[n] = SO3[n-1] - h*kSO3*SO3[n-1]*HOCl[n-1],
          HOCl[n] =HOCl[n-1] - h*kMCD*MCD[n-1]*HOCl[n-1]- h*kSO3*SO3[n-
1]*HOCl[n-1],
          n=n+1
          }] //N;
    percentMCD[x]= 100*MCD[n-1]/MCD[0]//N;
    },
  {x,0,xsteps-1}] //N;
percentdata = Table[{SO30*(n+1),percentMCD[n]}, {n, 0, xsteps-1}]
percentPlot=ListPlot[percentdata,Frame -> True, PlotStyle->
{RGBColor[1,0,0],PointSize[0.02]},PlotLabel="Percent MCD vs.
[SO3]",PlotRange=All];
```

Appendix H: Simulated data for the competition reaction of MCD/Sulfite with HOCl, comparing [MCD]=100 µM (circle) versus [MCD]=200 µM (diamonds).



Sodium sulfite reacts with HOCl with a rate constant around 10^9 $M^{-1}s^{-1}$ (Fogelman *et al.* "Hypochlorite and Hypochlorous Acid Reactions with Sulfite," Inorganic Chemistry, 28 (6) 986-993, 1989) much faster than the rate constant of 10^6 $M^{-1}s^{-1}$ for HOCl with MCD. When the rate constant of the inhibitor (sulfite in this particular example) is orders of magnitude faster than the competitor (or vice versa), HOCl gets used up by the faster reacting species, and then any HOCl that remains reacts with the slower reacting species, making it non-competitive. Take the following example, X (inhibitor) and Y (competitor, remains constant) compete for reaction with Z. X and Z react with a rate constant of 10^9 $M^{-1}s^{-1}$ and Y and Z react with a rate constant of 10^6 $M^{-1}s^{-1}$. Since X reacts orders of magnitude faster than Y, any X that is present (up to the

amount of Z available) will react, and then any Z remaining will react with Y. When X and Y are not competitive, a plot of X versus %Z remaining yields a graph which fits to a linear equation (y=mx+b). When X and Y are competitive (i.e. have similar rate constants), there is typically some curvature/non-linearity to the fit. This curvature can be modified by changing experimental conditions such as the concentration of the competitor (i.e. MCD). The curvature and shape of the fit, as well as investigating how experimental conditions change the fit, can both provide valuable insight into the reaction.